E. De Filippo (INFN Catania) (EXOCHIM  collaboration)

Probing the nuclear symmetry energy with heavy ion collisions

The nuclear EOS describes the relation between pressure, density, temperature and isospin asymmetry. It is an essential ingredient in nuclear physics and astrophysics, but how $E/A(\rho, \delta)$ depends on the density ρ and isospin asymmetry δ ?

IWM-EC 2014

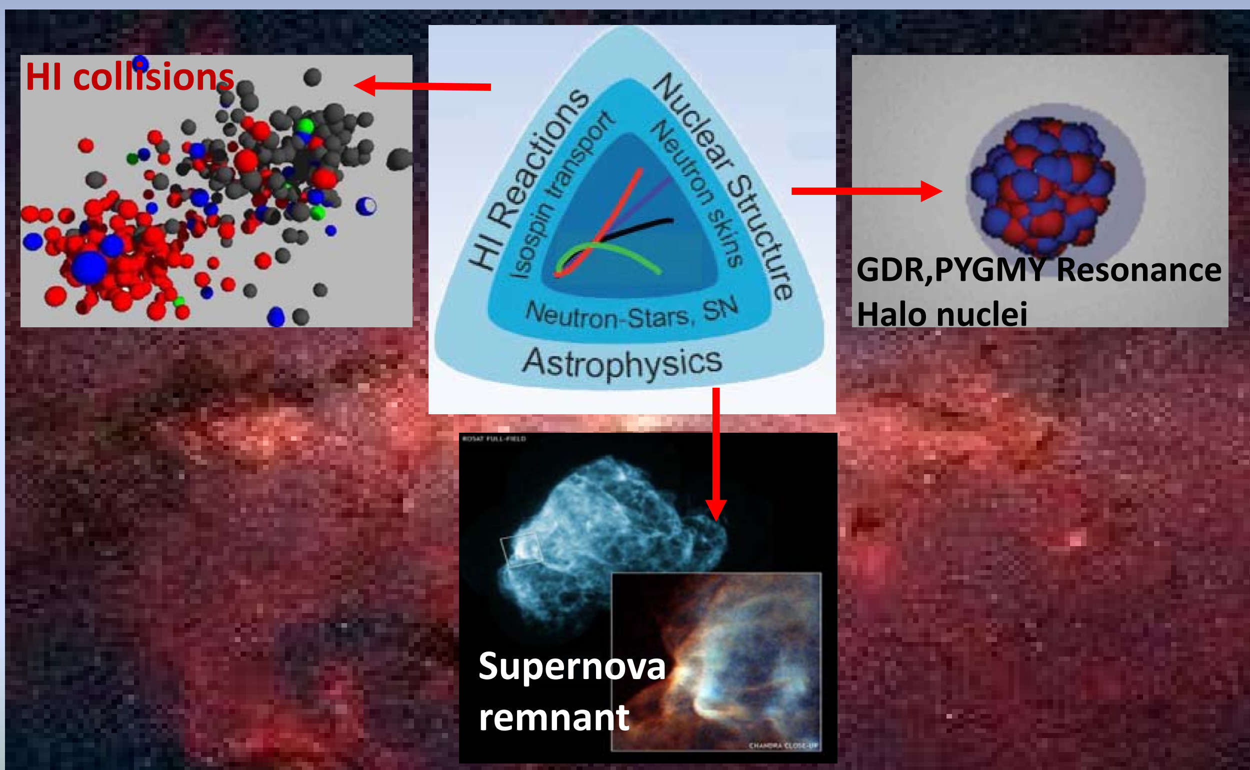

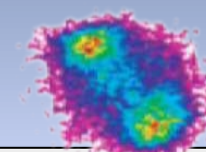

The density dependence of symmetry energy should be determined in a coherent way between astrophysical observations and heavy ion phenomenology

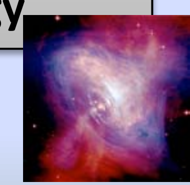

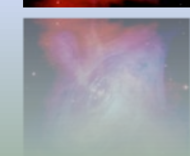

The role of isospin asymmetry in nuclear processes in the laboratory and in the cosmos

From laboratory

Nuclear structure

Nuclear reactions

Experimental Heavy ion reactions

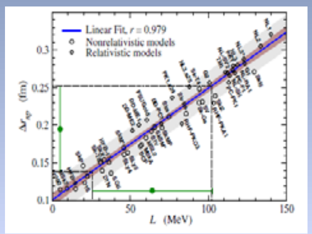

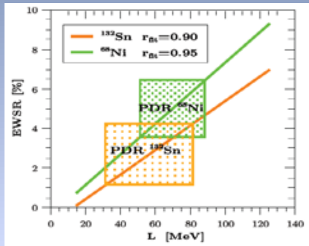

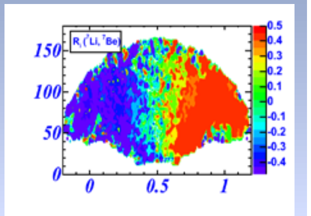

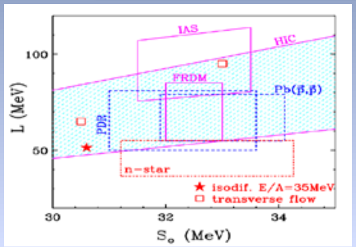

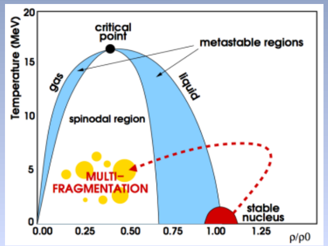

Theory

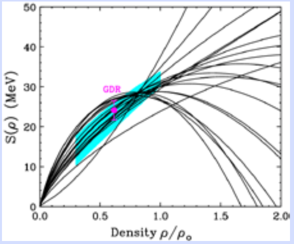

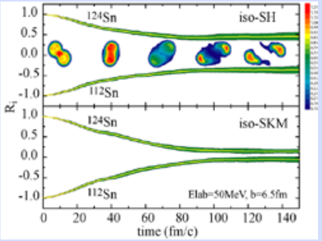

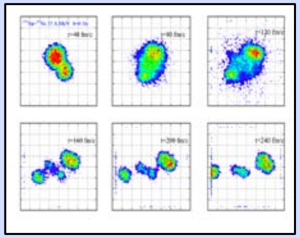

Models

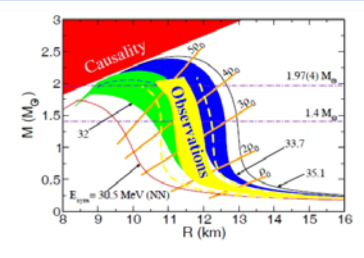

To compact stars

The key problem: the symmetry energy as a function of the barionic density

$$E(\rho,\delta) = E(\rho,\delta=0) + S(\rho)\delta^2$$

$$\delta = \frac{\rho_n - \rho_p}{\rho_n + \rho_p} = \frac{N-Z}{A}$$

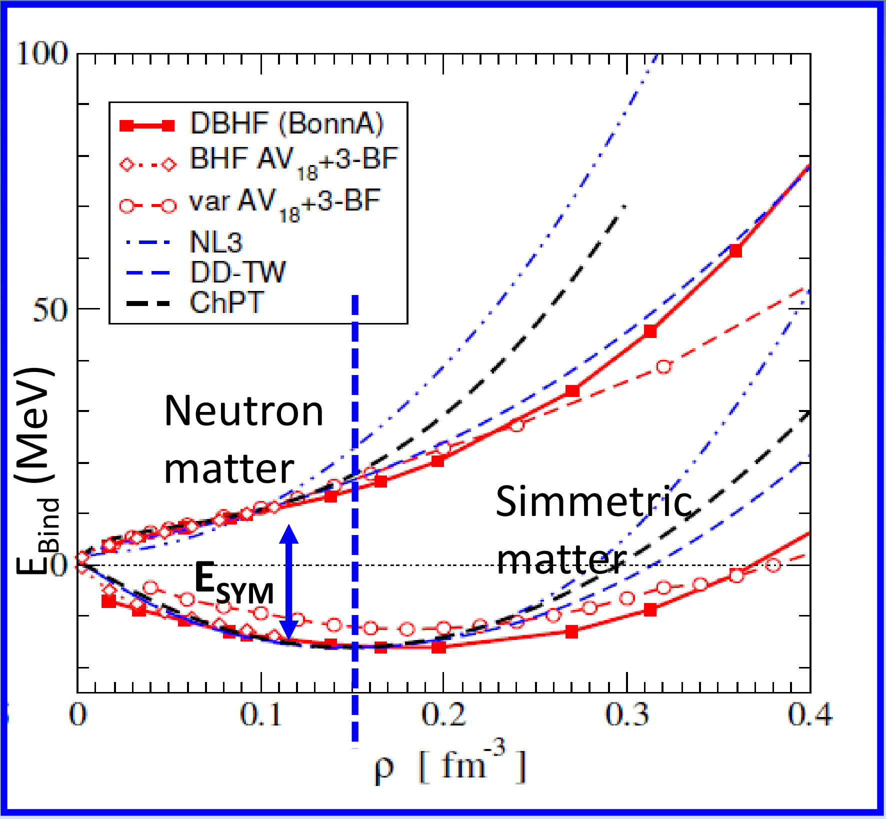

Fuchs and Wolter, EPJA 30, 5 (2006)

Large deviations at high densities, lack of experimental probes

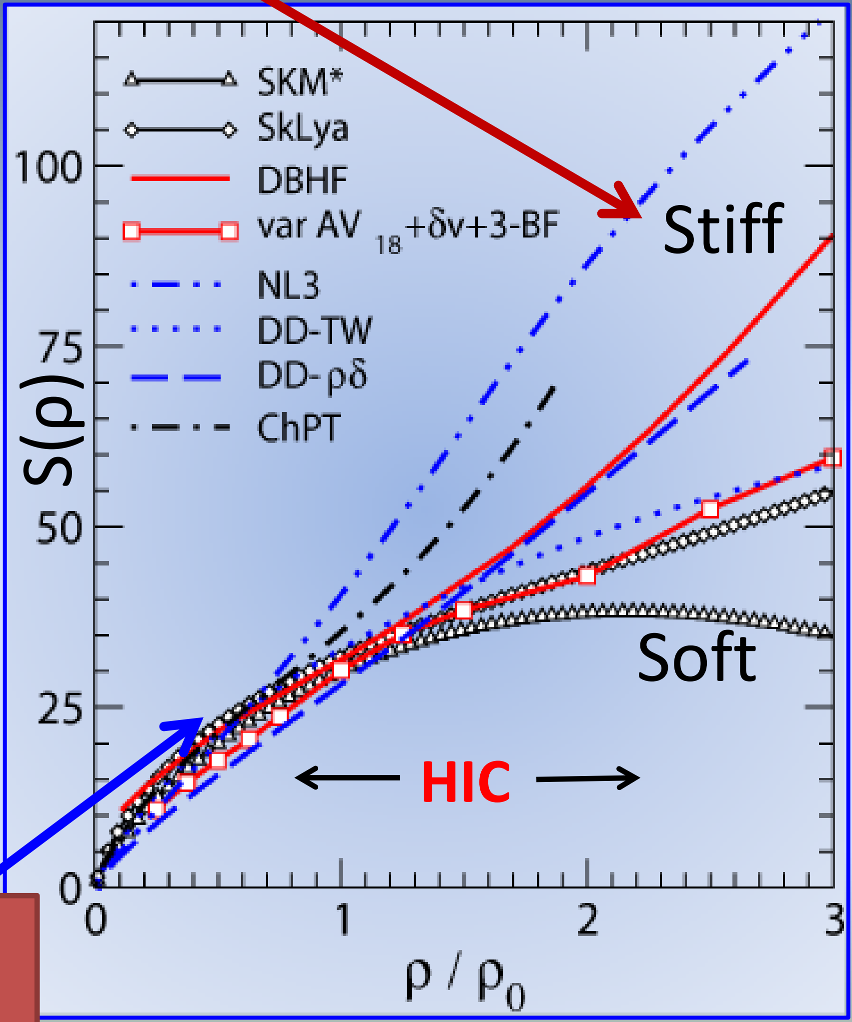

Sensitivity to observables based on N/Z asymmetry

Symmetry energy in neutron stars and neutron skin radius

$$S(\rho) = S_0 + \frac{L}{3}\left(\frac{\rho-\rho_0}{\rho_0}\right) + \frac{K_{sym}}{18}\left(\frac{\rho-\rho_0}{\rho_0}\right)^2 + \ldots.$$

$$L = 3\rho_0 \frac{dS(\rho)}{d\rho}$$

Slope

$$P_{SYM} = \rho^2 \left(\frac{dS}{d\rho}\right)_{\rho=\rho_0} = \frac{\rho_0}{3} L$$

Pressure

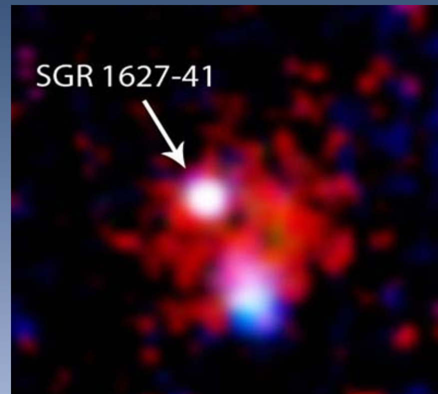

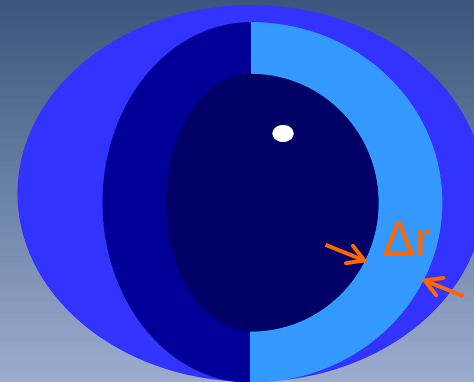

Neutron star
≈10^4 m

Neutron skin in ^{208}Pb
≈10^{-15} m

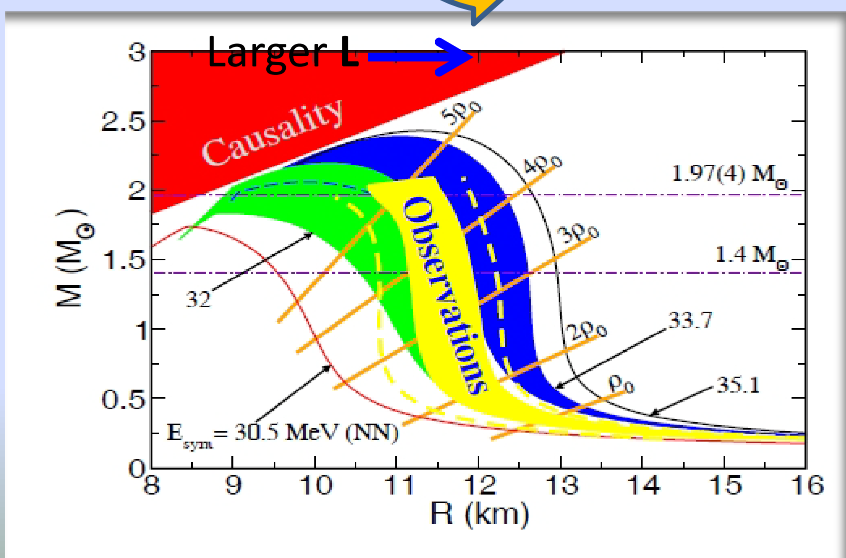

S. Gandolfi et al. EPJA 50:10 (2014)

Larger **L** → **Thicker** neutron skin

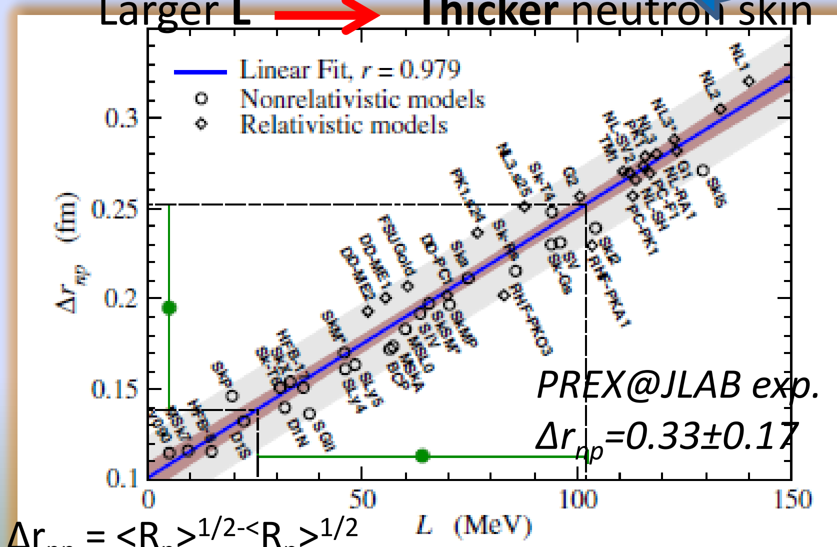

$\Delta r_{np} = \langle R_n \rangle^{1/2} - \langle R_p \rangle^{1/2}$

Roca-Maza et al., PRL 106, 252501 (2011)

Symmetry energy in neutron stars and neutron skin radius

$$S(\rho) = S_0 + \frac{L}{3}\left(\frac{\rho-\rho_0}{\rho_0}\right) + \frac{K_{sym}}{18}\left(\frac{\rho-\rho_0}{\rho_0}\right)^2 + \ldots$$

$$L = 3\rho_0 \frac{dS(\rho)}{d\rho}$$

Slope

$$P_{SYM} = \rho^2 \left(\frac{dS}{d\rho}\right)_{\rho=\rho_0} = \frac{\rho_0}{3} L$$

Pressure

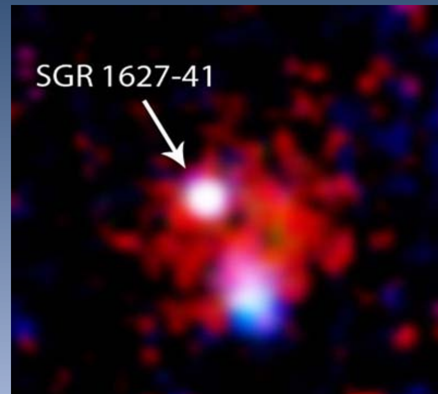

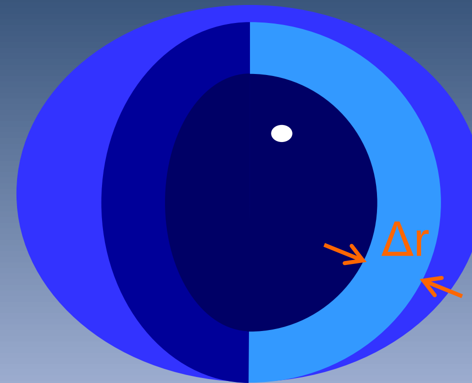

Neutron star

≈10^4 m

Neutron skin in ^{208}Pb

≈10^{-15} m

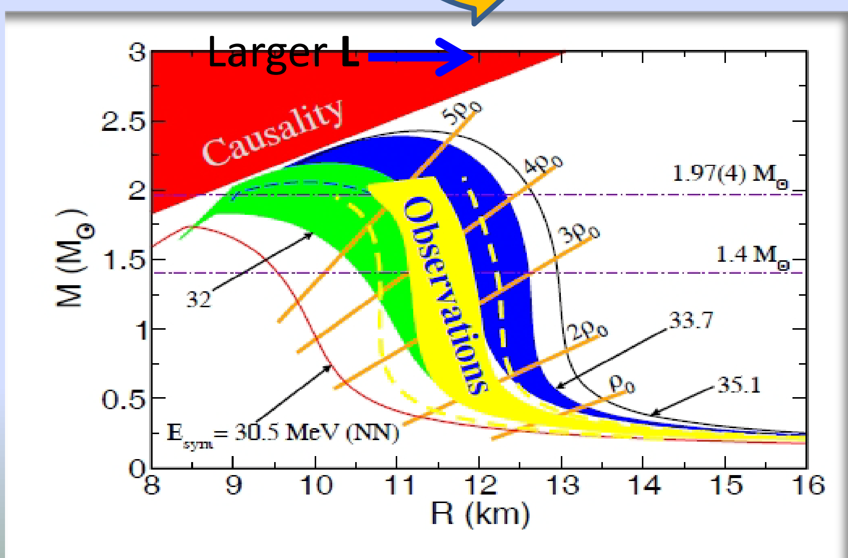

S. Gandolfi et al. EPJA 50:10 (2014)

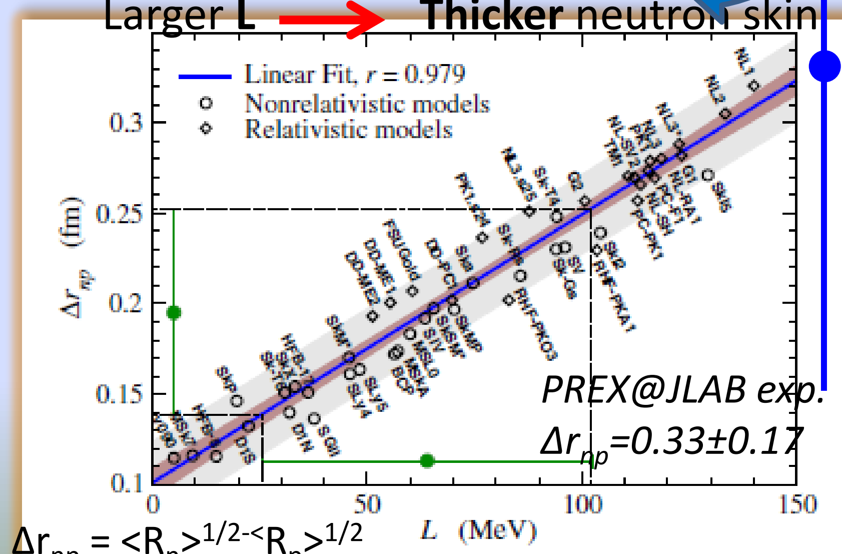

$\Delta r_{np} = \langle R_n \rangle^{1/2} - \langle R_p \rangle^{1/2}$

Roca-Maza et al., PRL 106, 252501 (2011)

Symmetry energy in neutron stars and neutron skin radius

$$S(\rho) = S_0 + \frac{L}{3}\left(\frac{\rho-\rho_0}{\rho_0}\right) + \frac{K_{sym}}{18}\left(\frac{\rho-\rho_0}{\rho_0}\right)^2 + \ldots.$$

$$L = 3\rho_0 \frac{dS(\rho)}{d\rho}$$

Slope

$$P_{SYM} = \rho^2 \left(\frac{dS}{d\rho}\right)_{\rho=\rho_0} = \frac{\rho_0}{3} L$$

Pressure

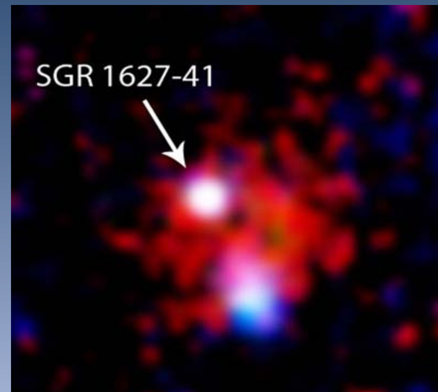

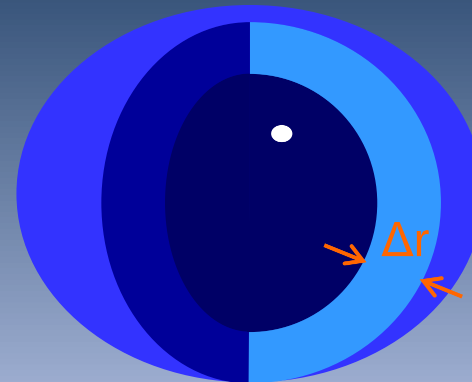

Neutron star $\approx 10^4$ **m**

Neutron skin in ^{208}Pb $\approx 10^{-15}$ **m**

Larger **L** → **Thicker** neutron skin

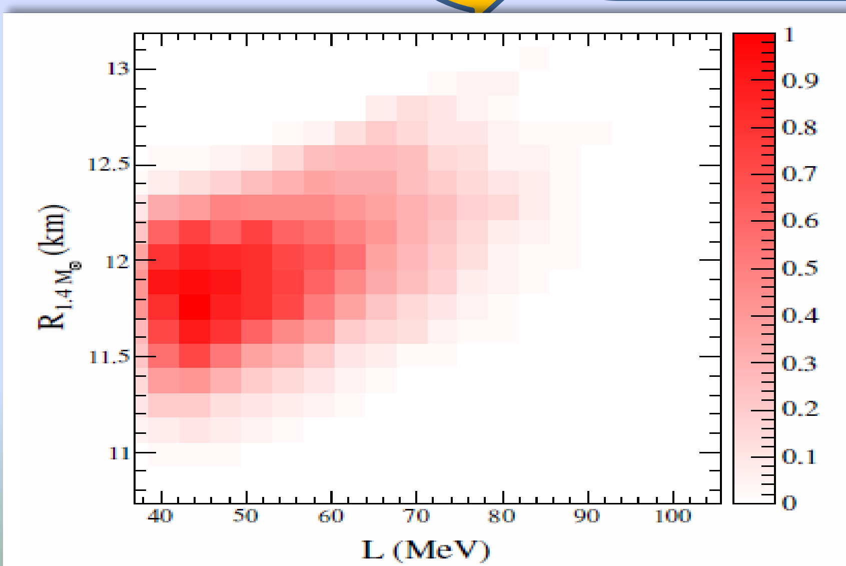

S. Gandolfi et al. EPJA 50:10 (2014)

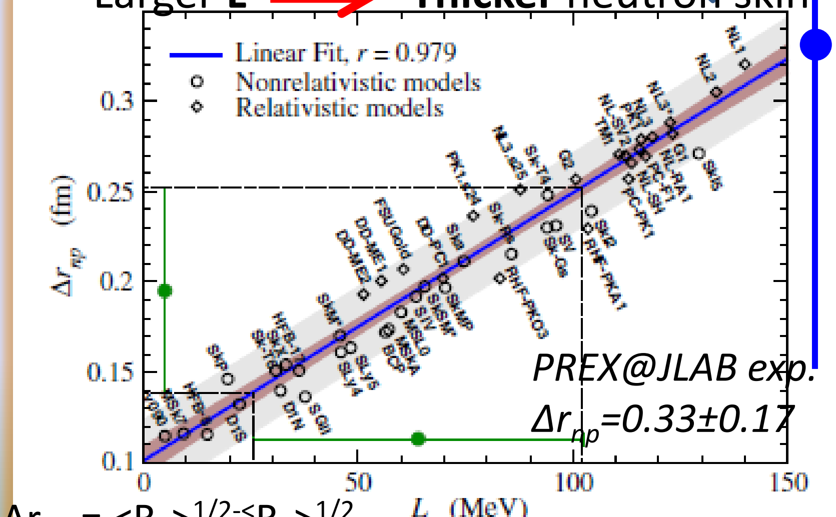

$\Delta r_{np} = \langle R_n\rangle^{1/2} - \langle R_p\rangle^{1/2}$

Roca-Maza et al., PRL 106, 252501 (2011)

Symmetry energy and heavy ion collisions (HIC): Why ?

With heavy ion collisions it is possible to access nuclear matter from low densities ($\rho \le \rho_0$, Fermi energies) to high densities ($\rho = 2\text{-}3\rho_0$)

SMF $^{124}Sn+^{64}Ni$ 35 A.MeV

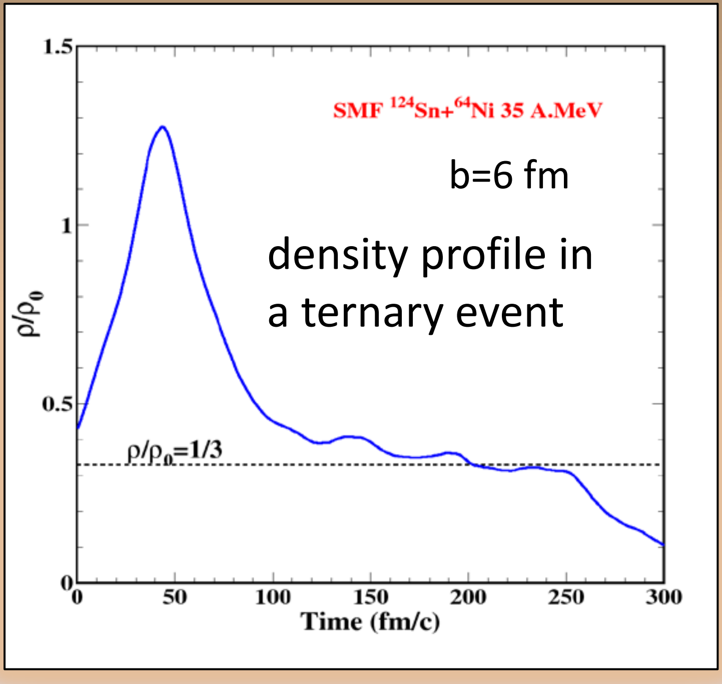

With HIC large density variations (density gradients) in nuclear matter can be obtained in a short timescale.

Symmetry energy and heavy ion collisions (HIC): Why ?

With heavy ion collisions it is possible to access nuclear matter from low densities ($\rho \leq \rho_0$, Fermi energies) to high densities ($\rho = 2\text{-}3\rho_0$)

SMF $^{124}Sn+^{64}Ni$ 35 A.MeV

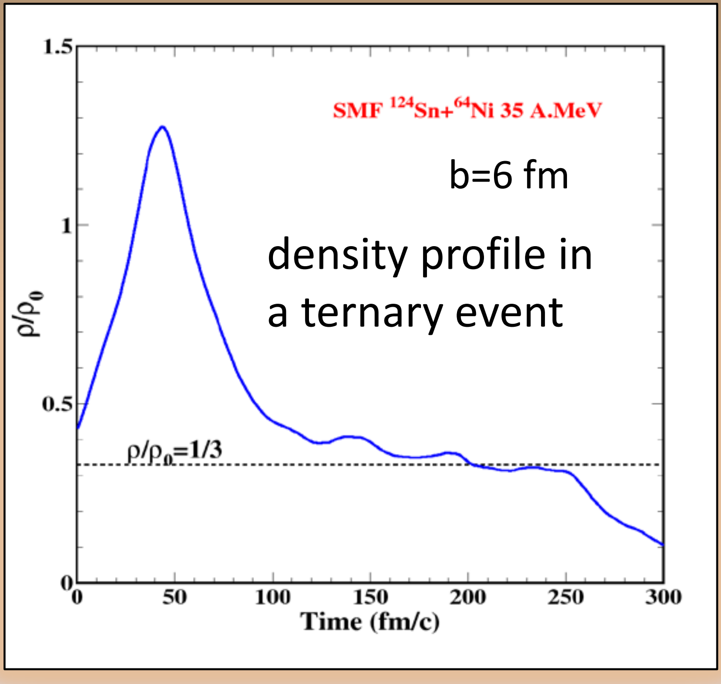

With HIC large density variations (density gradients) in nuclear matter can be obtained in a short timescale.

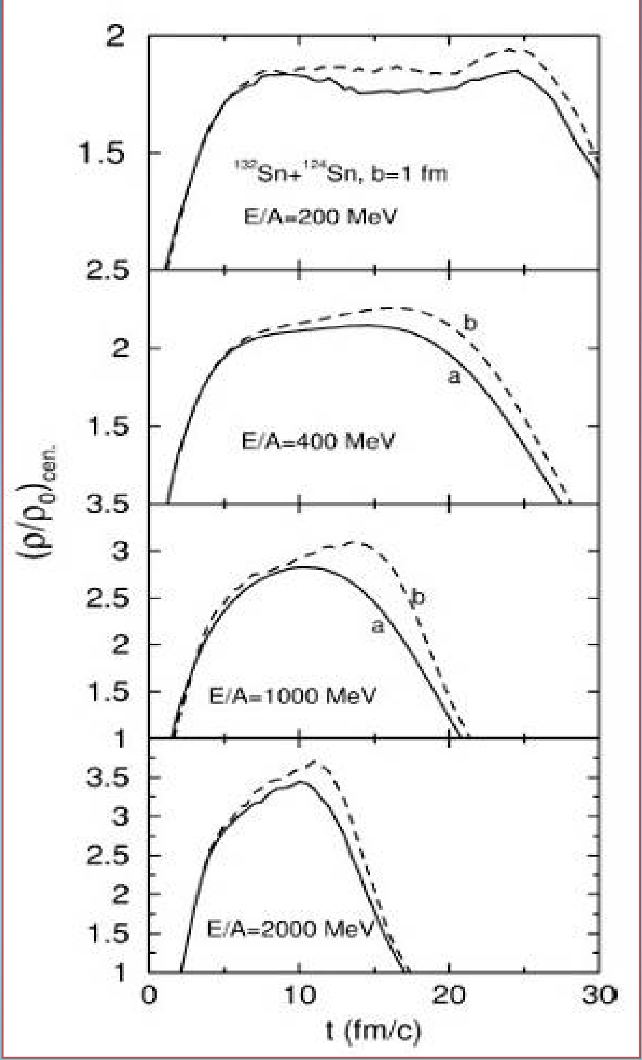

Bao-An Li, NPA 708 365 (2002)

Heavy ion collisions at Fermi energies: different scenarios and mechanisms

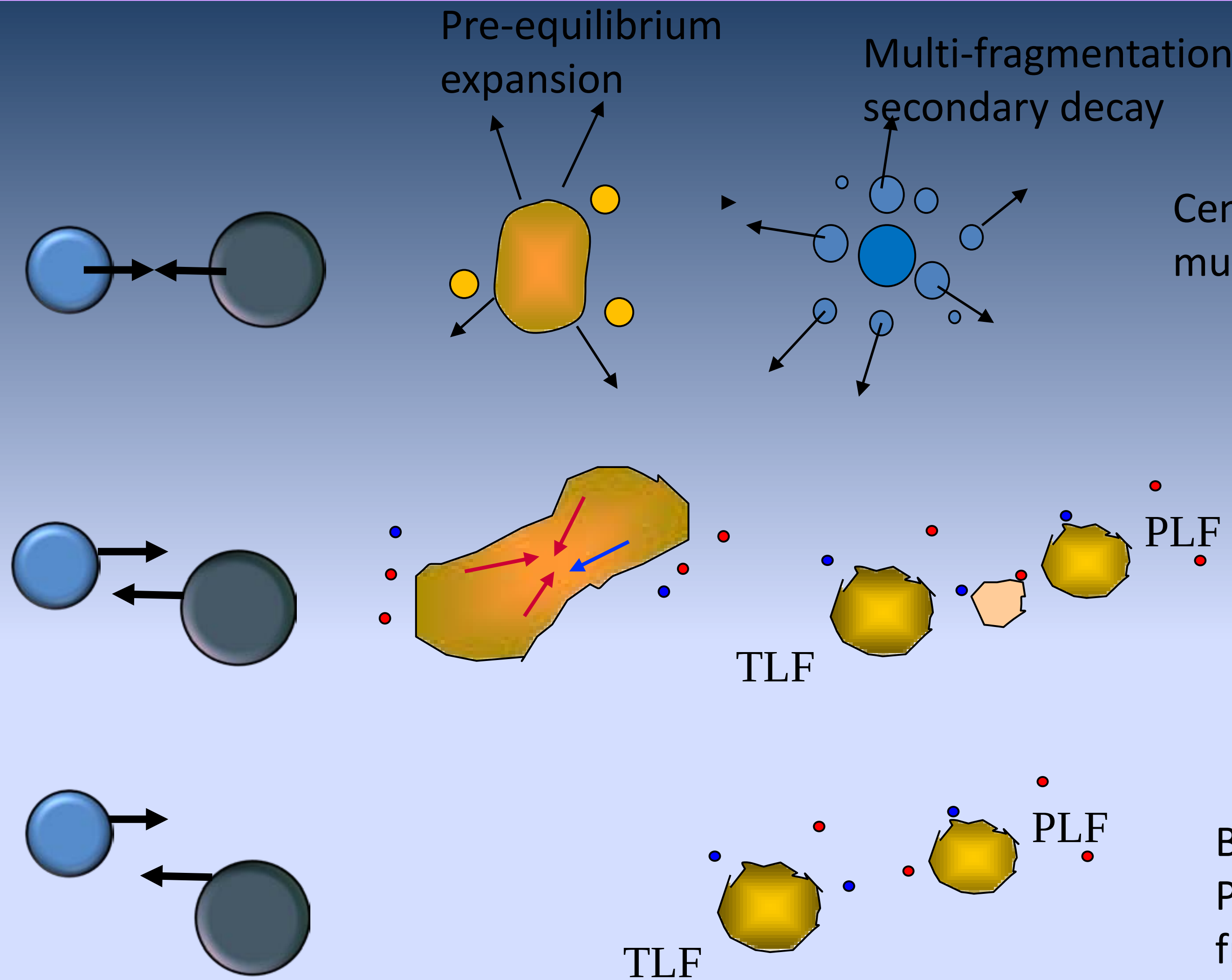

Central collisions: multifragmentation

Semi-peripheral collisions: ternary vs binary events competiton, projectile or target fission

Binary events: Projectile and target fragmentation, break-up

Particle emissions from the early phase of the dynamical evolution (**few fm/c**) up to later stages of statistical decay (**several hundreds of fm/c**) have been measured and are expected to coexist in the reaction products.

Heavy ion collisions at Fermi energies: different scenarios and mechanisms

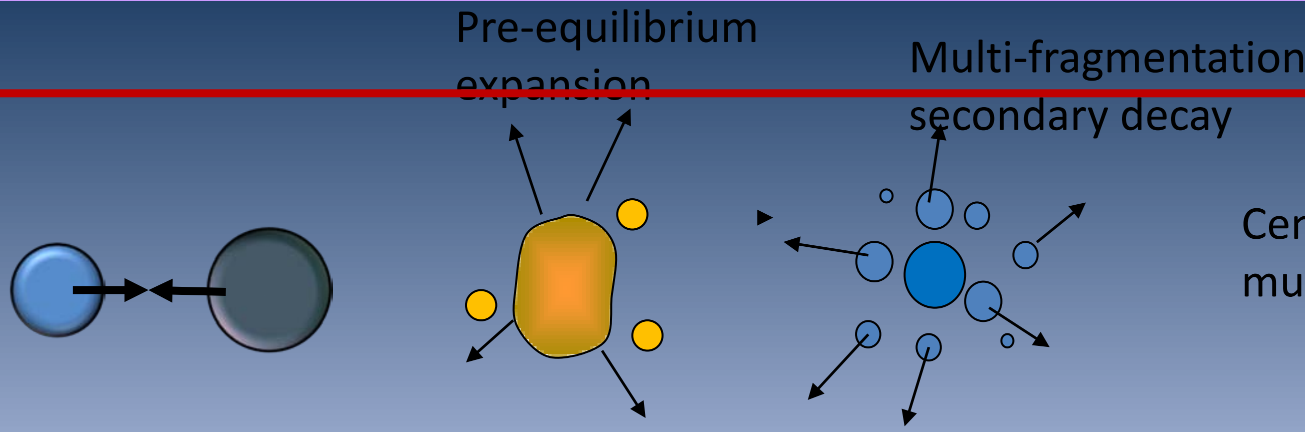

Central collisions:
multifragmentation

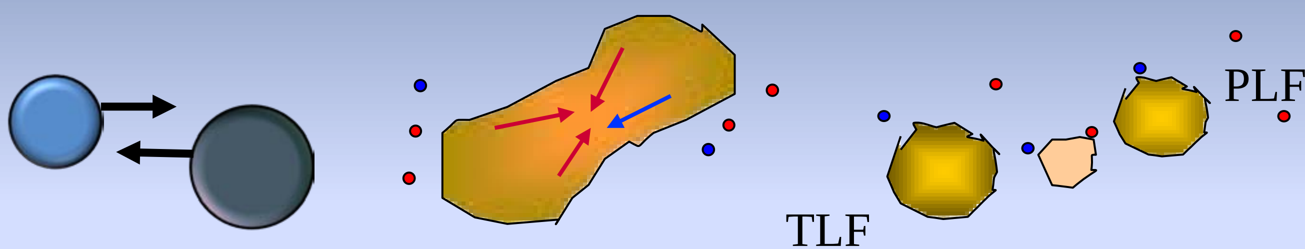

Semi-peripheral collisions: ternary vs binary events competiton, projectile or target fission

Binary events:
Projectile and target fragmentation, break-up

Particle emissions from the early phase of the dynamical evolution (**few fm/c**) up to later stages of statistical decay (**several hundreds of fm/c**) have been measured and are expected to coexist in the reaction products.

Nuclear matter symmetry energy at low density ($\rho/\rho_0 \leq 0.2$)

Temperature and density determination from intermediate velocity source in ^{40}Ar,^{64}Zn + ^{112,124}Sn at 47 A.MeV

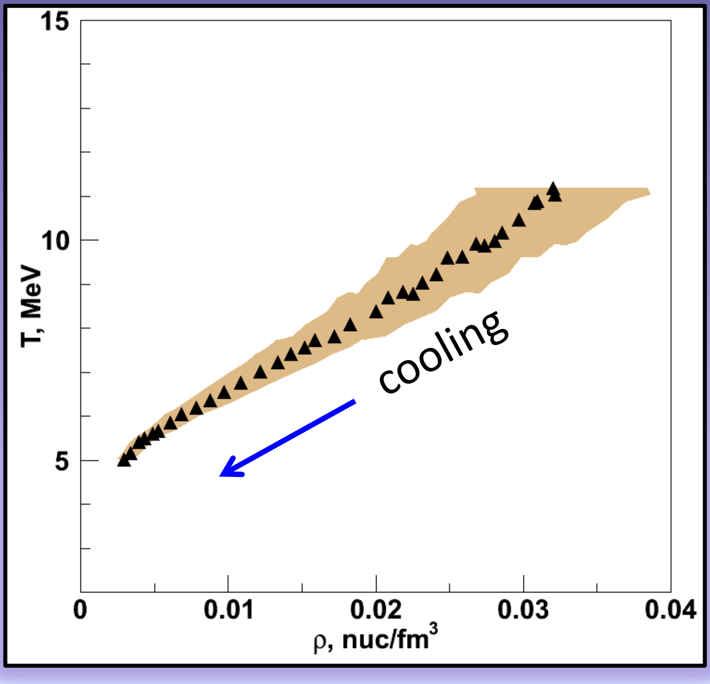

NIMROD@TAMU

Formation of light clusters at very low densities

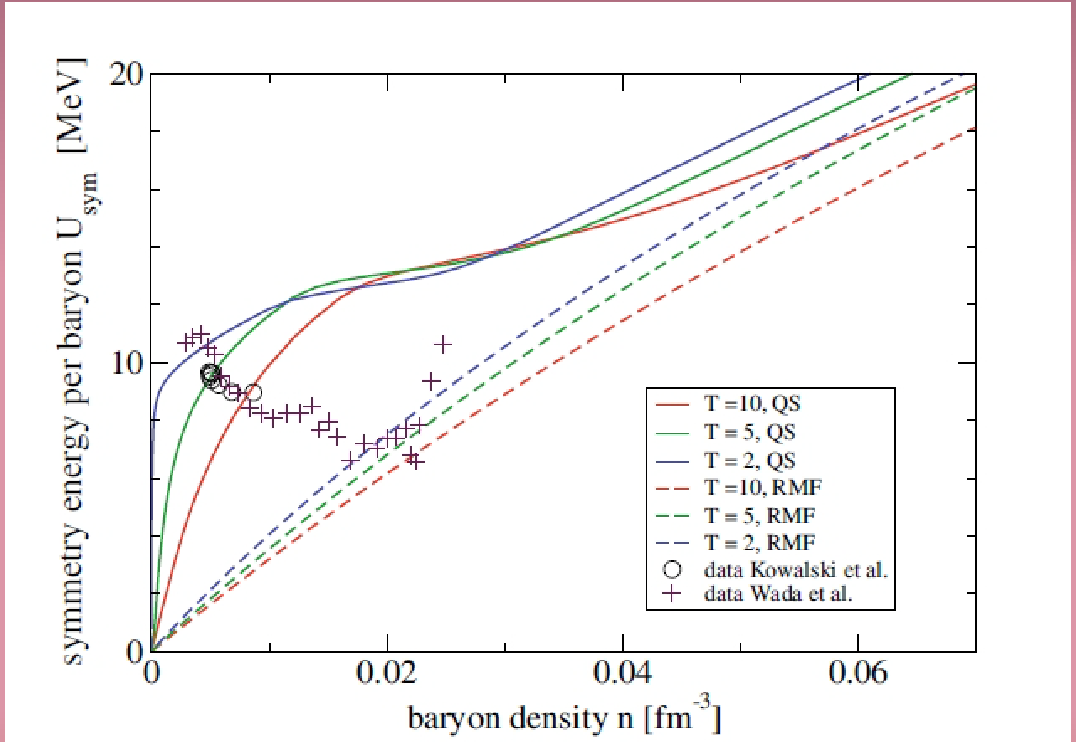

R. Wada et al., PRC85, 064618 (2012)
J.B. Natowitz et al., PRL 104 202501 (2010)
K. Hagel et al., EPJA 50:39 (2014)

QS = Quantum Statistical model including clusterization by Typel, Roepke et al.,
RMF = Relativistic mean field approaches

Nuclear matter symmetry energy at low density ($\rho/\rho_0 \leq 0.2$)

Temperature and density determination from intermediate velocity source in $^{40}Ar, ^{64}Zn + ^{112,124}Sn$ at 47 A.MeV

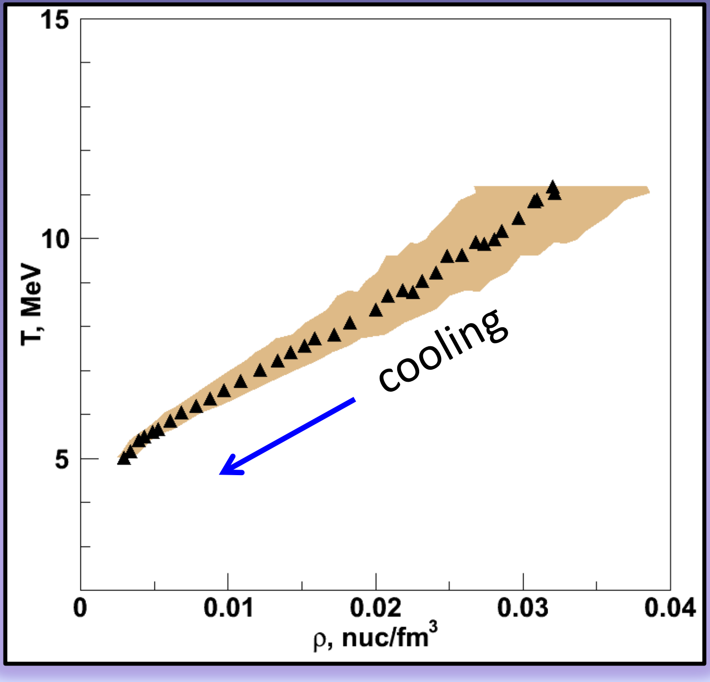

NIMROD@TAMU

Formation of light clusters at very low densities

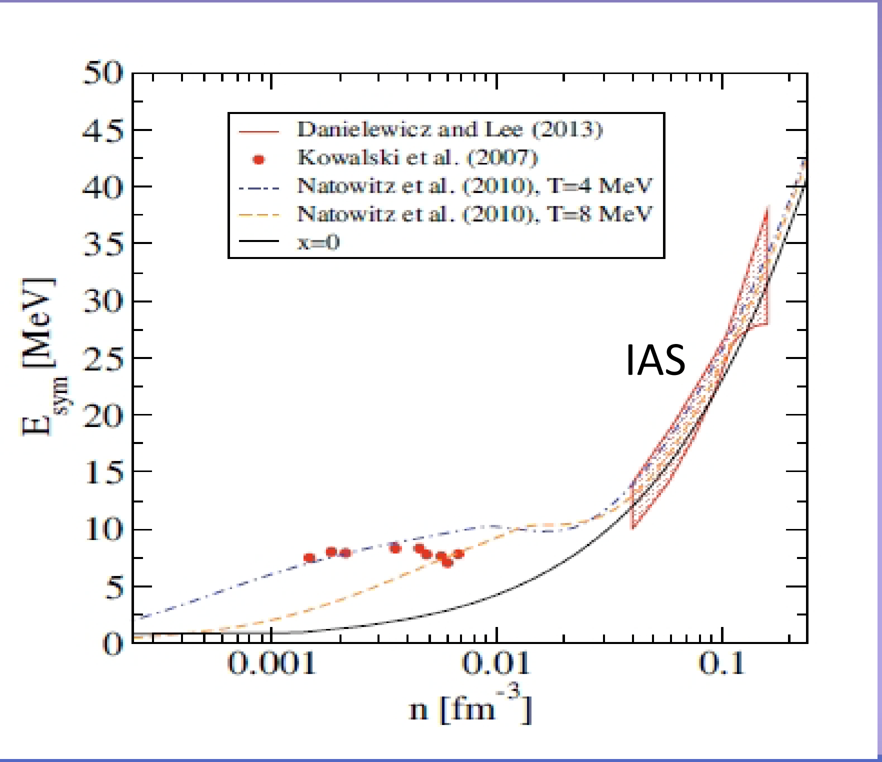

R. Wada et al., PRC85, 064618 (2012)
J.B. Natowitz et al., PRL 104 202501 (2010)
K. Hagel et al., EPJA 50:39 (2014)

QS = Quantum Statistical model including clusterization by Typel, Roepke et al.,
RMF = Relativistic mean field approaches

Pre-equilibrium nucleons: n/p and scalings laws for clusters

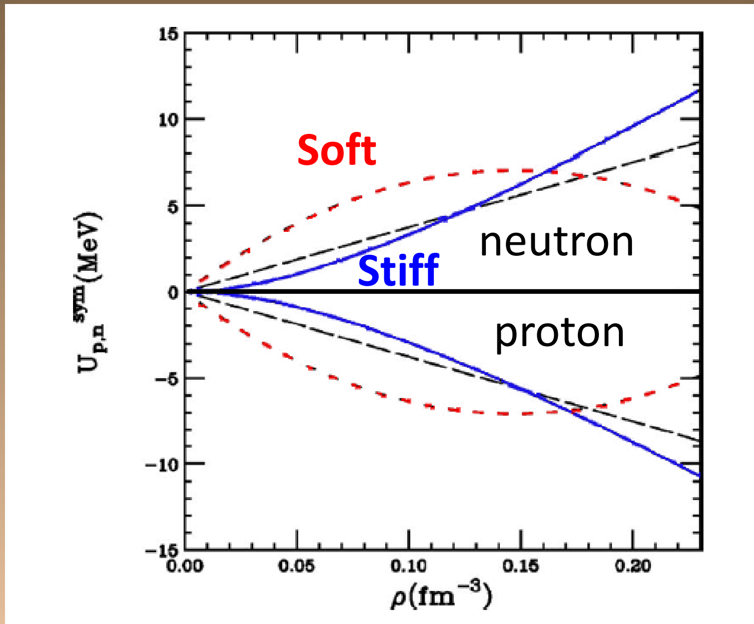

The idea is to look to the ratio of neutron/proton yield in central collisions (energy spectra of transversely emitted nucleons around 90° in the c.m. system.)

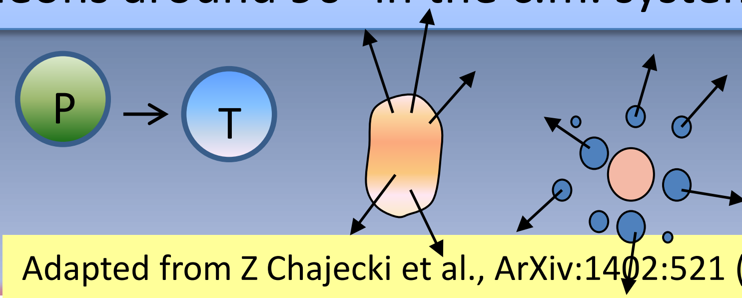

V. Baran et al. Phys. Rep. 410, (2005)
Skyrme-like form for mean-field potential seen by protons and neutrons for ^{124}Sn

Adapted from Z Chajecki et al., ArXiv:1402:521 (2014)

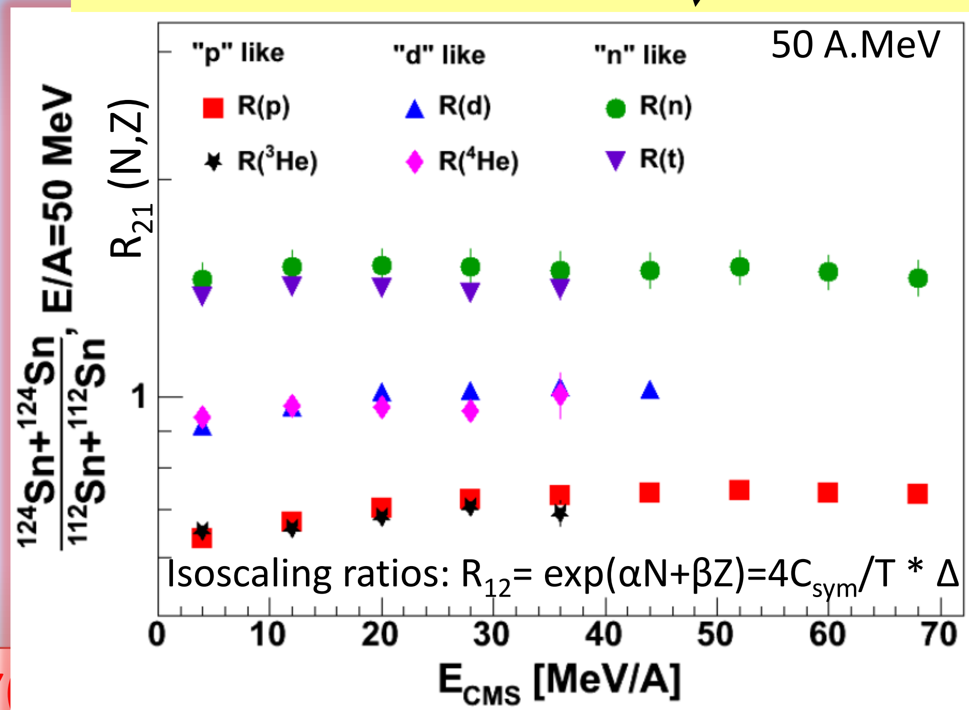

Double Ratio R(n/p) minimizes systematic errors, efficiency problems, etc

$$\frac{\text{Neutron rich} \quad Y(n)/Y(\ldots}{\text{Neutron poor} \quad Y(n)/Y(p)}$$

Pre-equilibrium nucleons: n/p and scalings laws for clusters

Asy-soft more repulsive for neutrons

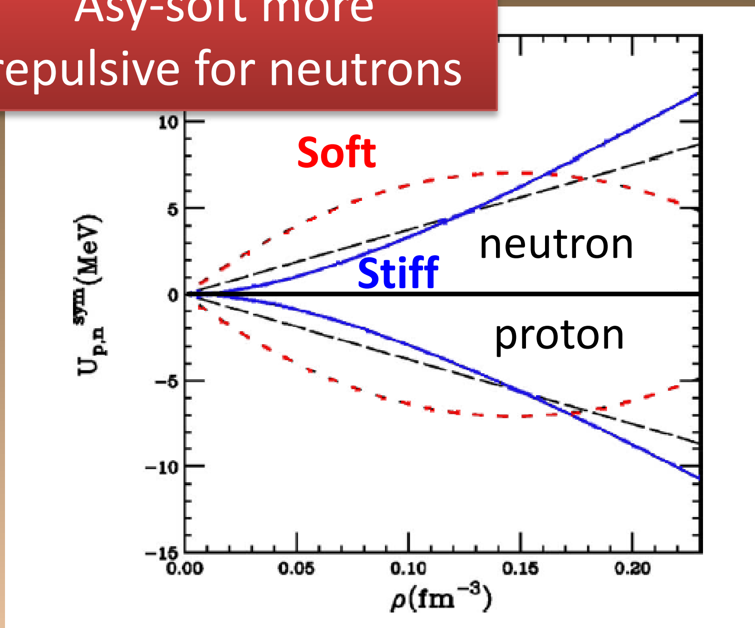

The idea is to look to the ratio of neutron/proton yield in central collisions (energy spectra of transversely emitted nucleons around 90° in the c.m. system.)

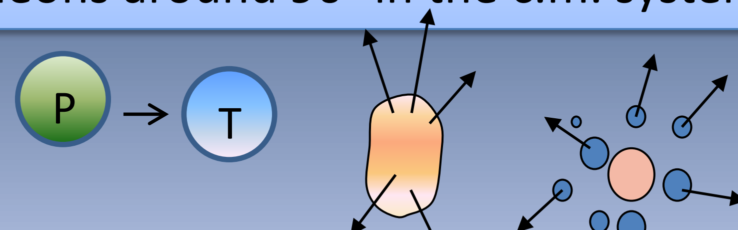

Adapted from Z Chajecki et al., ArXiv:1402:521 (2014)

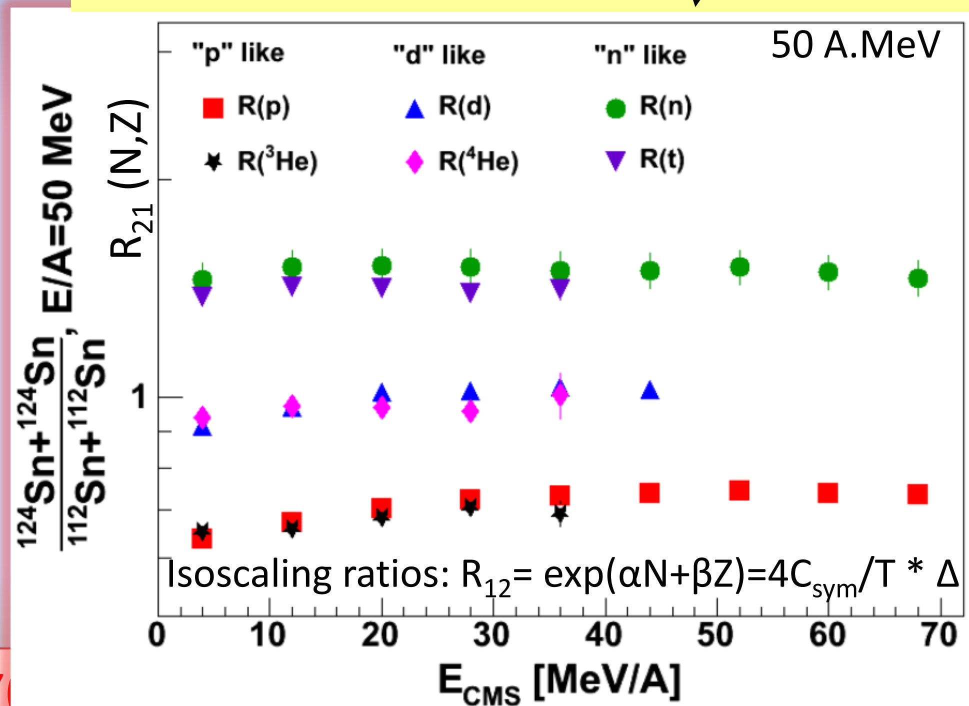

V. Baran et al. Phys. Rep. 410, (2005)
Skyrme-like form for mean-field potential seen by protons and neutrons for ^{124}Sn

Double Ratio R(n/p) minimizes systematic errors, efficiency problems, etc

$$\frac{\text{Neutron rich } Y(n)/Y(p)}{\text{Neutron poor } Y(n)/Y(p)}$$

Pre-equilibrium nucleons: n/p and scalings laws for clusters

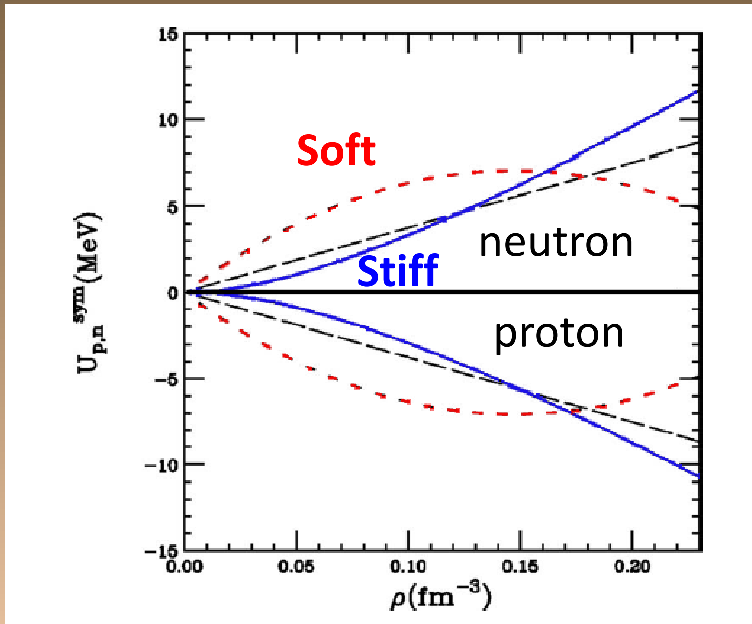

The idea is to look to the ratio of neutron/proton yield in central collisions (energy spectra of transversely emitted nucleons around 90° in the c.m. system.)

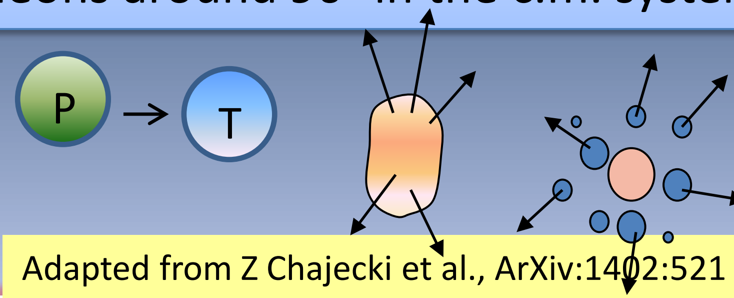

Adapted from Z Chajecki et al., ArXiv:1402:521 (2014)

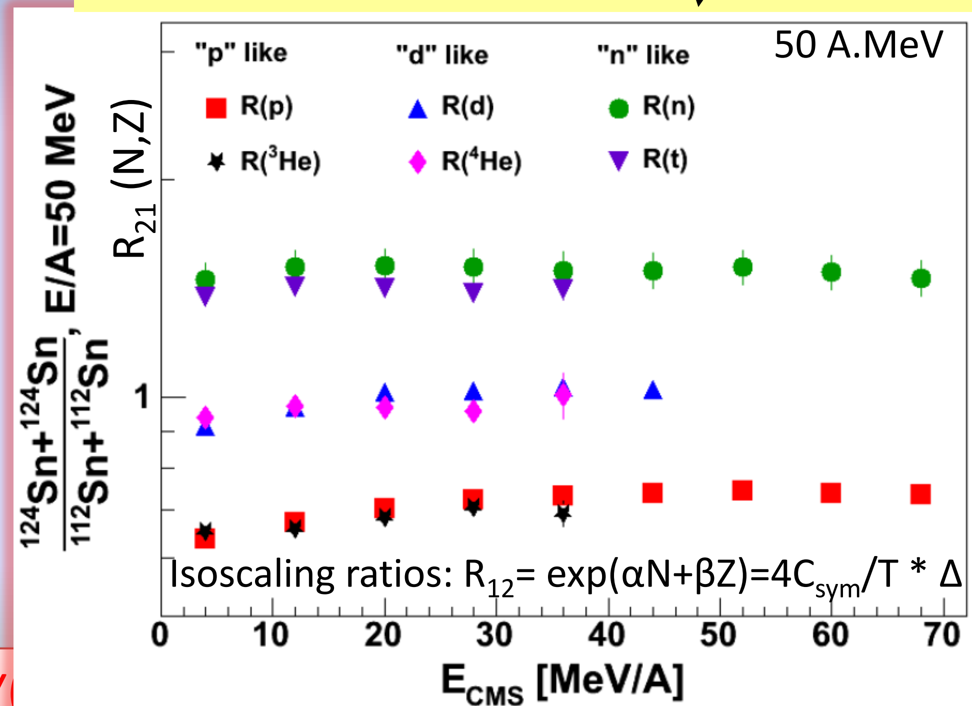

V. Baran et al. Phys. Rep. 410, (2005)
Skyrme-like form for mean-field potential seen by protons and neutrons for ^{124}Sn

Double Ratio R(n/p) minimizes systematic errors, efficiency problems, etc

$$\frac{\text{Neutron rich}\quad Y(n)/Y(}{\text{Neutron poor}\quad Y(n)/Y(p)}$$

Neutron – Protons ratio (pre-equilibrium nucleons)

Nucleons are mostly emitted when system expands and breaks-up at subsaturation densities.

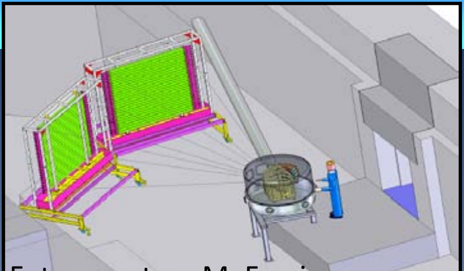
Foto: courtesy M. Famiano

LASSA+MBall + NEUTRON WALL@MSU

$$S(\rho) = 12.3 \cdot (\rho/\rho_0)^{2/3} + 17.6 \cdot (\rho/\rho_0)^{\gamma}$$

M. Famiano et al. data

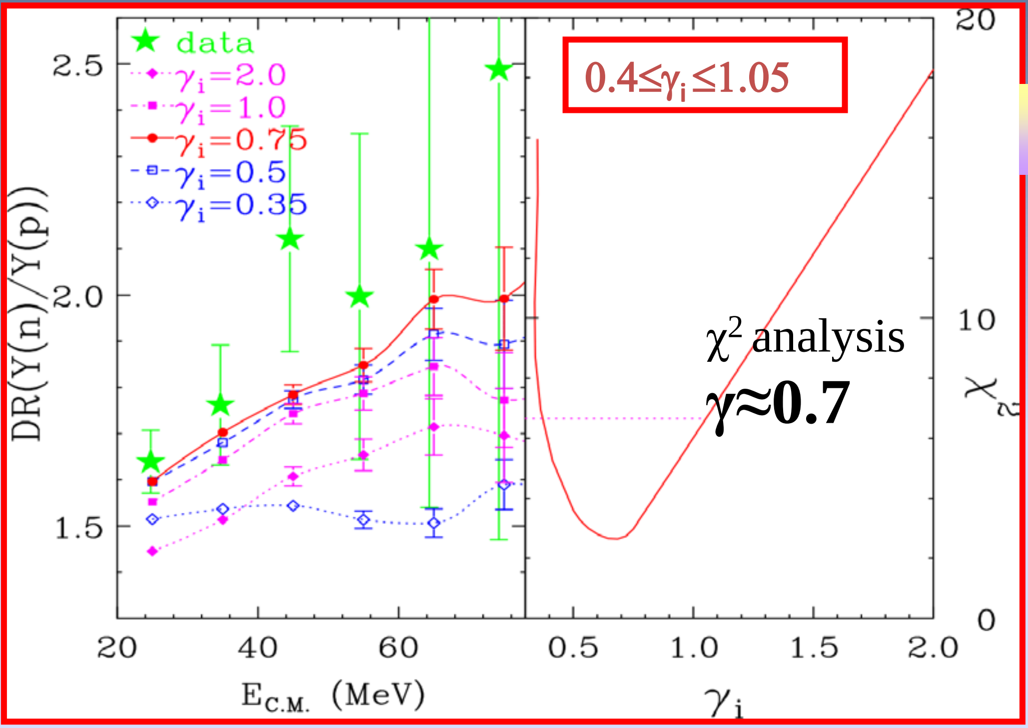

M.B. Tsang et al., PRL 102 122701 (2009)
Y. Zhang et al., PLB 664 145 (2008)

ImQMD model with γ between 0.35 and 2.0 (momentum dependent mean field)

Neutron – Protons ratio (pre-equilibrium nucleons)

Nucleons are mostly emitted when system expands and breaks-up at subsaturation densities.

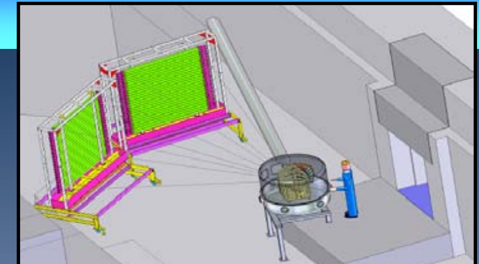

Foto: courtesy M. Famiano

LASSA+MBall + NEUTRON WALL@MSU

M. Famiano et al. data

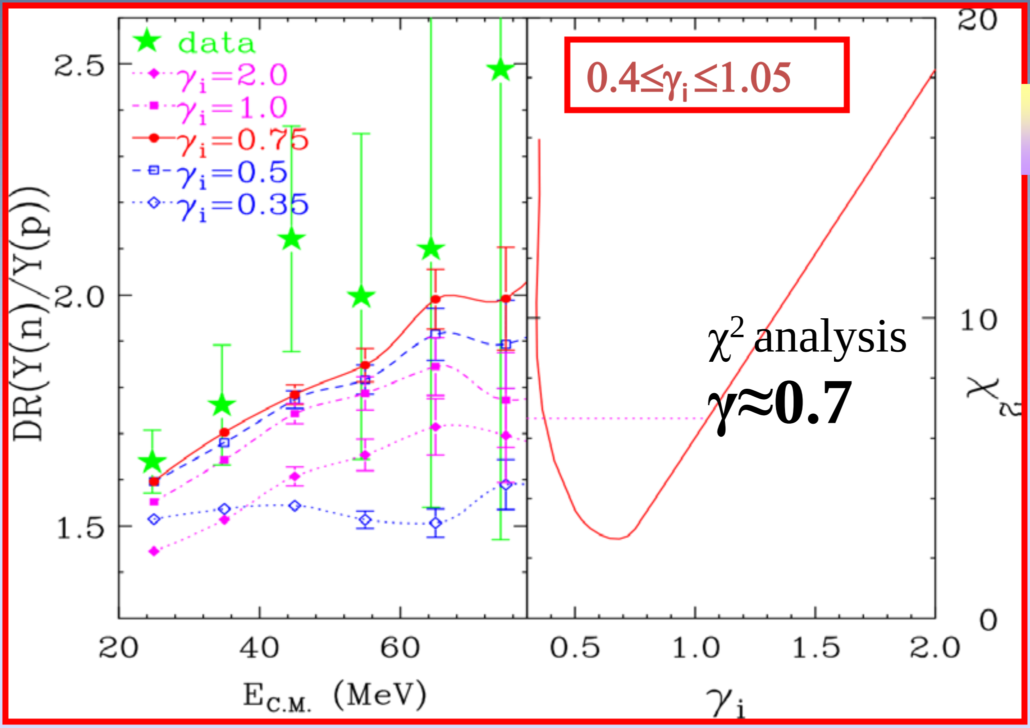

$$S(\rho) = 12.3\cdot(\rho/\rho_0)^{2/3} + 17.6\cdot(\rho/\rho_0)^{\gamma}$$

see J. Rizzo et al., PRC72 064609

Adapted from Zhang et al ArXiv:1402.3790 (2014)

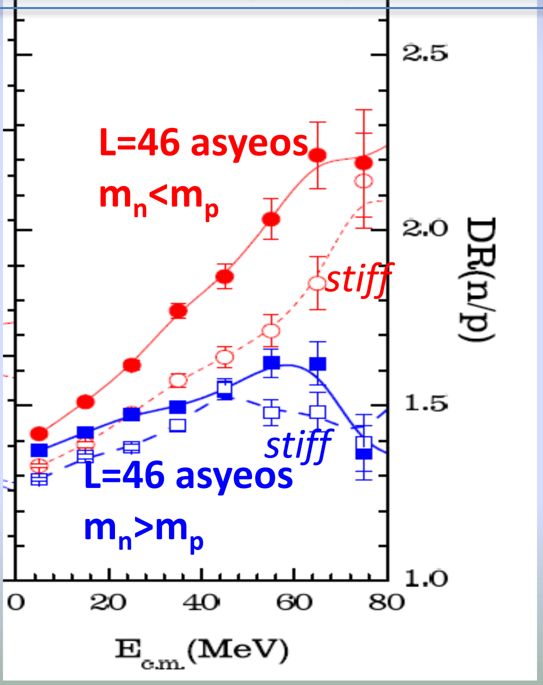

M.B. Tsang et al., PRL 102 122701 (2009)

Y. Zhang et al., PLB 664 145 (2008)

ImQMD model with γ between 0.35 and 2.0 (momentum dependent mean field)

But: **WARNING!!**
The role of effective masses can give effects comparable to that of symmetry energy

Competition of reaction mechanisms

N/Z effects in competition between binary reactions and incomplete fusion. Higher probability for fusion using neutron rich systems

$^{48}Ca+^{48}Ca$ $^{40}Ca+^{48}Ca$
$^{48}Ca+^{40}Ca$ $^{40}Ca+^{40}Ca$
25 A.MeV

CHIMERA @ LNS

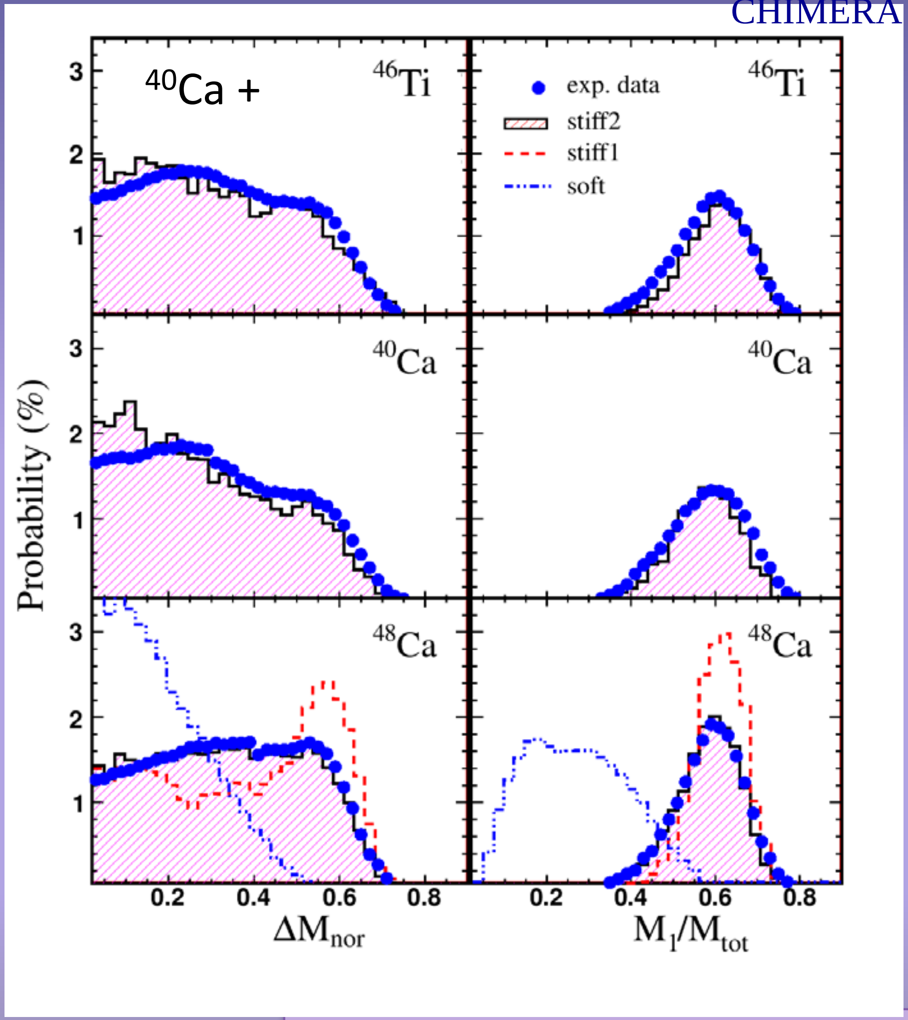

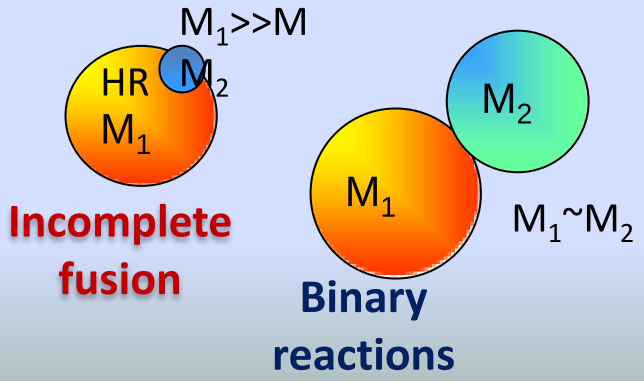

G. Cardella et al., PRC 85 084609 (2012)
F. Amorini et al., PRL102, 112, 701 (2009)

Competition of reaction mechanisms

N/Z effects in competition between binary reactions and incomplete fusion. Higher probability for fusion using neutron rich systems

$^{48}Ca+^{48}Ca$ **$^{40}Ca+^{48}Ca$**
$^{48}Ca+^{40}Ca$ **$^{40}Ca+^{40}Ca$**
25 A.MeV

CHIMERA @ LNS

Comparison with **CoMD** model *(M. Papa et G. Giuliani, EPJA 39, 17 (2009): the good matching with experimental data is obtained by a stiff symmetry energy term* ***(γ=1.1±0.1)***

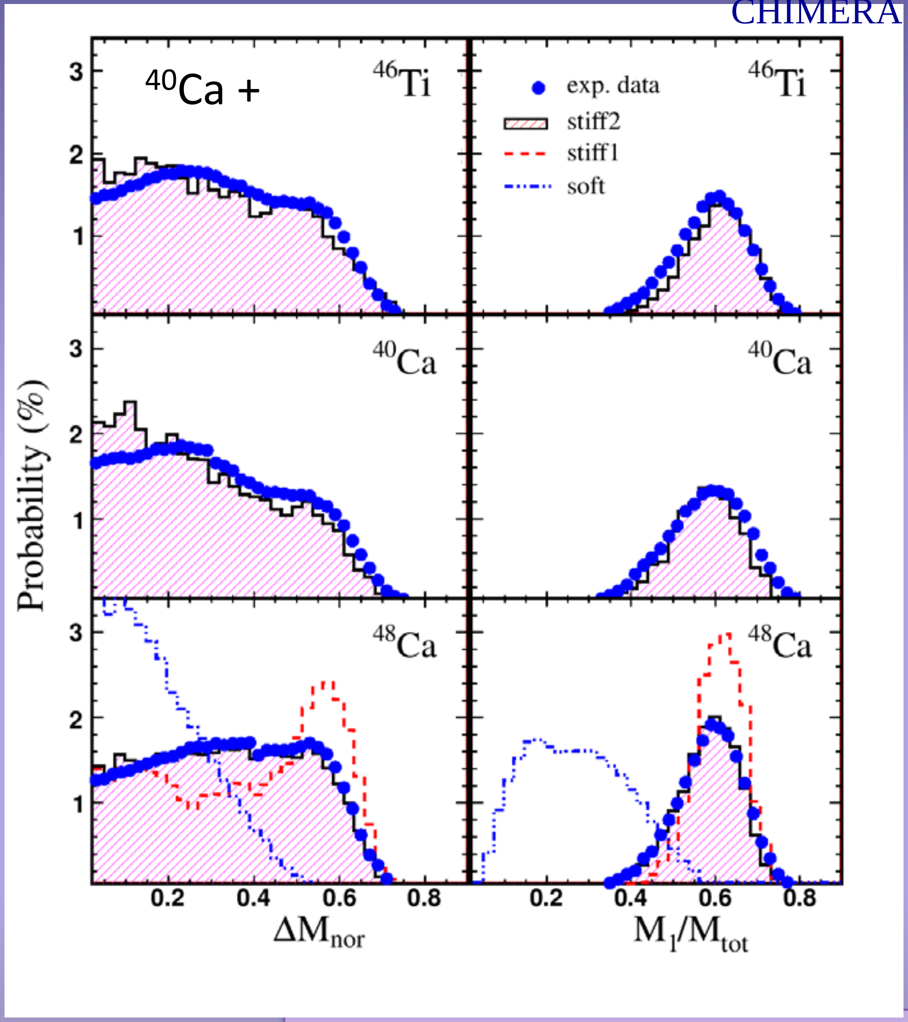

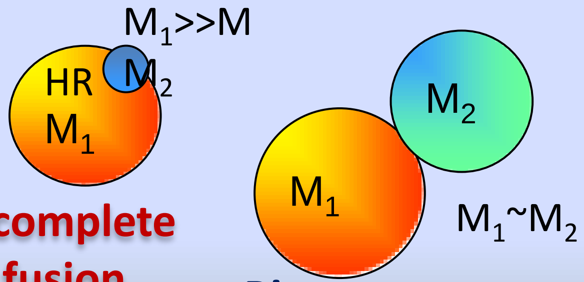

Incomplete fusion

Binary reactions

G. Cardella et al., PRC 85 084609 (2012)
F. Amorini et al., PRL102, 112, 701 (2009)

Heavy ion collisions at Fermi energies: different scenarios and mechanisms

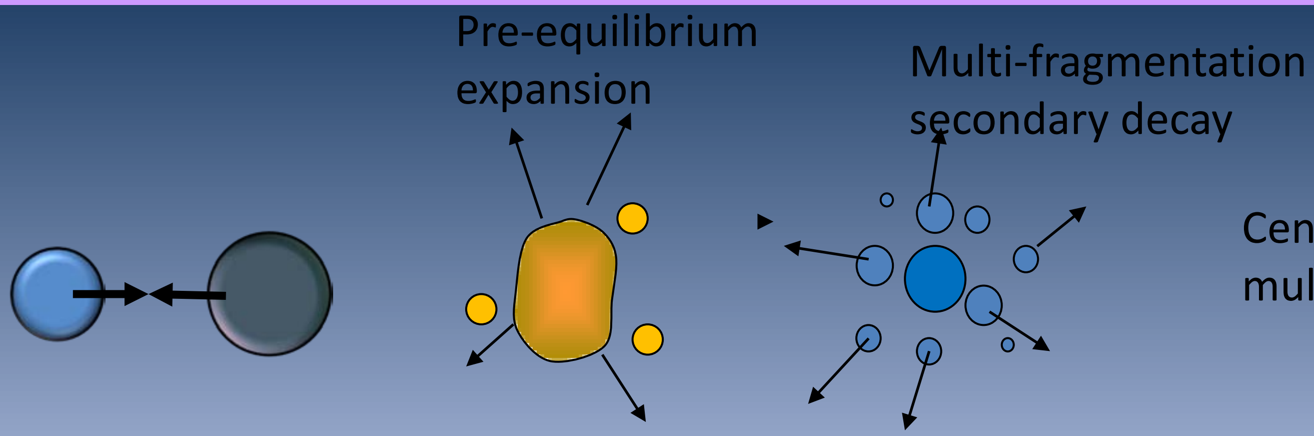

Central collisions:
multifragmentation

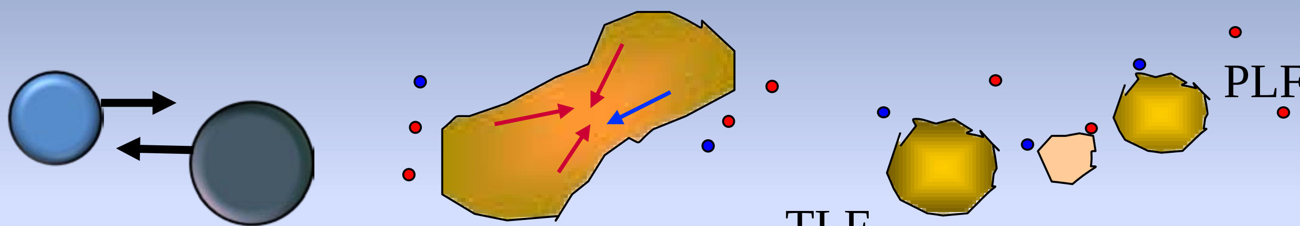

Semi-peripheral collisions: ternary vs binary events competiton, projectile or target fission

Binary events
Projectile and target fragmentation, break-up

Semi-peripheral events are characterized by binary reactons where projectile and target nuclei experience a substantial overlap of matter.

Isospin transport through the "neck"

V. Baran et al., PRC 72 064620 (2005)

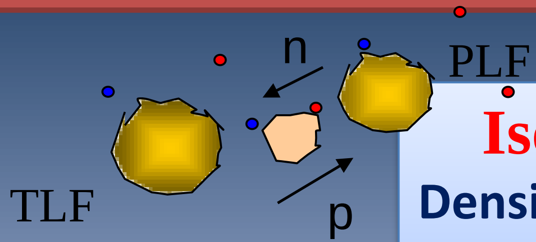

Isospin drift (fast timescale: around 100 fm/c

Density gradient

Depending on slope of the symmetry energy

Migration of neutrons in low density region

$$j_n - j_p \propto E_{sym}(\rho)\nabla I + \frac{\partial E_{sym}(\rho)}{\partial \rho} I \nabla \rho$$

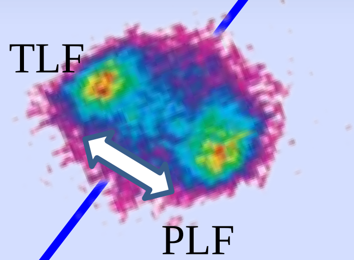

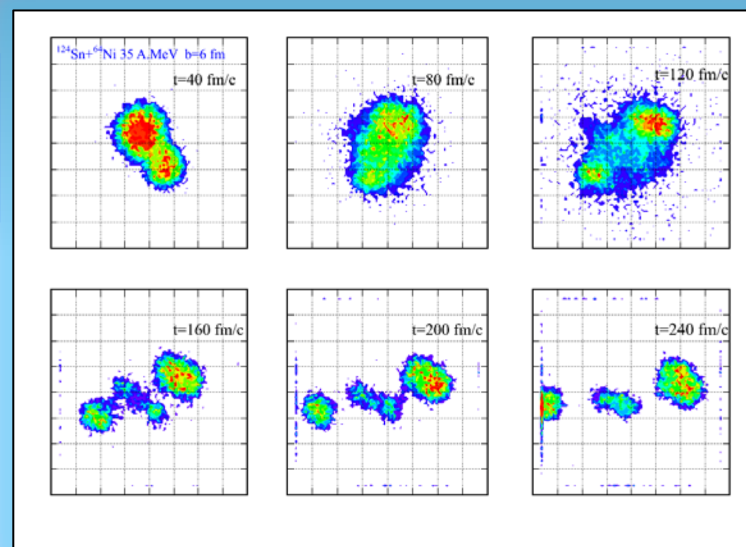

Isospin diffusion

Isospin gradient (N/Z asymmetry in the initial system)

Depending on absolute value of the symmetry energy

Isospin equilibration between projectile and target

Isospin transport through the "neck"

V. Baran et al., PRC 72 064620 (2005)

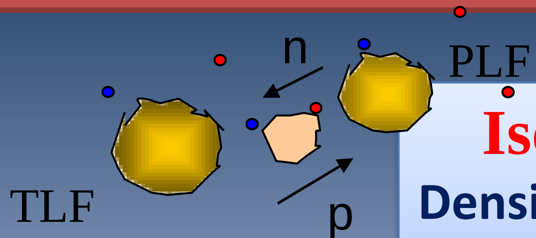

Isospin drift (fast timescale: around 100 fm/c

Density gradient

Depending on slope of the symmetry energy

Migration of neutrons in low density region

$$\boxed{j_n - j_p \propto E_{sym}(\rho)\nabla I + \frac{\partial E_{sym}(\rho)}{\partial \rho} I \nabla \rho}$$

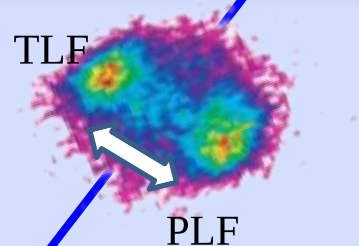

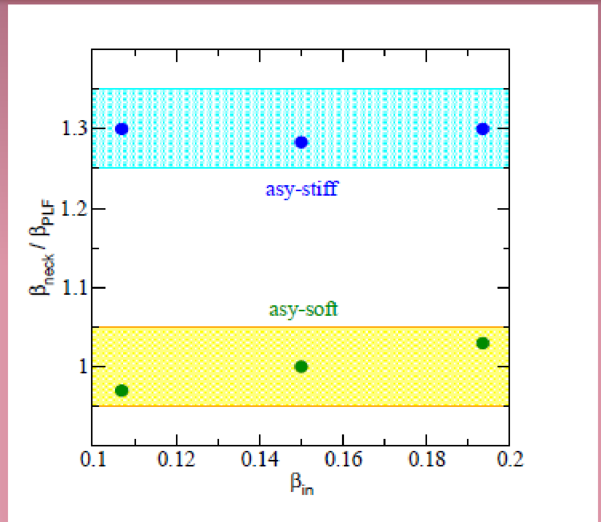

M. Colonna et al., J. Phys. CS, 413, 012018 (2013)

Isospin diffusion

Isospin gradient (N/Z asymmetry in the initial system)

Depending on absolute value of the symmetry energy

Isospin equilibration between projectile and target

Isospin diffusion → diffusion of neutrons and protons across the neck

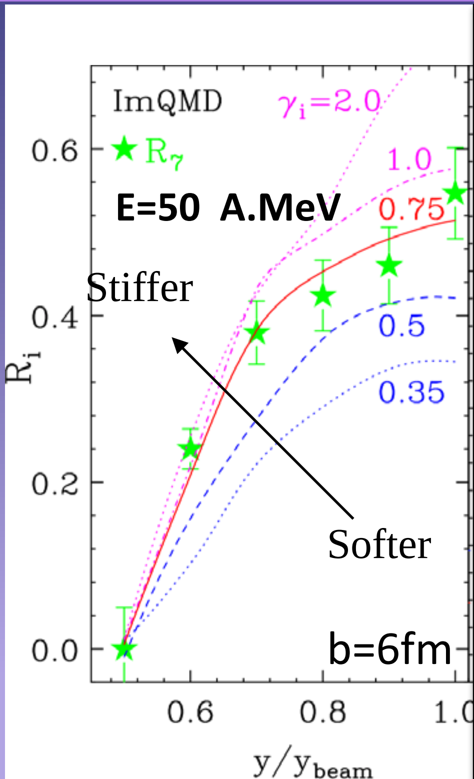

Comparison with **ImQMD** model (Best fit obtained with γ=0.75 at b=6 fm.

Results of χ^2 analysis on compared isospin diffusion and n/p ratios data:

$0.45 \leq \gamma \leq 1$
$50 \leq L \leq 85$ MeV

^{124}Sn + ^{112}Sn (AB) mixed → diffusion
^{112}Sn + ^{124}Sn (BA) mixed → diffusion 50 A.MeV

$$R_i(x_{AB}) = 2 \cdot \frac{x_{AB} - (x_{AA} + x_{BB})/2}{x_{AA} - x_{BB}}$$

$R_i = \pm 1$ no diffusion; $R_i = 0$ equilibration

X is an "isospin" observable and is rescaled according to R_i (transport ratio)

$R_7 = f(Y(^7Li)/Y(^7Be)$

Isospin equilibration depends from **S (ρ)** value at subsaturation density and is favoured by a **SOFT term of ASY-EOS. Less mixing with a STIFF asy-EOS.**

Lassa@MSU

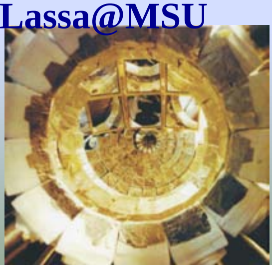

Isospin diffusion → diffusion of neutrons and protons across the neck

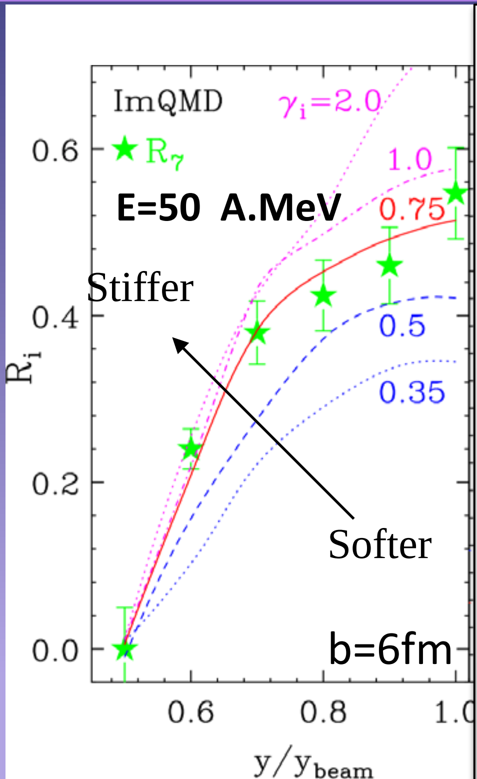

Comparison with **ImQMD** model (Best fit obtained with γ=0.75 at b=6 fm.

Results of χ^2 analysis on compared isospin diffusion and n/p ratios data:

$0.45 \leq \gamma \leq 1$
$50 \leq L \leq 85$ MeV

^{124}Sn + ^{112}Sn (AB) mixed → diffusion
^{112}Sn + ^{124}Sn (BA) mixed → diffusion 50 A.MeV

$E_{sym} = E_{sym}^{kin} + E_{sym}^{pot}$

$= 12\text{MeV}\cdot(\rho/\rho_0)^{2/3} + 22\text{MeV}\cdot(\rho/\rho_0)^{\gamma}$

$R_i = \pm 1$ no diffusion; $R_i = 0$ equilibration

X is an "isospin" observable and is rescaled according to R_i (transport ratio)

$R_7 = f(Y(^7Li)/Y(^7Be))$

Isospin equilibration depends from **S (ρ)** value at subsaturation density and is favoured by a **SOFT term of ASY-EOS. Less mixing with a STIFF asy-EOS.**

Lassa@MSU

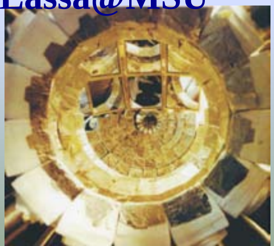

Isospin diffusion → diffusion of neutrons and protons across the neck

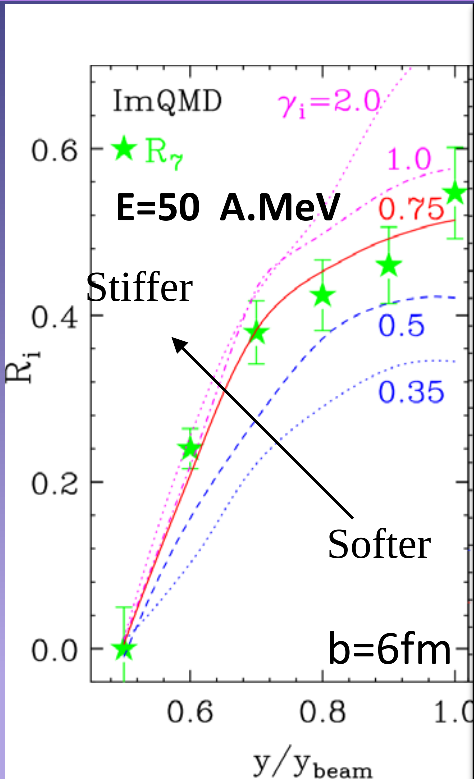

Comparison with **ImQMD** model (Best fit obtained with γ=0.75 at b=6 fm.

Results of χ^2 analysis on compared isospin diffusion and n/p ratios data:

$0.45 \leq \gamma \leq 1$

$50 \leq L \leq 85$ MeV

^{124}Sn + ^{112}Sn (AB) mixed → diffusion

^{112}Sn + ^{124}Sn (BA) mixed → diffusion 50 A.MeV

$$E_{sym} = E_{sym}^{kin} + E_{sym}^{pot}$$

$$= 12\text{MeV}\cdot(\rho/\rho_0)^{2/3} + 22\text{MeV}\cdot(\rho/\rho_0)^{\gamma}$$

$R_i = \pm 1$ no diffusion; $R_i = 0$ equilibration

X is an "isospin" observable and is rescaled according to R_i (transport ratio)

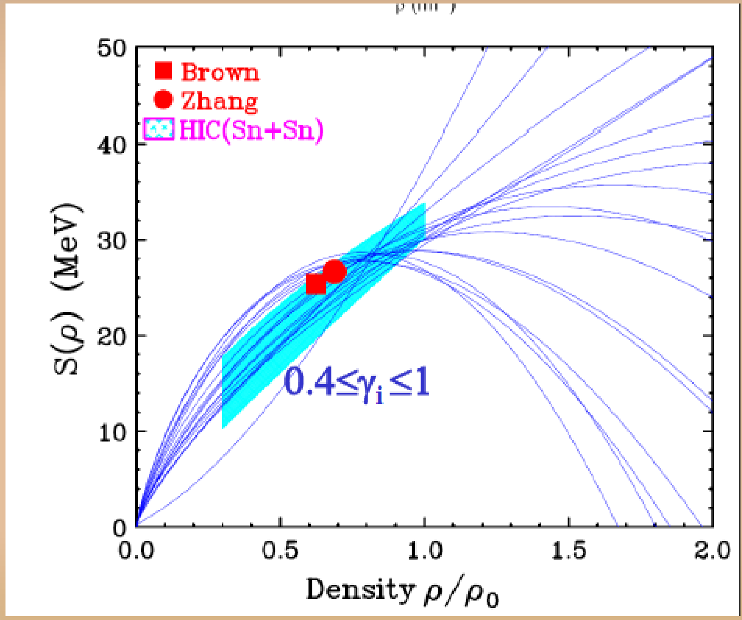

$R_7 = f(Y(^7Li)/Y(^7Be)$

Isospin equilibration depends from **S (ρ)** value at subsaturation density and is favoured by a **SOFT term of ASY-EOS. Less mixing with a STIFF asy-EOS.**

Lassa@MSU

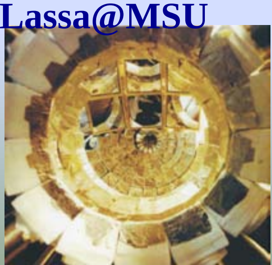

Isospin diffusion → diffusion of neutrons and protons across the neck

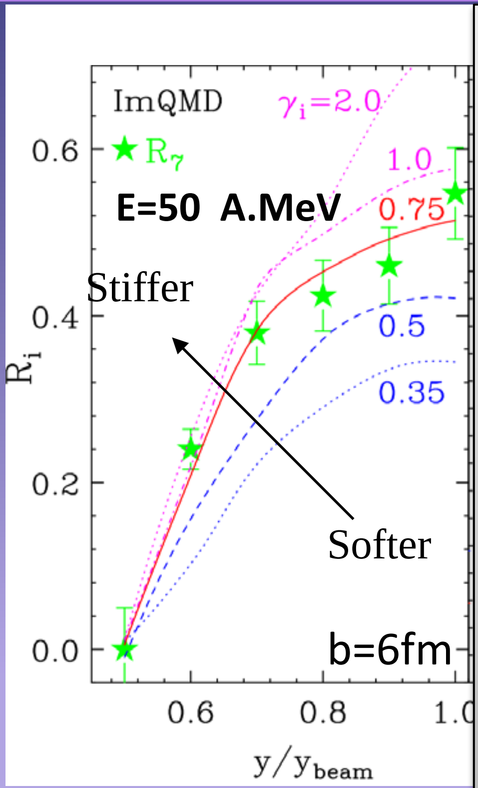

Comparison with **ImQMD** model (Best fit obtained with γ=0.75 at b=6 fm.

Results of χ^2 analysis on compared isospin diffusion and n/p ratios data:

$0.45 \leq \gamma \leq 1$

$50 \leq L \leq 85$ MeV

^{124}Sn + ^{112}Sn (AB) mixed → diffusion

^{112}Sn + ^{124}Sn (BA) mixed → diffusion 50 A.MeV

$E_{sym} = E_{sym}^{kin} + E_{sym}^{pot}$

$= 12\text{MeV}\cdot(\rho/\rho_0)^{2/3} + 22\text{MeV}\cdot(\rho/\rho_0)^{\gamma}$

$R_i = \pm 1$ no diffusion; $R_i = 0$ equilibration

X is an "isospin" observable and is rescaled according to R_i (transport ratio)

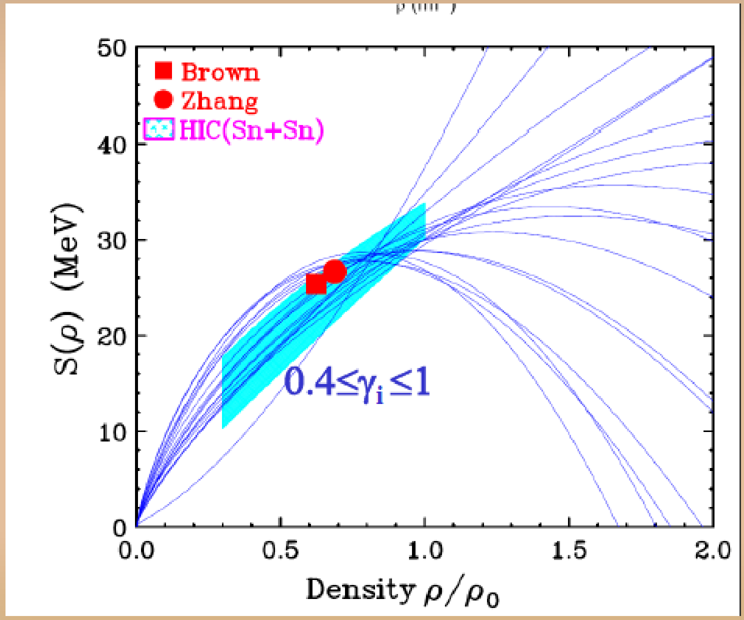

$R_7 = f(Y(^7Li)/Y(^7Be))$

Isospin equilibration depends from **S (ρ)** value at subsaturation density and is favoured by a **SOFT term of ASY-EOS. Less mixing with a STIFF asy-EOS.**

Lassa@MSU

Improvement with RIBS

Isospin diffusion: Sn+Sn@35 A.MeV


CHIMERA@LNS

Z.Y. Sun et al, CHIMERA-MSU collaboration PRC82, 051603 (2011)

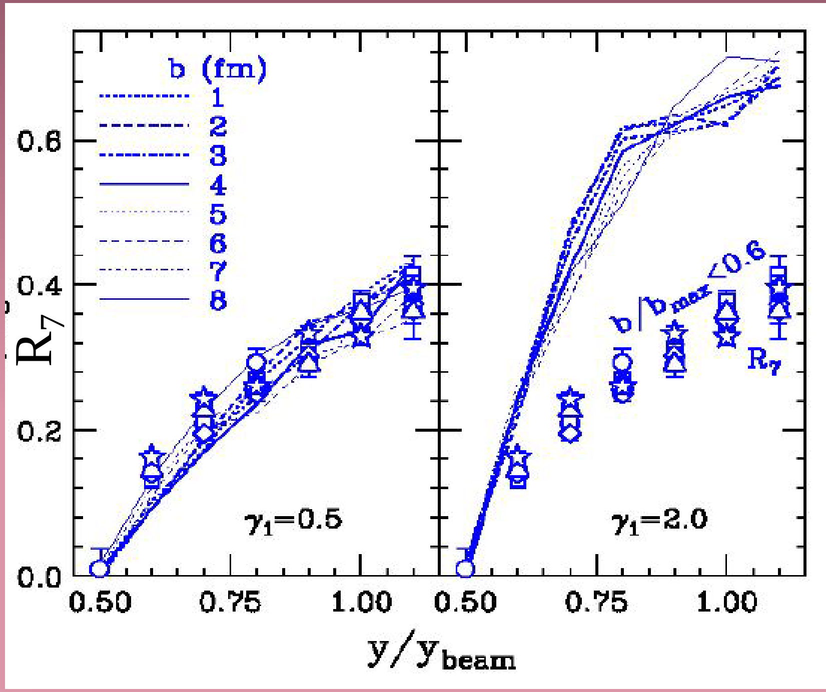

Isospin diffusion: Sn+Sn@35 A.MeV

CHIMERA@LNS

Z.Y. Sun et al, CHIMERA-MSU collaboration PRC82, 051603 (2011)

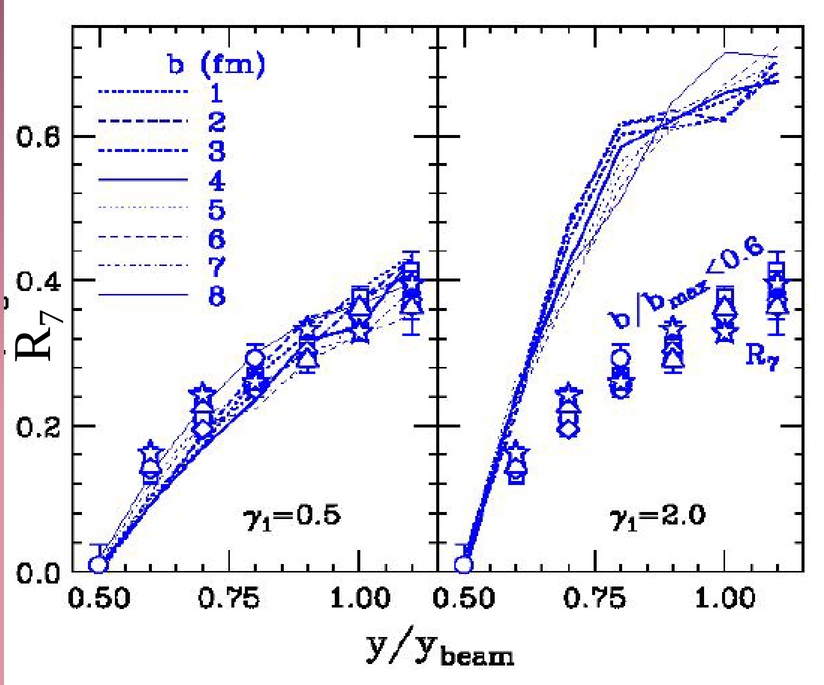

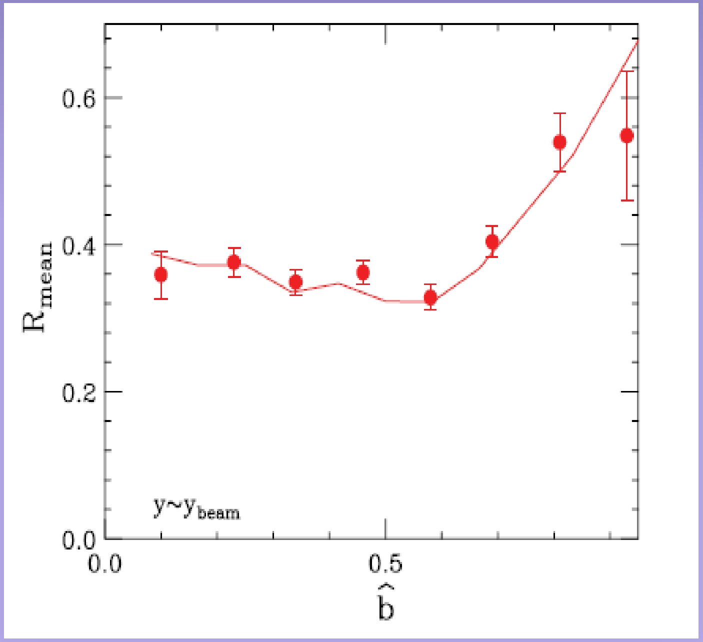

Isospin transport by looking at the quasi-projectile

Indra@GANIL

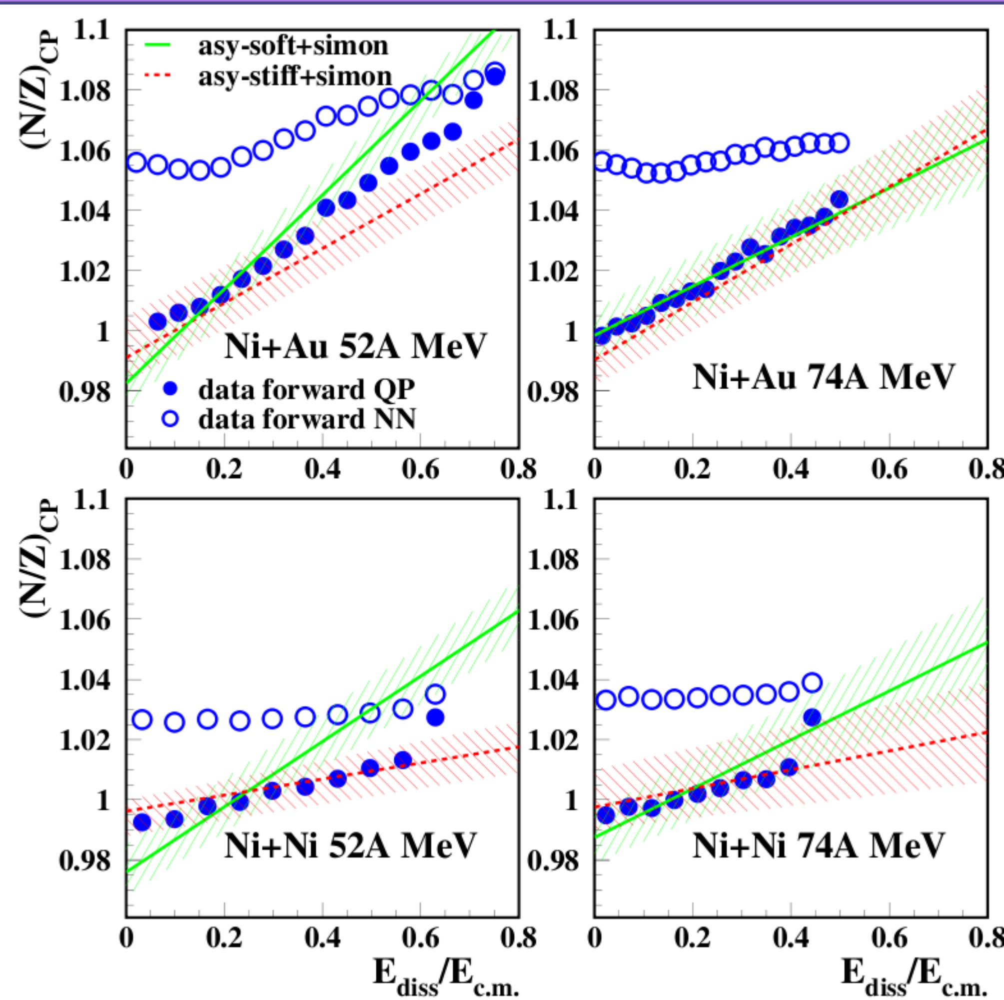

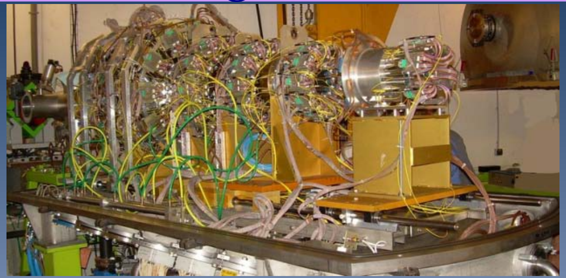

Isospin equilibration is reached for more dissipative collisions. Here X (isospin variable in R^t) = **triton multiplicity**

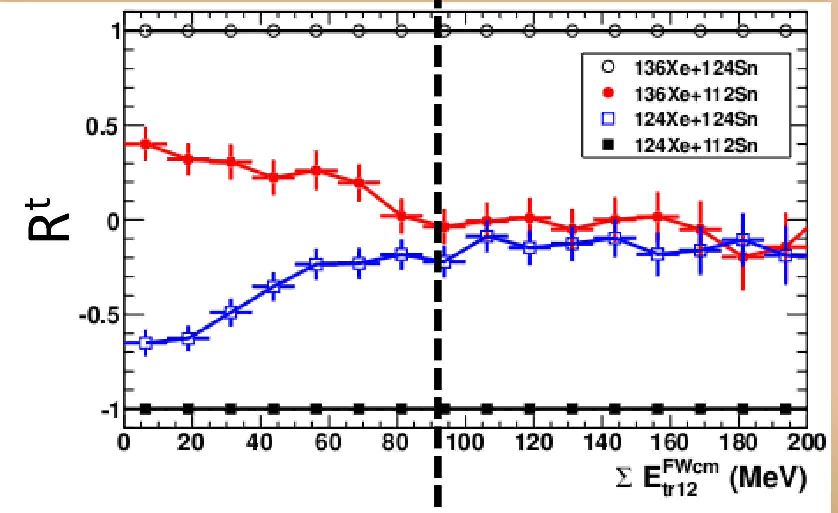

Data compared to Stochastic Mean Field (SMF)
Asy-stiff parametrization better reproduce data

see E. Galichet et al., PRC79 064615 (2009)
G. Ademard et al., EPJA 50:33 (2014)

Disentangling dynamical vs. statistical emission in ternary events

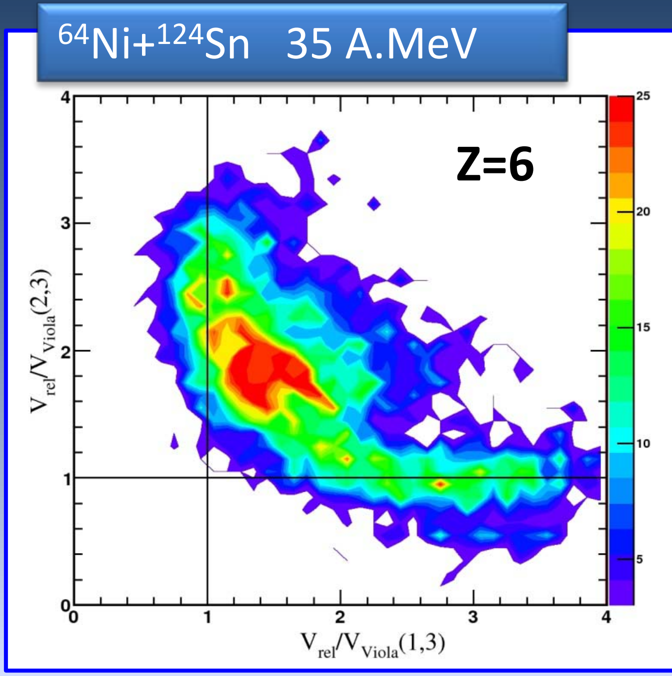

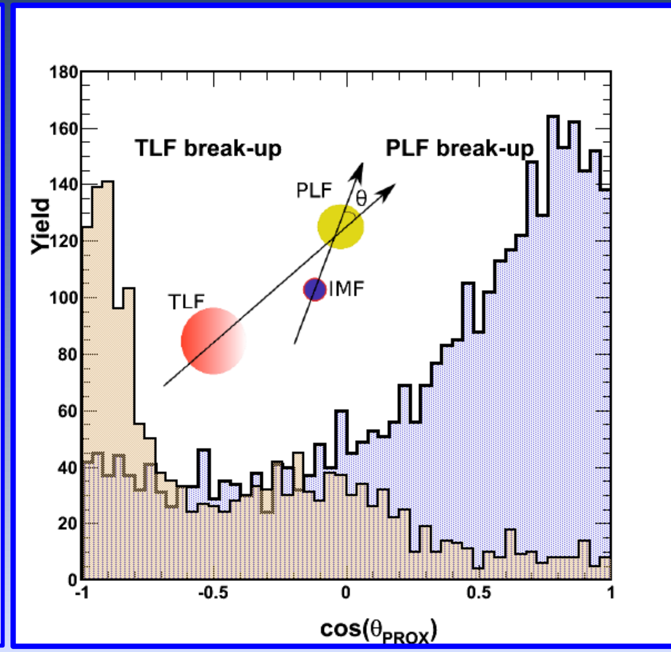

cos(θ)≈±1
aligned emission of the lighter fragment in the backward emisphere of **PLF** (+1) and **TLF** (-1) towards midrapidity

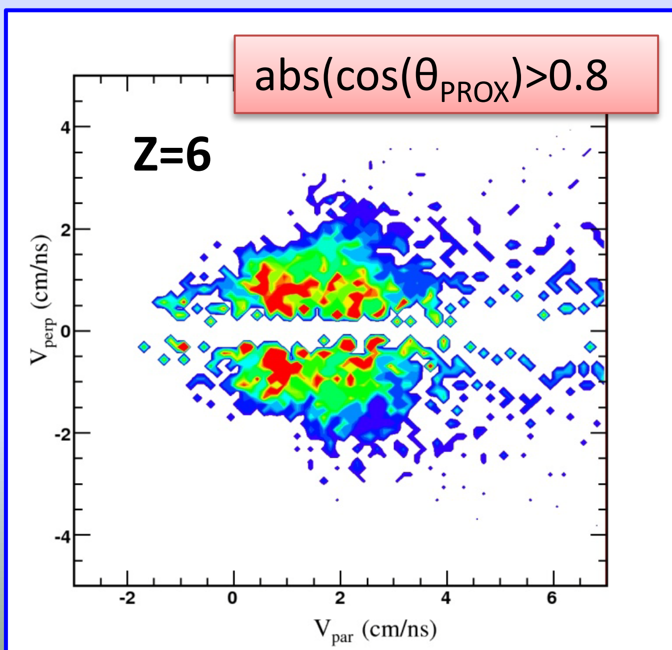

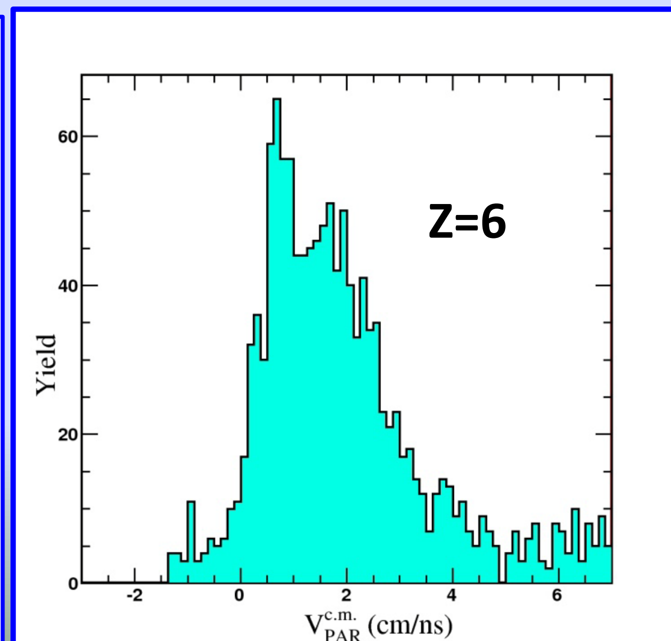

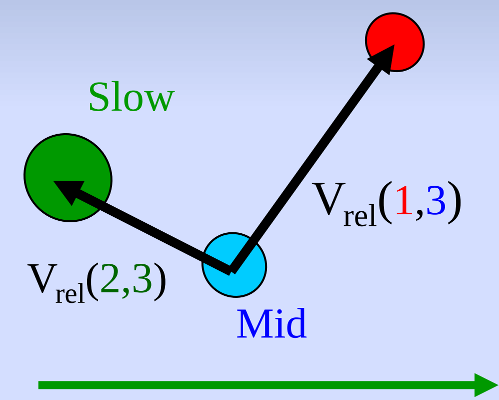

The three heaviest fragments are ordered according to decreasing value of parallel velocity.

Disentangling dynamical vs. statistical emission in ternary events

$^{64}Ni + ^{124}Sn$ 35 A.MeV

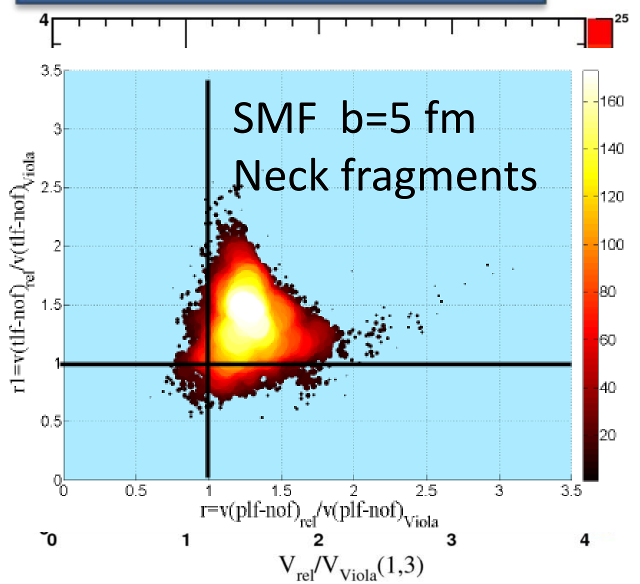

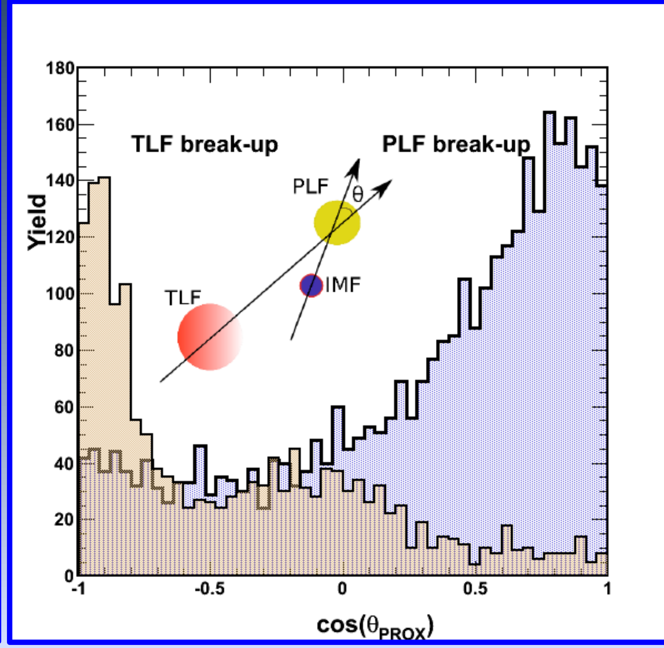

cos(θ)≈±1
aligned emission of the lighter fragment in the backward emisphere of **PLF** (+1) and **TLF** (-1) towards midrapidity

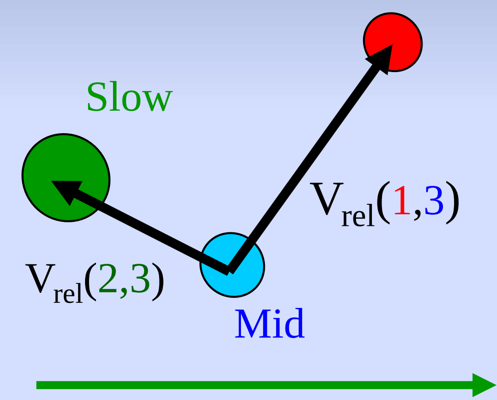

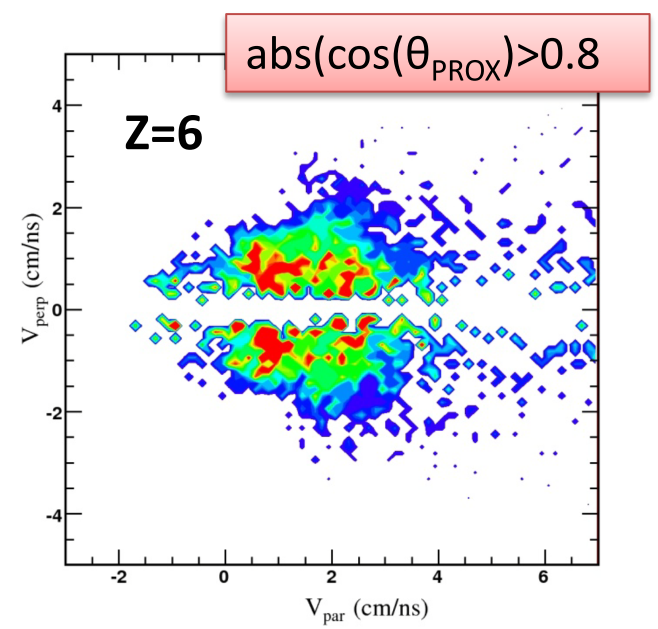

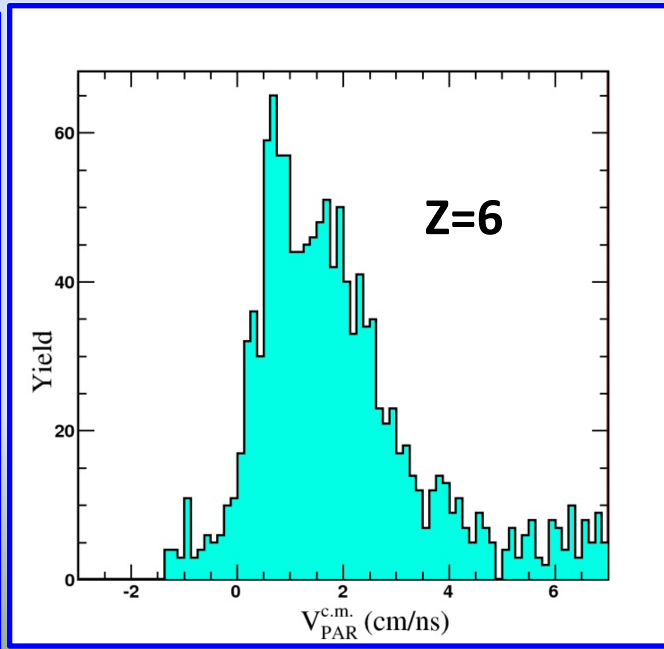

The three heaviest fragments are ordered according to decreasing value of parallel velocity.

Disentangling dynamical vs. statistical emission in ternary events

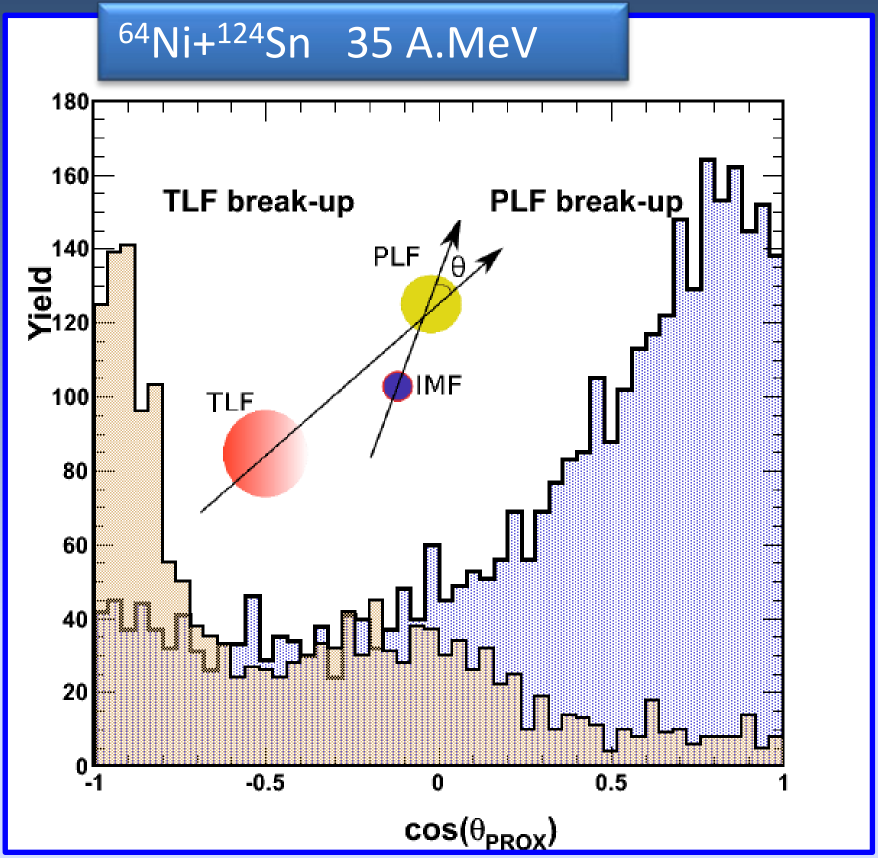

cos(θ)≈±1
aligned emission of the lighter fragment in the backward emisphere of **PLF** (+1) and **TLF** (-1) towards midrapidity

Enhancement of backward fragment yield relative to the forward component

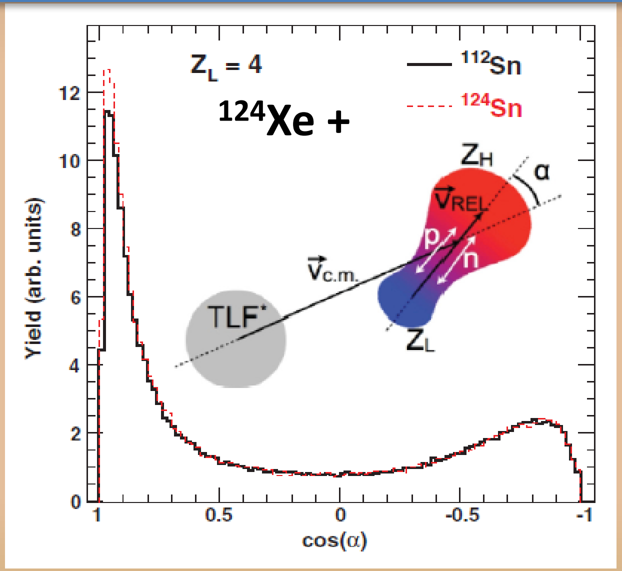

S. Hudan et al., PRC **86** 021603 (2012)

R. Brown et al., PRC 87 061601 (2013)

Stochastic Mean Field (SMF) + GEMINI calculation

CHIMERA @ LNS

$^{124}Sn+^{64}Ni$ 35 A.MeV

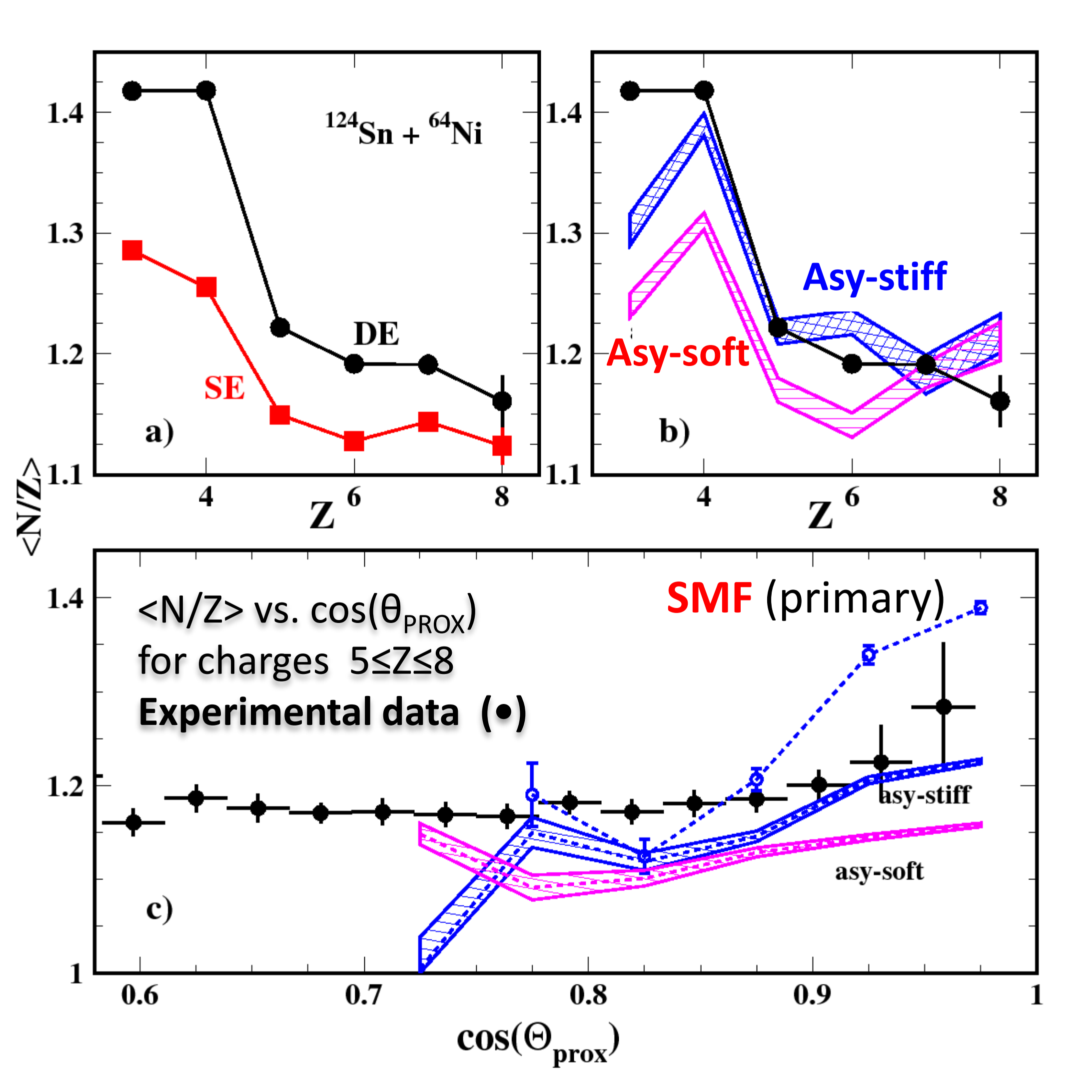

Experimental <N/Z> distribution of IMFs as a function of their atomic number compared with results **SMF+GEMINI** calculations (hatchad area) for two different parametrizations of the symmetry potential (asy-soft and asy-stiff)

- Dynamically emitted particles
- Statistically emitted particles

*E.d.F. et al., Phys. Rev. C **86** 014610 (2012)*

See also: S. Hudan et al., PRC **86** 021603(R) 2012.
K. Brown et al., PRC **87** 061601 (2013)

Stochastic Mean Field (SMF) + GEMINI calculation

$^{124}Sn+^{64}Ni$ 35 A.MeV

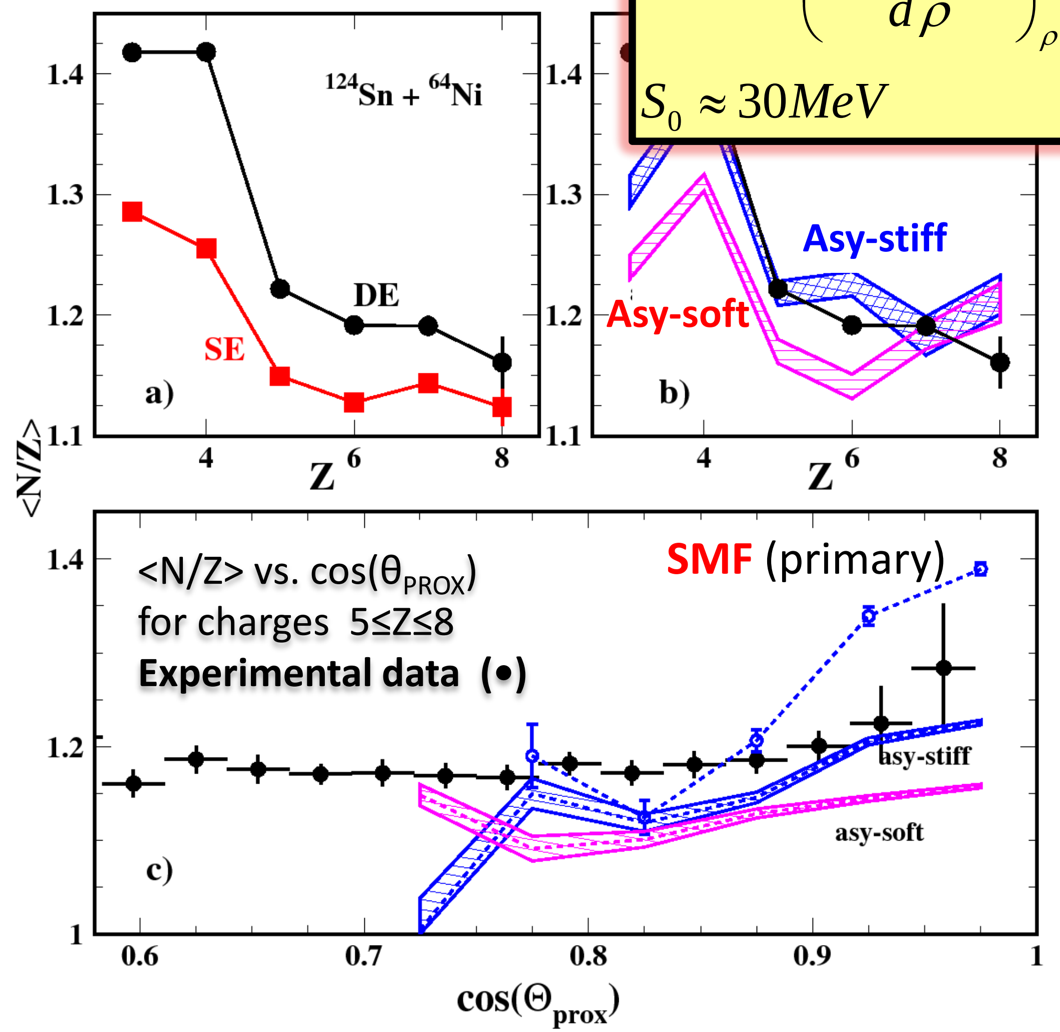

$$L = 3\rho_0 \left(\frac{dE_{sym}(\rho)}{d\rho} \right)_{\rho=\rho_0} =$$

≈ 80±10 MeV for the asy-stiff

≈ 25 MeV for the asy-soft

$$S_0 \approx 30MeV$$

function of their atomic number compared with results **SMF+GEMINI** calculations (hatchad area) for two different parametrizations of the symmetry potential (**asy-soft** and **asy-stiff**)

- Dynamically emitted particles
- Statistically emitted particles

E.d.F. et al., Phys. Rev. C ***86*** *014610 (2012)*

See also: S. Hudan et al., PRC **86** 021603(R) 2012.
K. Brown et al., PRC **87** 061601 (2013)

Stochastic Mean Field (SMF) + GEMINI calculation

CHIMERA @ LNS

$^{124}Sn+^{64}Ni$ 35 A.MeV

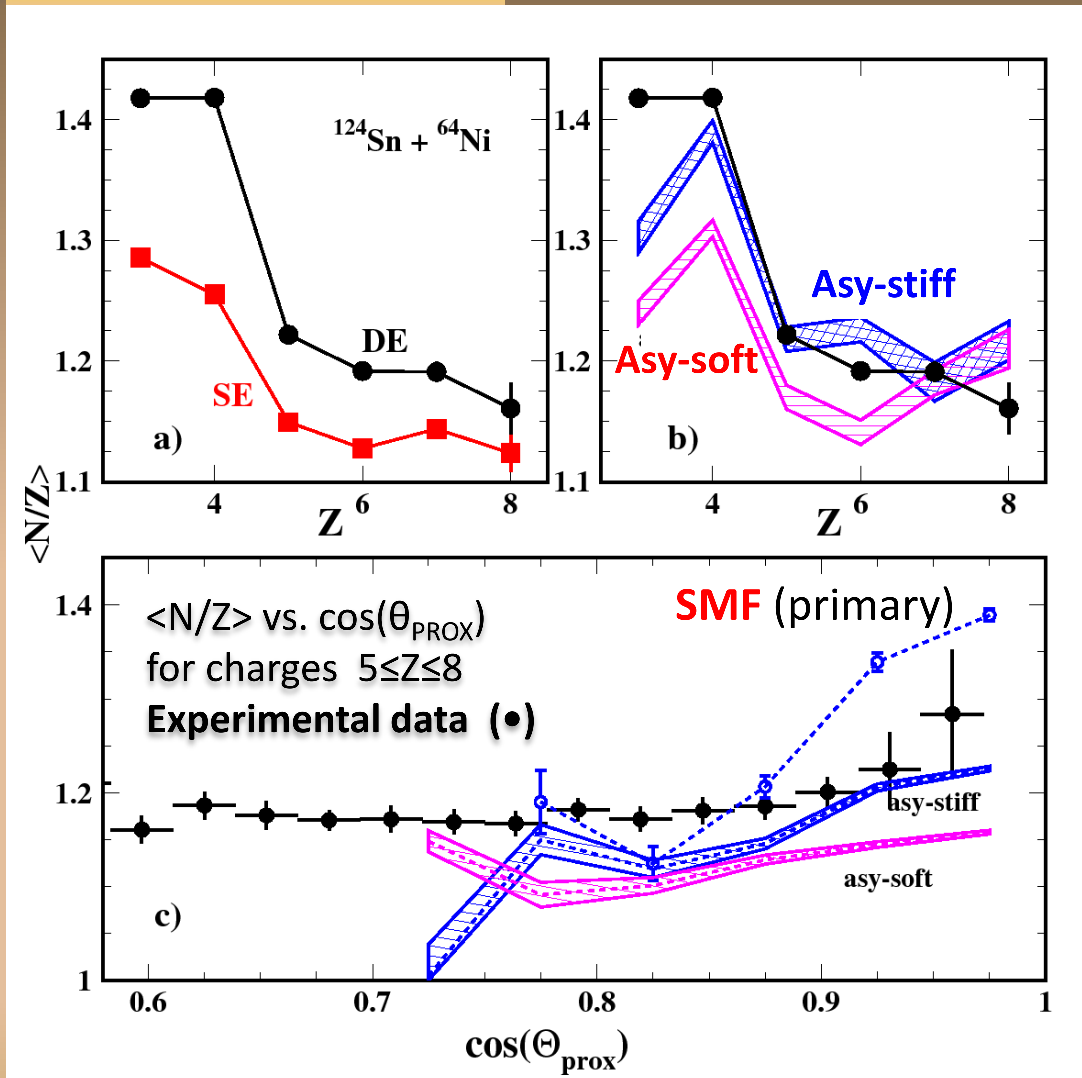

Experimental <N/Z> distribution of IMFs as a function of their atomic number compared with results SMF+GEMINI calculations (hatchad area) for two different parametrizations of the symmetry potential (asy-soft and asy-stiff)

- Dynamically emitted particles
- Statistically emitted particles

*E.d.F. et al., Phys. Rev. C **86** 014610 (2012)*

See also: S. Hudan et al., PRC **86** 021603(R) 2012.
K. Brown et al., PRC **87** 061601 (2013)

Stochastic Mean Field (SMF) : ratio (a) $^{124}Sn+^{64}Ni$ / $^{124}Xe+^{64}Zn$

Very Preliminary

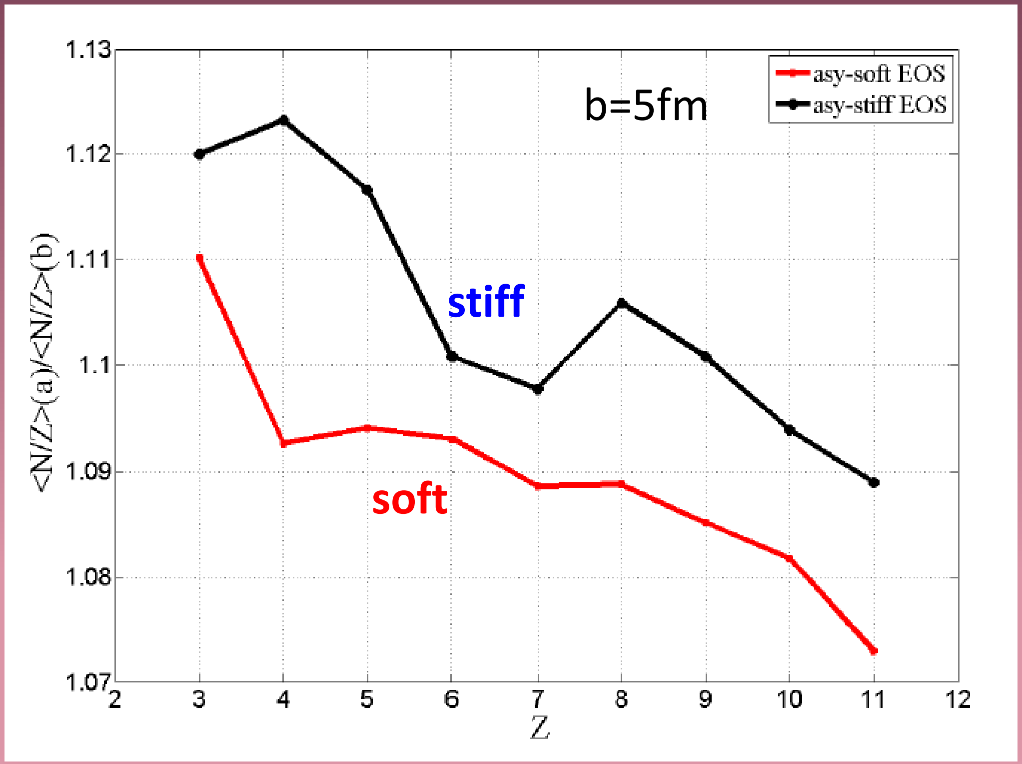

V. Baran, M. Marciu

Comparison with FAZIA data $^{84}Kr + ^{112,124}Sn$ data 35 A.MeV

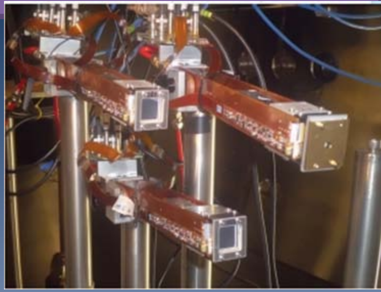

Fazia@LNS

FAZIA data: **$^{84}Kr+^{112,124}Sn$**
Selection based on particles velocity

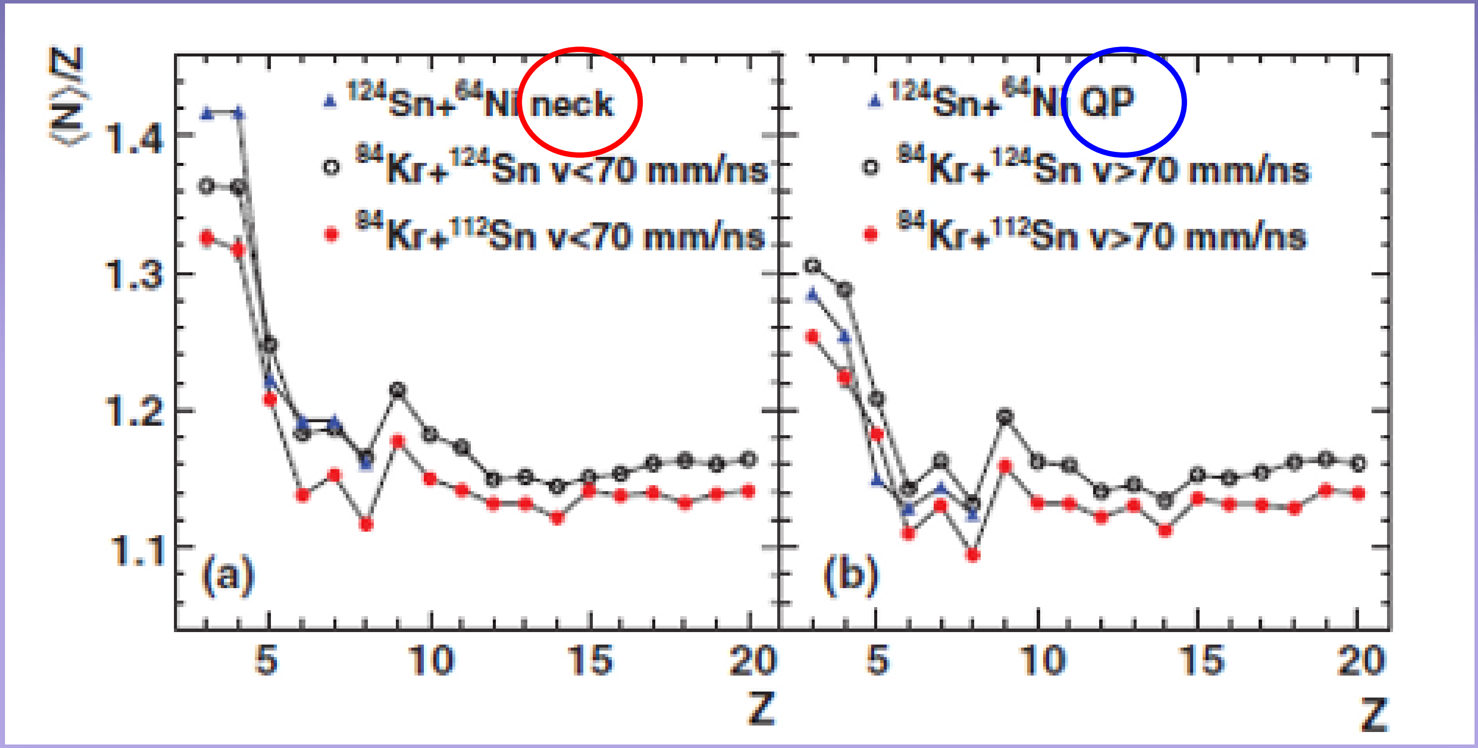

Chimera data (**triangles**): **$^{124}Sn+^{64}Ni$**
Selection based on angular correlations

S. Barlini et al., Phys. Rev. C**87**, 054607 (2013)

Density determination: three body analysis in the experimental data

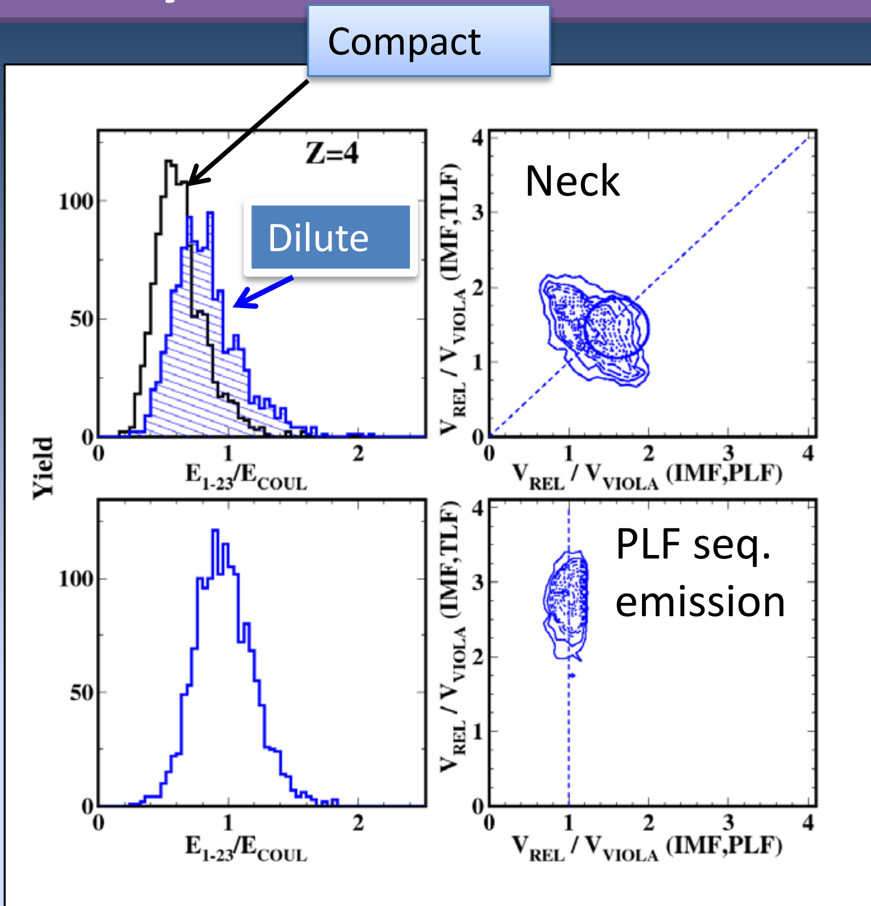

$^{124}Sn+^{64}Ni$ 35 A.MeV

CHIMERA@LNS

In the 3-bodies center-of-mass system:

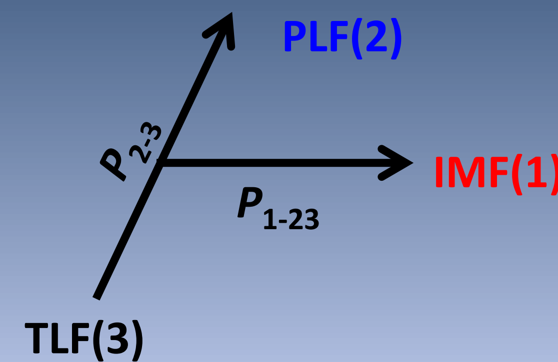

$$E_{TOT}^{c.m.} = E_1 + E_2 + E_3 = \frac{p_{1-23}^2}{\mu_{1-23}} + \frac{p_{23}^2}{\mu_{23}} = E_{1-23} + E_{23}$$

The ratio $E_{1\text{-}23}/E_{COULOMB}$ is calculated considering for the IMFs a dilute configuration with r_0=1.8$A^{1/3}$ fm (filled histogram corresponding to about 0.05 ρ_0) resulting from average values of SMF calculation (ρ=0.05-0.06 1/fm^3)

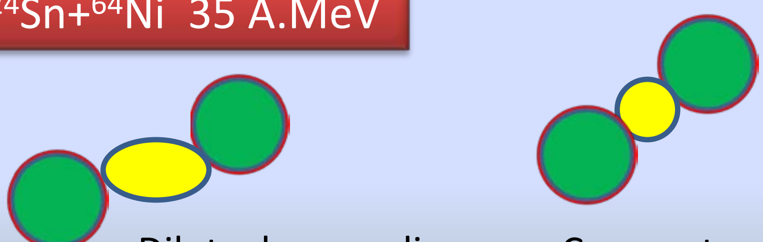

Dilute, large radius

Compact, normal radius

Proceedings INPC2013: E.d.F. et al., EPJ WoC 66, 03032 (2014)

From early prompt neck fragmentation to PLF dynamical fission

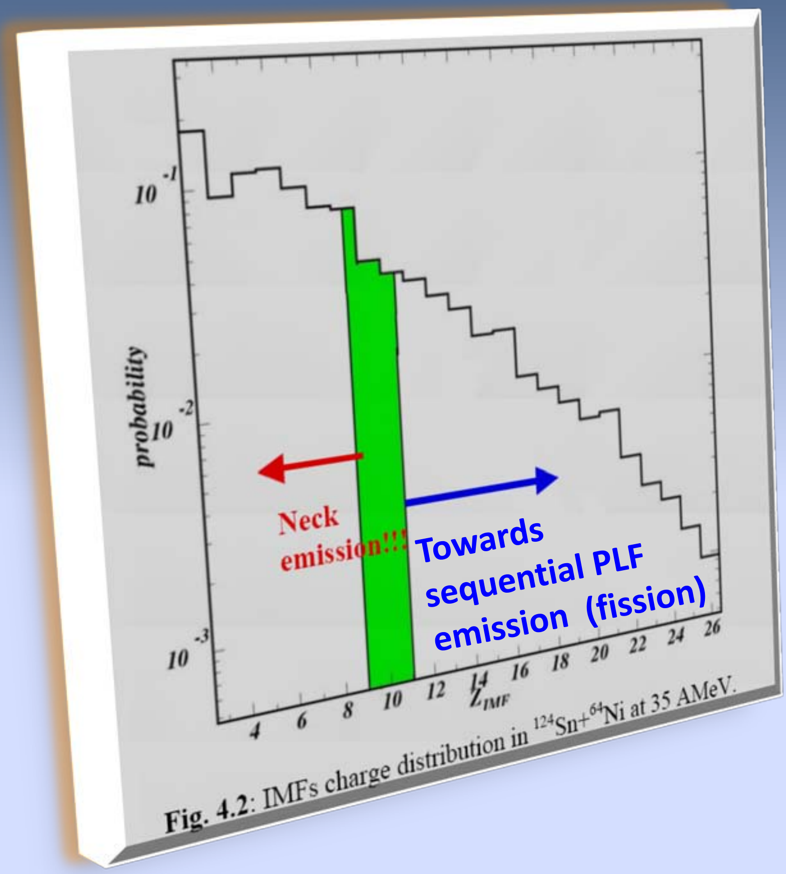

Fig. 4.2: IMFs charge distribution in $^{124}Sn+^{64}Ni$ at 35 AMeV.

The time-scale of the process as a function of the incident energy and impact parameter could be the main signature among different mechanisms:

1) Early neck fragmentation (40-120 fm/c)
2) Dynamical fission (120-300 fm/c
3) Equilibrated fission (>1000 fm/c)

With respect to the prompt neck emission, the emission of heavy IMFs from projectile-like fragment break-up appears at a later stage

The inset of quasi-projectile dynamical fission

$^{124}Sn+^{64}Ni$ 35 AMeV
neutron rich

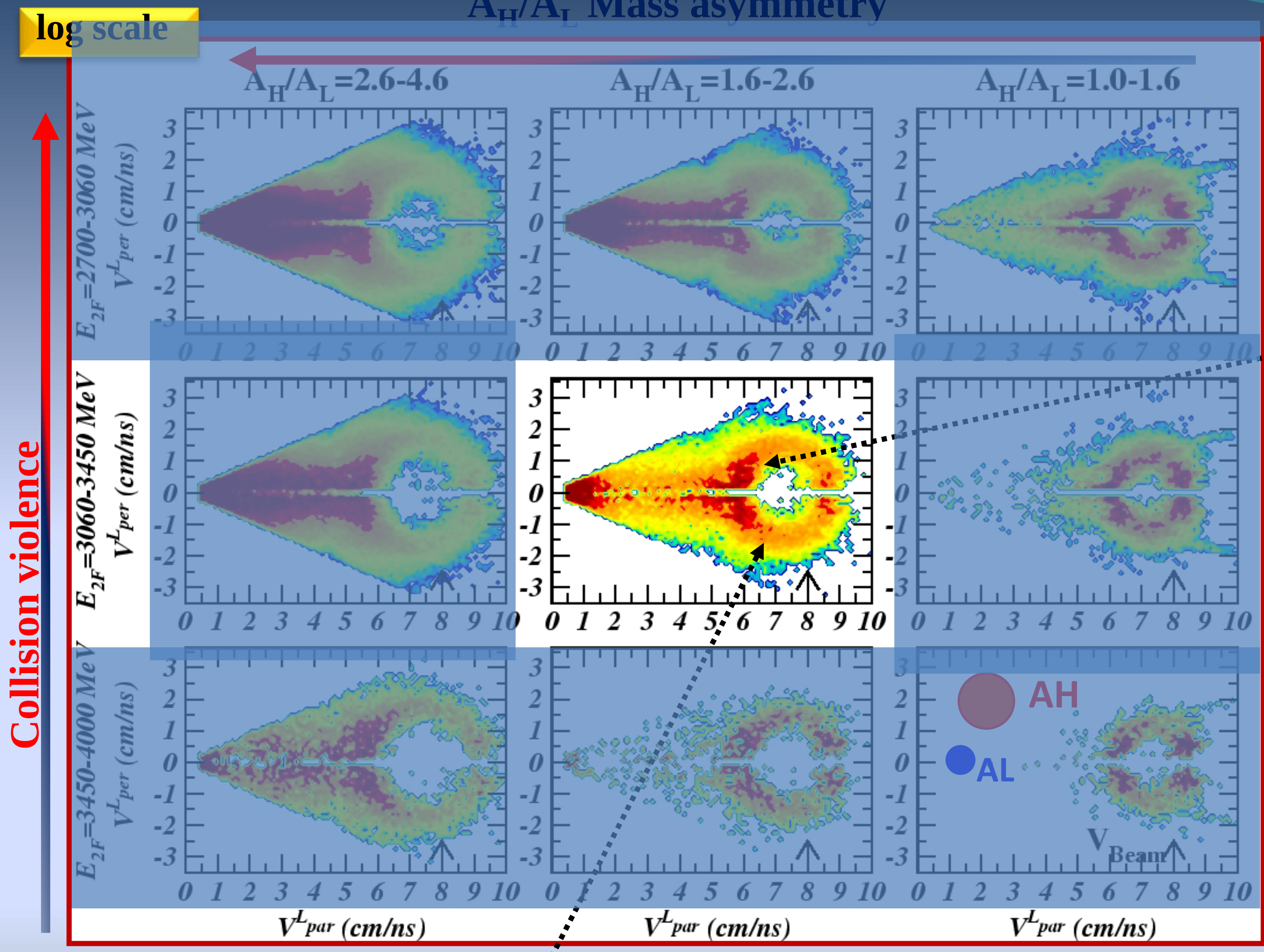

The lighter fragments are emitted preferentially backwards in the PLF reference system, i.e., towards the target nucleus: ***Dynamical Fission***
→ fast and non-equilibrated fission

E.De Filippo et al.,PRC 71 064604 (2005)
P. Russotto et al., PRC 81, 064605 (2010)

Coulomb ring 5<≈ V_{beam} = 8. cm/ns→ Well defined PLF source: scattering of PLF followed by its splitting in H&L fragments → sequential mechanism!!!

The inset of quasi-projectile dynamical fission

$^{124}Sn+^{64}Ni$ 35 AMeV neutron rich

A_H/A_L Mass asymmetry

log scale

Collision violence

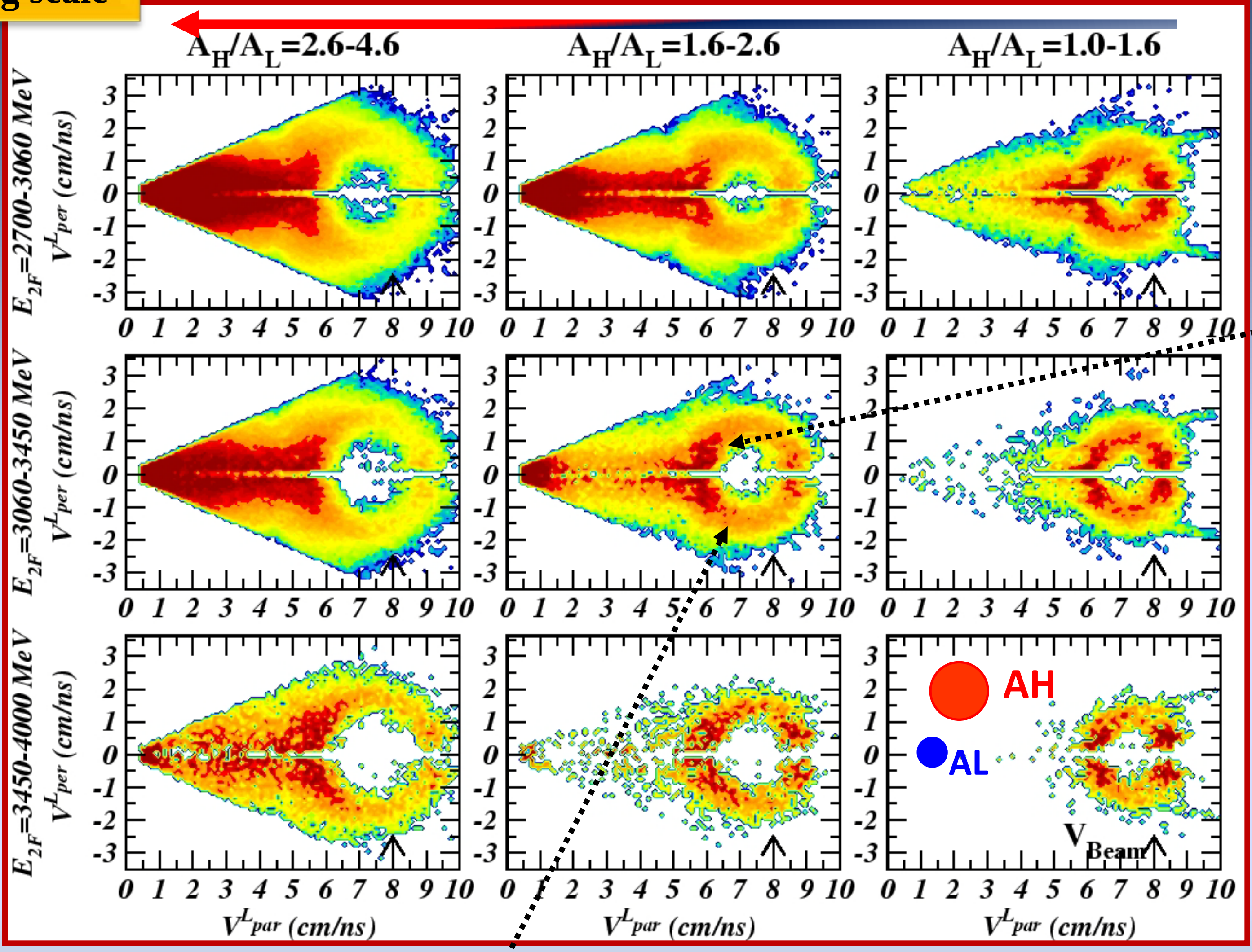

The lighter fragments are emitted preferentially backwards in the PLF reference system, i.e., towards the target nucleus: ***Dynamical Fission*** → fast and non-equilibrated fission

E.De Filippo et al.,PRC 71 064604 (2005)
P. Russotto et al., PRC 81, 064605 (2010)

Coulomb ring 5<≈ V_{beam} = 8. cm/ns→ Well defined PLF source: scattering of PLF followed by its splitting in H&L fragments → sequential mechanism!!!

Comparison of IMFs cross sections for $^{124}Sn+^{64}Ni$ and $^{112}Sn+^{58}Ni$

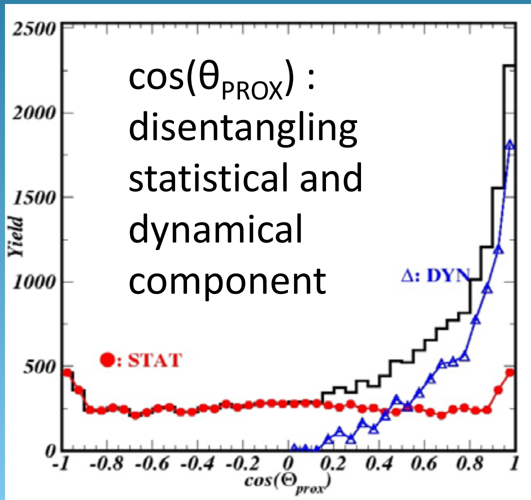

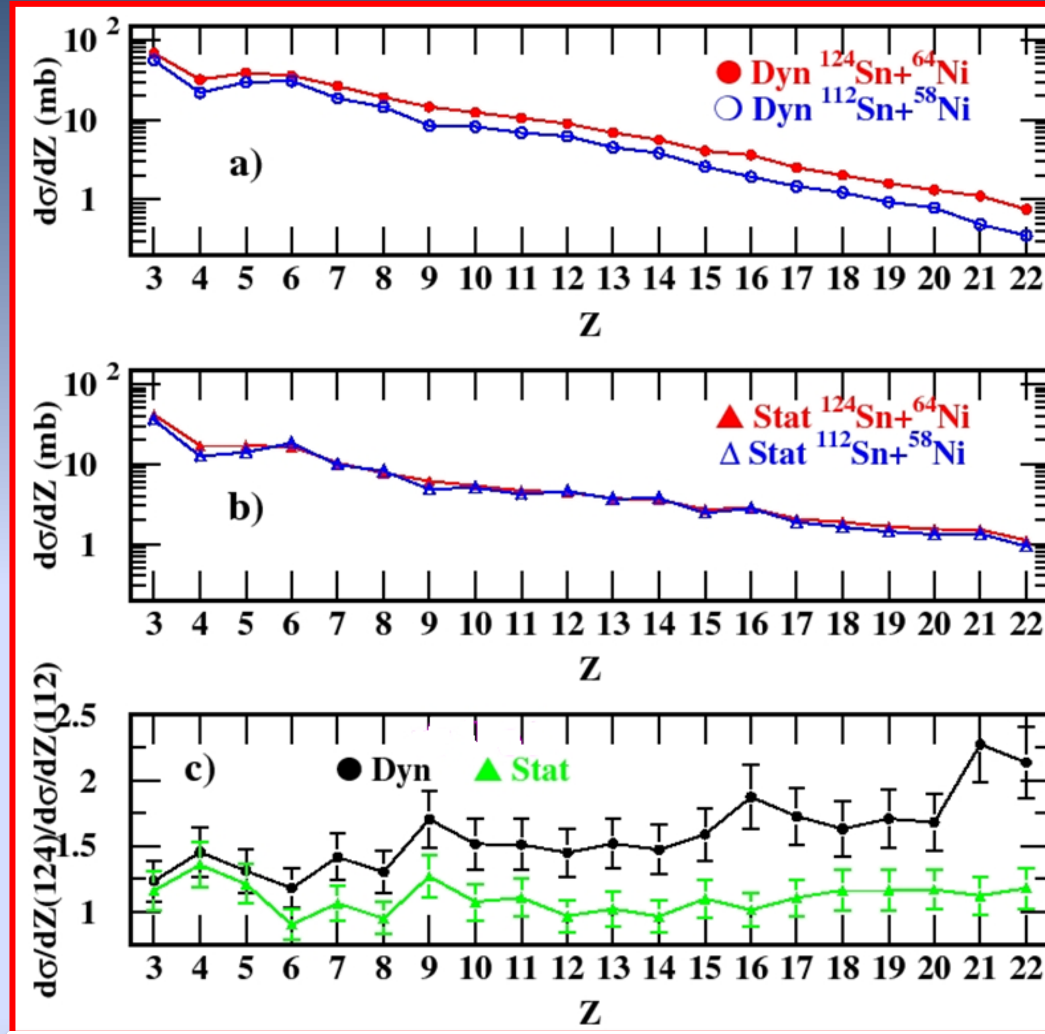

- Dynamical component: enhanced in the neutron rich
- Statistical component: almost equal (ratio: ~1.1)

P. Russotto et al. , to be submitted, PRC (2014)
P. Russotto et al., PRC 81, 064605 (2010)
E.De Filippo et al.,PRC 71 064604 (2005)

Comparison of IMFs cross sections for $^{124}Sn+^{64}Ni$ and $^{112}Sn+^{58}Ni$

Main experimental result: the dynamical component is enhanced for the neutron rich system.

Is it a size (mass) effect or isospin effect ?

The Inkiissy experiment at LNS

System	N/Z Projectile	N/Z target	N/Z compound
$^{124}Sn+^{64}Ni$	1.48	1.29	1.41
$^{124}Xe+^{64}Zn$	1.30	1.13	1.24
$^{112}Sn+^{58}Ni$	1.24	1.07	1.18

see Lucia Quattrocchi poster for details

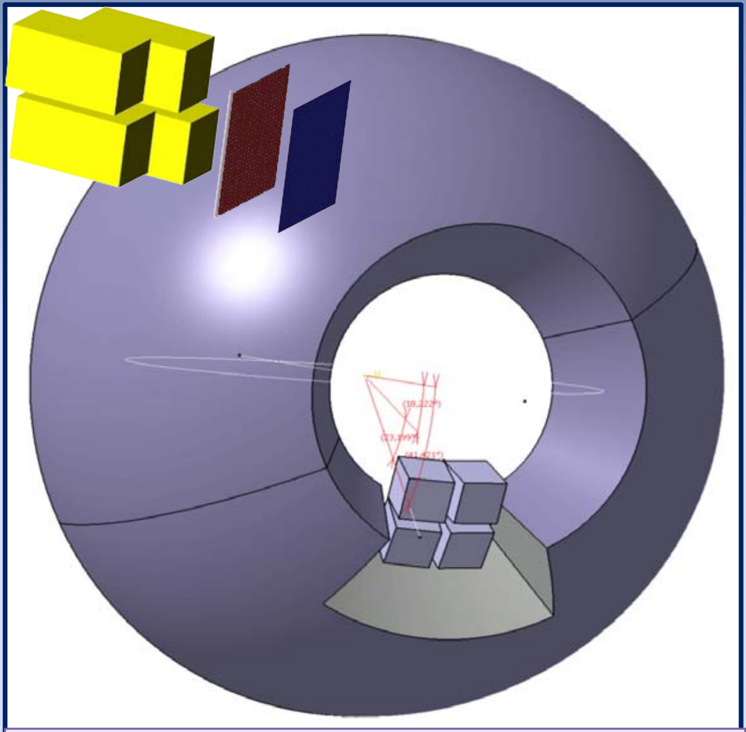

the 4π CHIMERA + a module of FARCOS prototype

4 telescopes 25 cm from the target
$\theta_{lab} \sim 16\text{-}44$ deg, $\Delta\phi \sim 45$ deg

See E.V. Pagano talk

Comparison of IMFs cross sections for $^{124}Sn+^{64}Ni$ and $^{112}Sn+^{58}Ni$

Main experimental result: the dynamical component is enhanced for the neutron rich system.

Is it a size (mass) effect or isospin effect ?

exotic beams for science

SPES letter of intent 2014

The Inkiissy experiment at LNS

System	N/Z Projectile	N/Z target	N/Z compound
$^{124}Sn+^{64}Ni$	1.48	1.29	1.41
$^{124}Xe+^{64}Zn$	1.30	1.13	1.24
$^{112}Sn+^{58}Ni$	1.24	1.07	1.18

see Lucia Quattrocchi poster for details

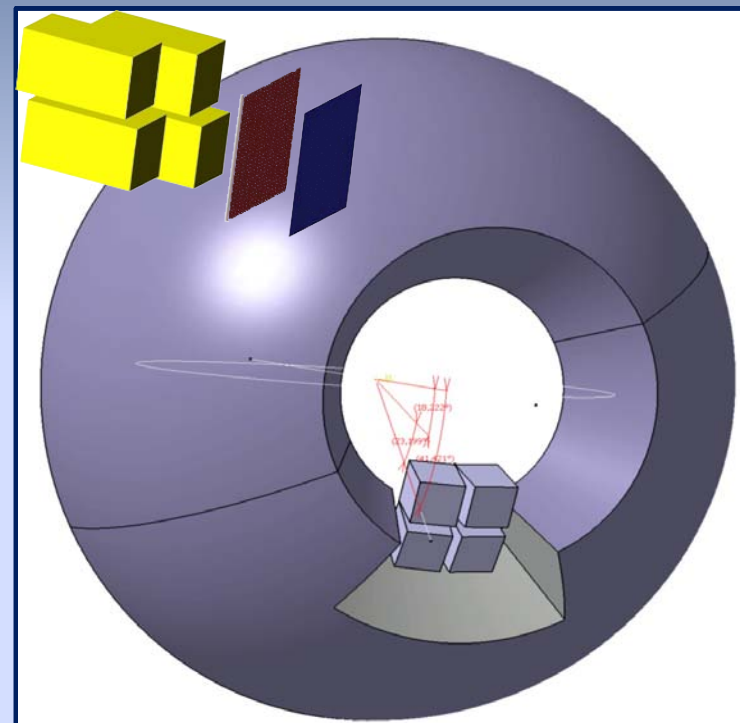

the 4π CHIMERA + a module of FARCOS prototype

4 telescopes 25 cm from the target
$\theta_{lab} \sim 16\text{-}44$ deg, $\Delta\phi \sim 45$ deg

See E.V. Pagano talk

Transverse flow of IMFs and symmetry energy

$$V_1(y,p_t)=\left\langle \frac{p_x}{p_t} \right\rangle$$

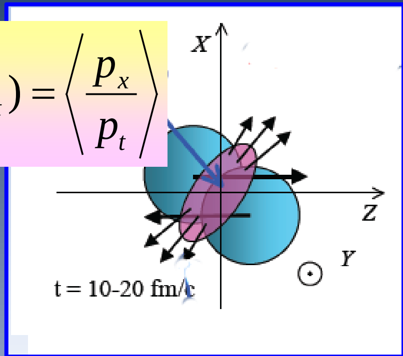

Transverse flow: *provides information on the azimuthal anisotropy in the reaction plane .*

$$V_2(y,p_t)=\left\langle \frac{p_x^2-p_y^2}{p_t^2} \right\rangle$$

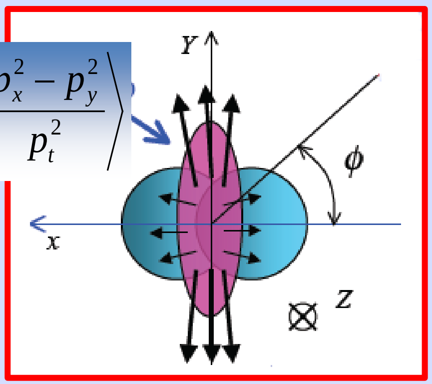

Elliptic flow: *measures the competition between in plane and out-of-plane emission*

$^{70}Zn+^{70}Zn$, $^{64}Zn+^{64}Zn$, $^{64}Ni+^{64}Ni$ E/A= 35 MeV

Main observable:

$$R_{\mathrm{flow}} = \frac{\overline{\langle Px\rangle}_{^{64}\mathrm{Zn}} - \overline{\langle Px\rangle}_{^{70}\mathrm{Zn}}}{\overline{\langle Px\rangle}_{^{64}\mathrm{Ni}} - \overline{\langle Px\rangle}_{^{70}\mathrm{Zn}}}$$

Z. Kohley et al., PRC82, 064601 (2010)

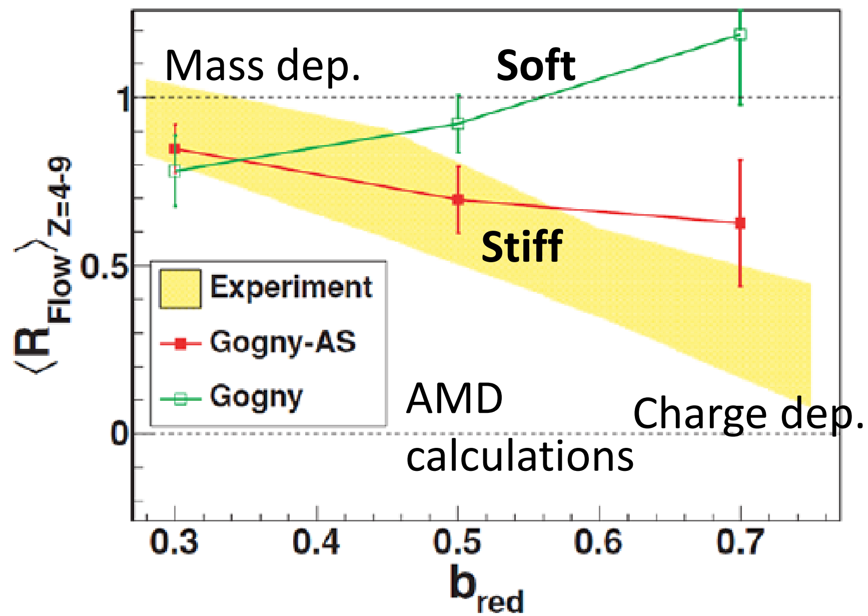

NIMROD-ISiS@TAMU

See P. Russotto talk for "flow" measurements at relativistic energies

Transverse flow of IMFs and symmetry energy

$^{70}Zn+^{70}Zn$, $^{64}Zn+^{64}Zn$, $^{64}Ni+^{64}Ni$ E/A= 35 MeV

$$V_1(y,p_t) = \left\langle \frac{p_x}{p_t} \right\rangle$$

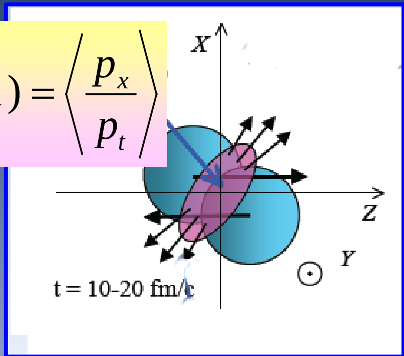

Main observable:

$$R_{\text{flow}} = \frac{\overline{\langle Px \rangle}_{^{64}\text{Zn}} - \overline{\langle Px \rangle}_{^{70}\text{Zn}}}{\overline{\langle Px \rangle}_{^{64}\text{Ni}} - \overline{\langle Px \rangle}_{^{70}\text{Zn}}}$$

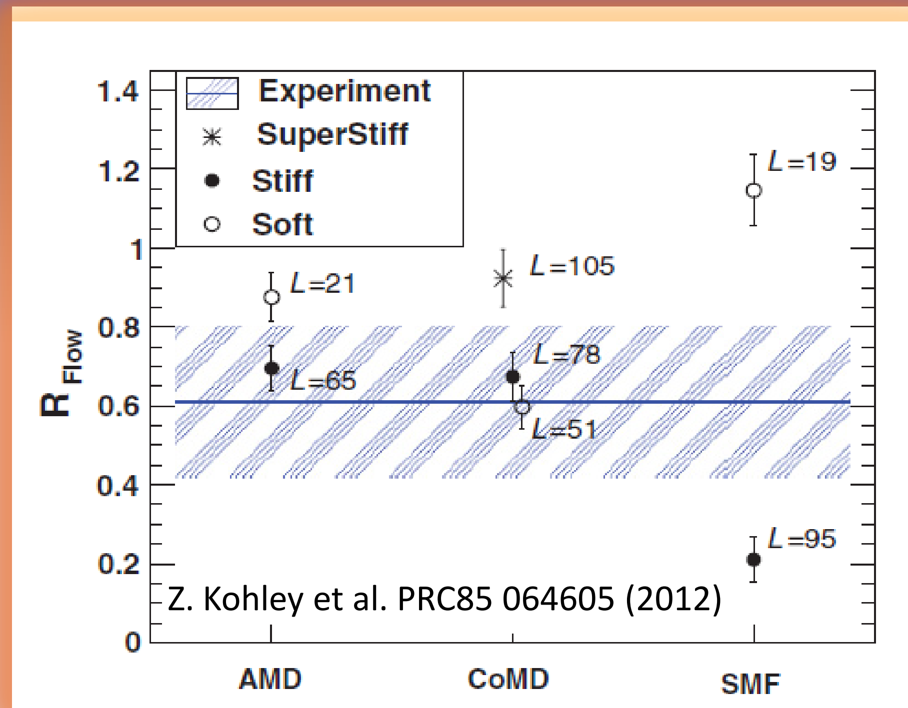

Transverse flow: *provides information on the azimuthal anisotropy in the reaction plane .*

$$V_2(y,p_t) = \left\langle \frac{p_x^2 - p_y^2}{p_t^2} \right\rangle$$

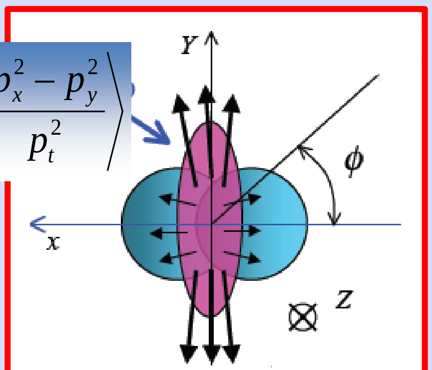

Elliptic flow: *measures the competition between in plane and out-of-plane emission*

NIMROD-ISiS@TAMU

See P. Russotto talk for "flow" measurements at relativistic energies

Exploiting RIBS and neutron detection (a way for the future ?)

CoMD calculation showing the sensitivity to L for the <N/Z> of the quasi-projectile residue in ^{32}Mg +^{9}Be respect to ^{24}Mg +^{9}Be at 73 MeV/A

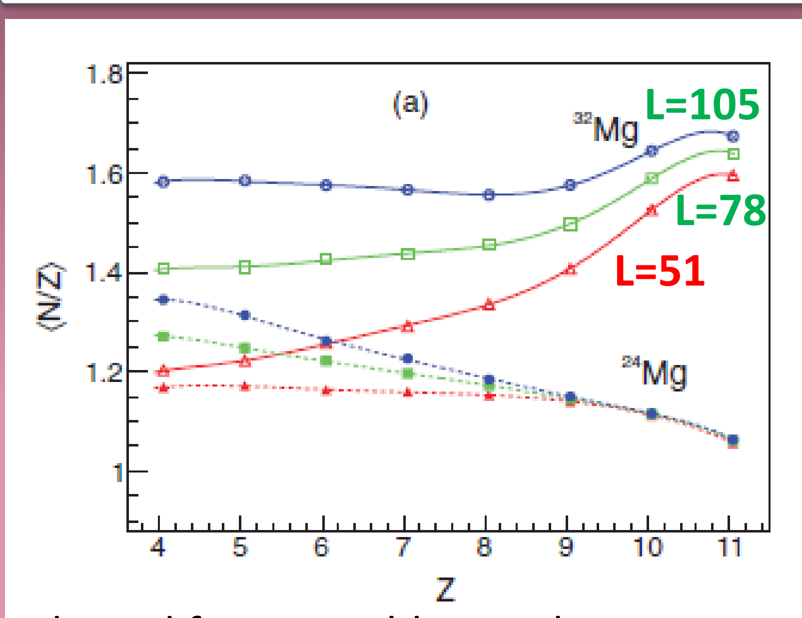

Adapted from Z. Kohley et al., PRC **88** 041601 (2013)

MoNA@MSU

Neutron angular distributions and velocity in coincidence with Z=4 fragments. CoMD calculations with **L=78 MeV** are in green (Data from Z.Kohley et al. PRC88 with the MoNA Neutron Array).

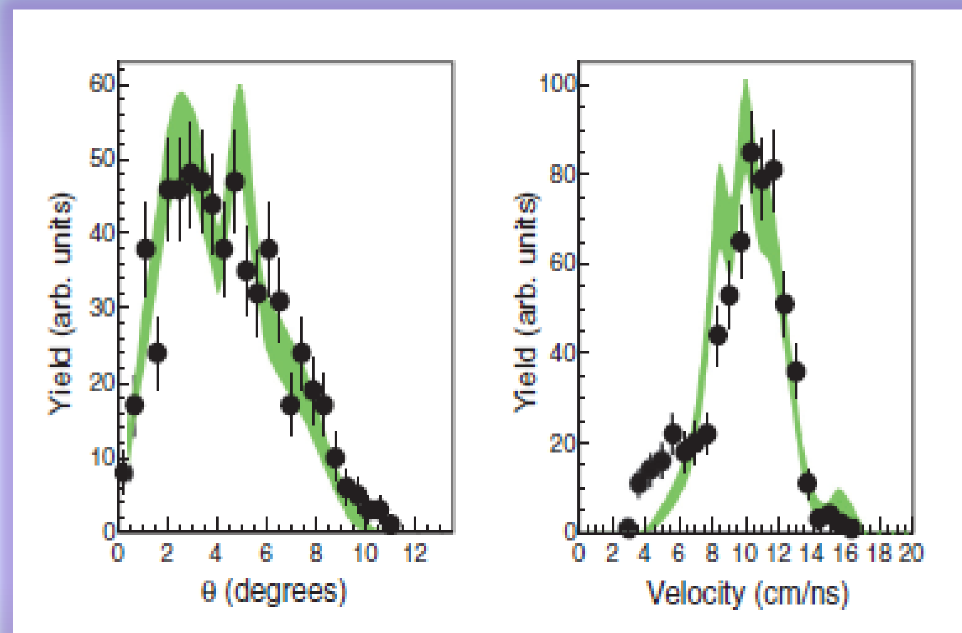

Collection of available estimates of the slope parameter L

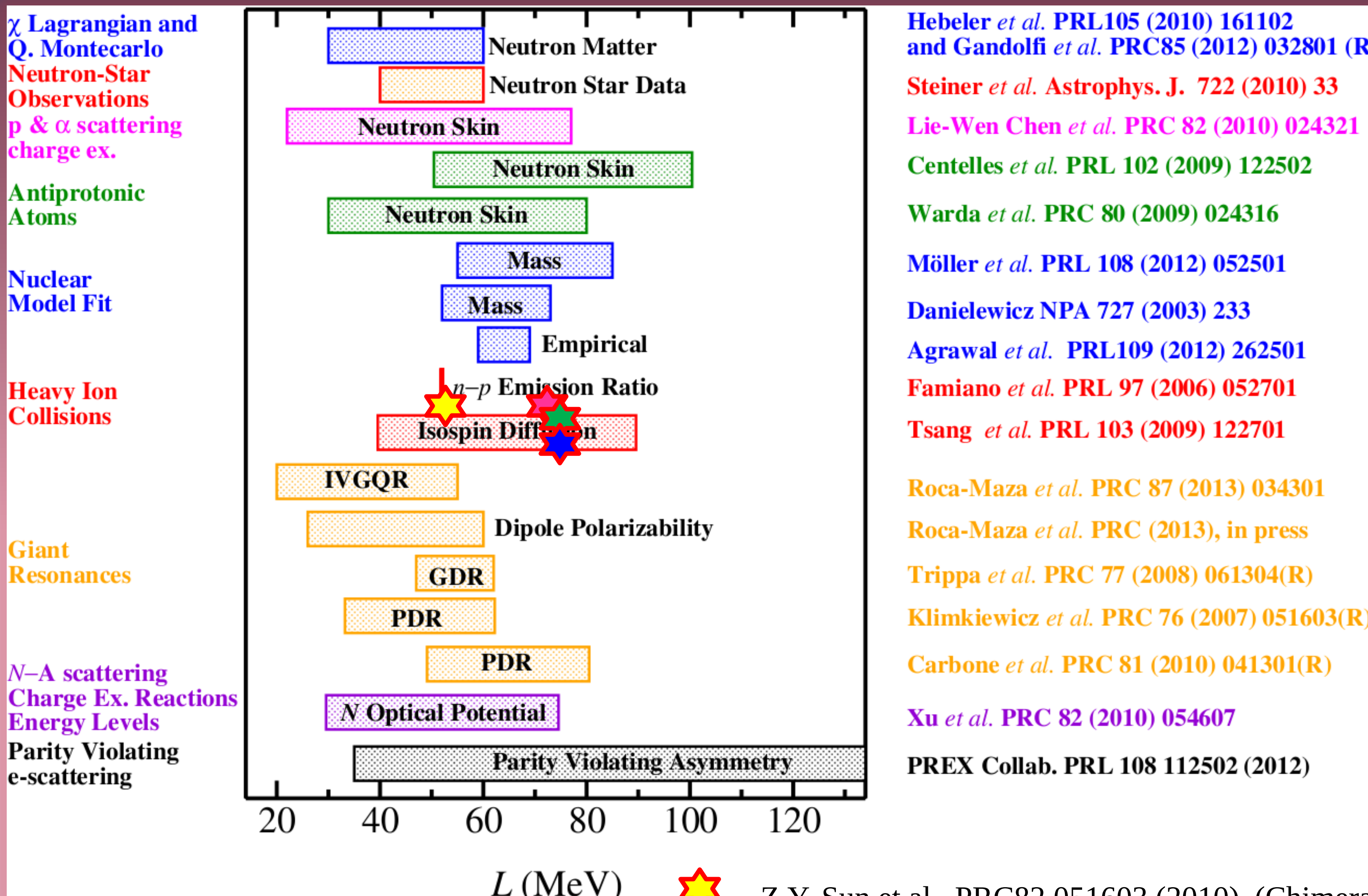

Z.Y. Sun et al., PRC82 051603 (2010) (Chimera/MSU data)
E. Galichet et al. PRC 79 064615 (2009) (INDRA data)
E.d.F. et al. PRC 86 014610 (2012) (Chimera data)
Z. Kohley et al., PRC 88 041601 (2013) (TAMU data)

Adapted from X. Vinas et al.,
EPJA 50:27 (2014)

What we learn from Heavy Ion collisions and nuclear structure probes ?

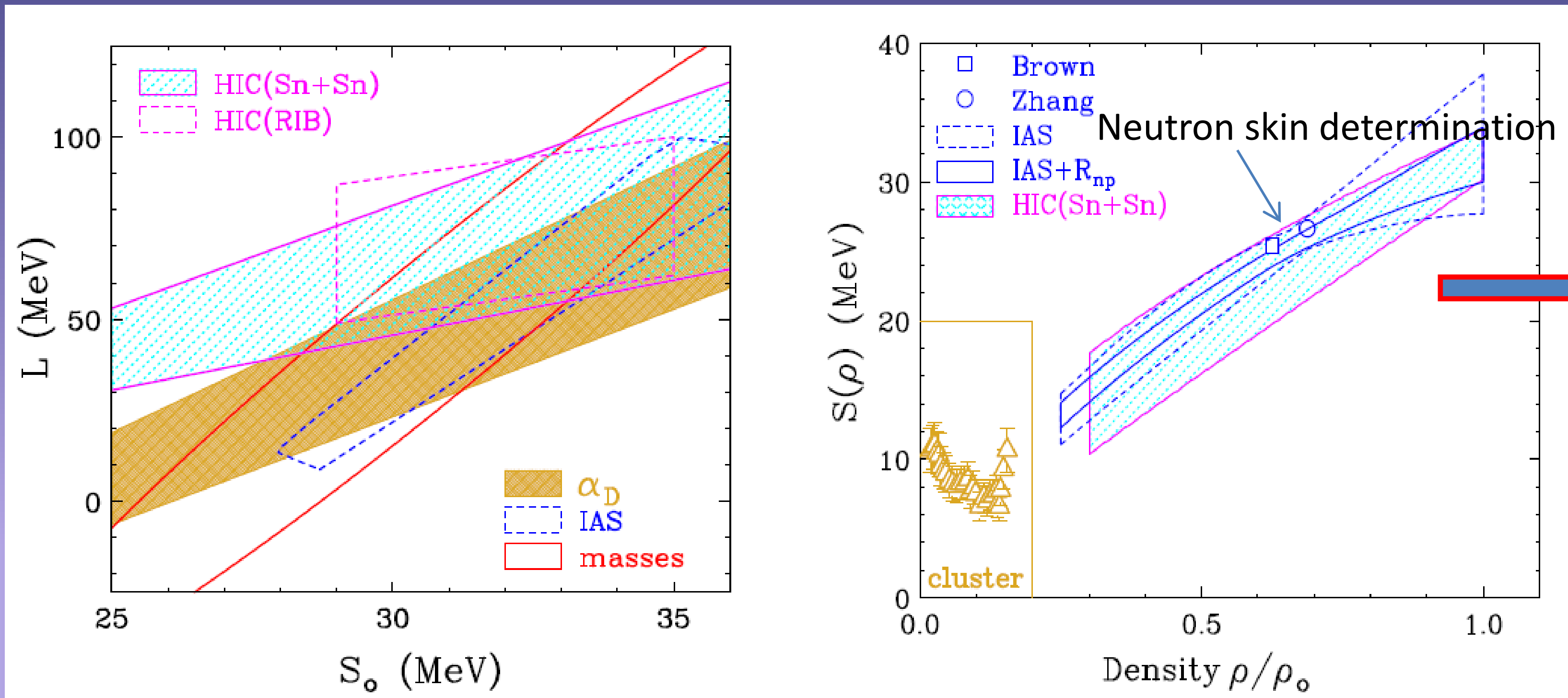

Adapted from C.J. Horowitz et al., ArXiv 1401:5839 (2014)

As a function of incident energy, impact parameter, isospin asymmetry, it is possible to span from low to high densities with HIC

A stringent test and constraint on trasport model and dynamical theories

Unique possibility to explore the critical region at 2-3ρ_0

High densities behaviour of symmetry energy: a controversial problem

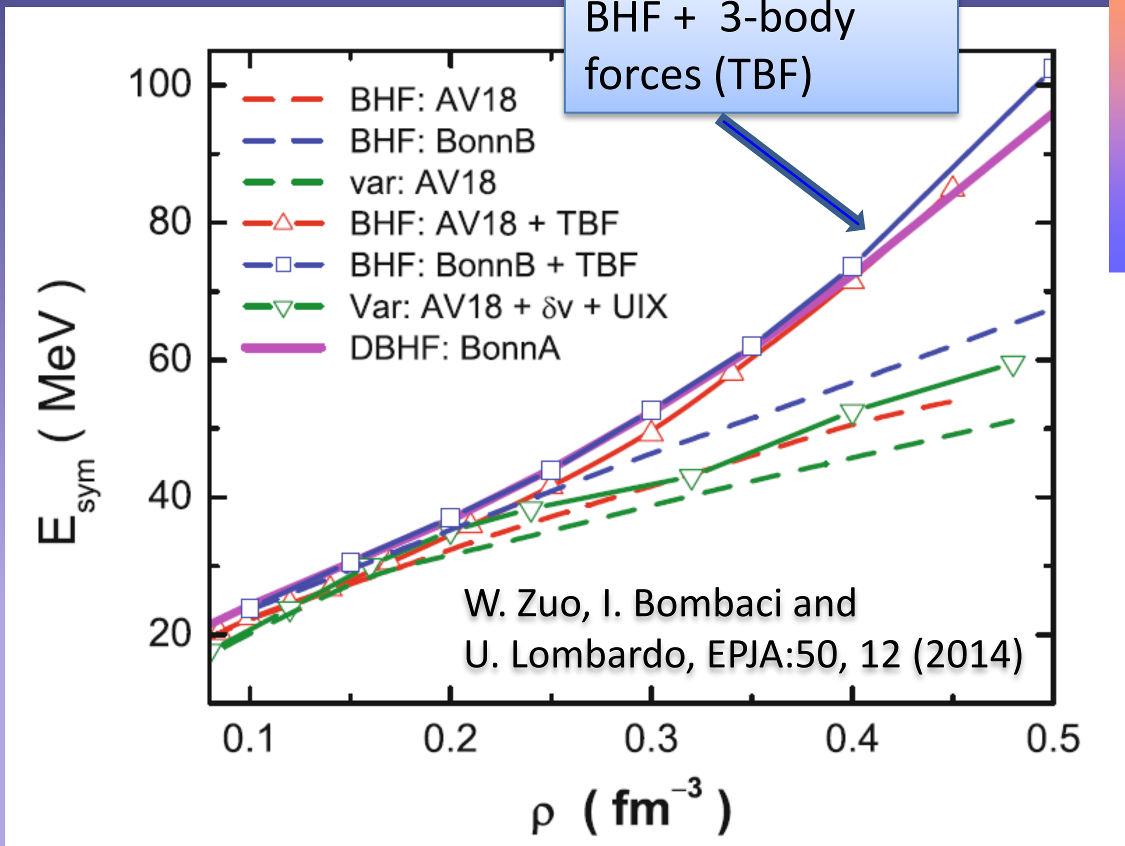

The dependency on density of the potential part of symmetry energy term is is largerly uncostrained for the high density behaviour $\rho \geq \rho_0$

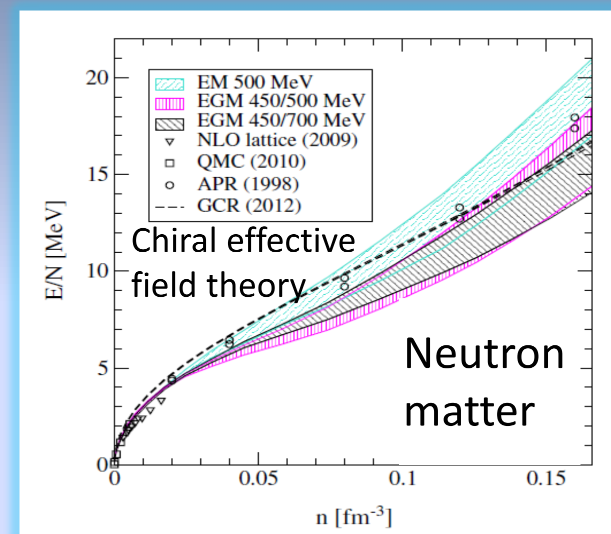

I. Tews et al., PRL110 032501 (2013)

The effect of three body forces (TBF) is weak at low density but at supra-saturation densities leads to a stiffening of the symmetry energy with density.
In neutron matter the short-range repulsive part of 3-body force is dominant.

Using Pion and Kaon probes

FOPI@GSI

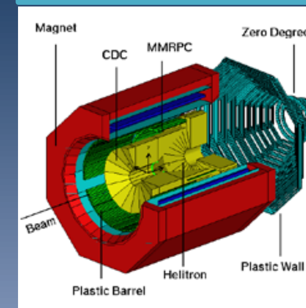

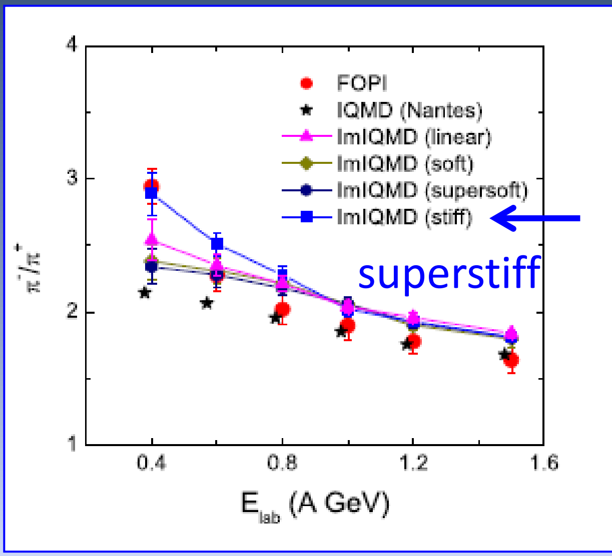

Z. Feng et al. PLB 683 140, 2010

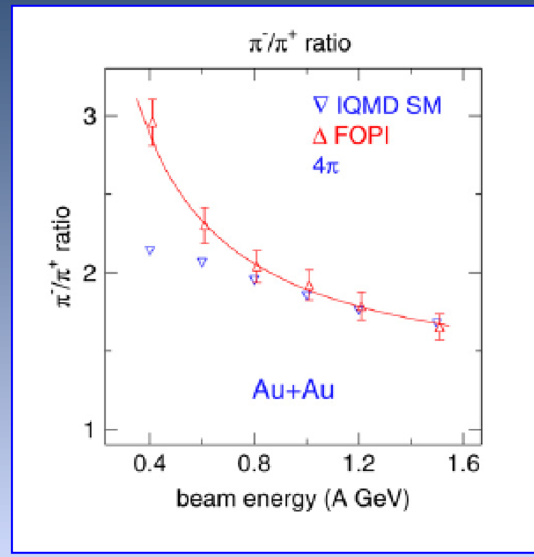

W. Reisdorf et al. NPA 781 459, 2007

Δ resonance:

$Y(\pi-)/Y(\pi+) \approx (N/Z)^2_{dense}$

Statistic model:

$\mu(\pi^+)-\mu(\pi^-)=2\ (\mu_p-\mu_n)$

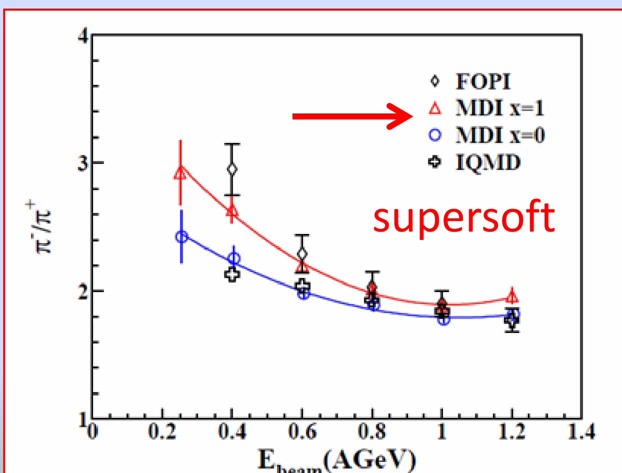

Z. Xiao et al. PRL 102 062509, 2009

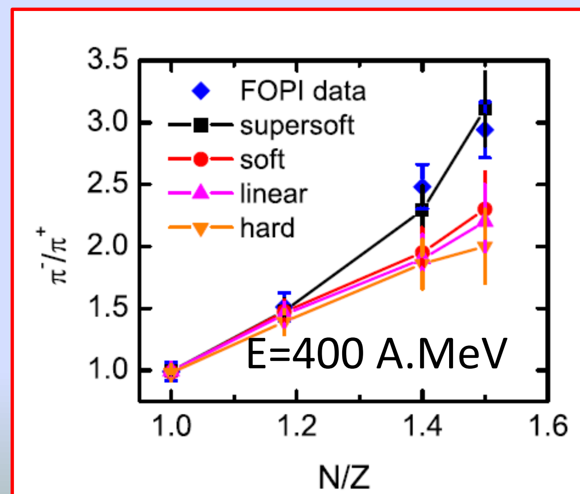

W. Xie et al. PLB 718 1510, 2013

Using Pion and Kaon probes

FOPI@GSI

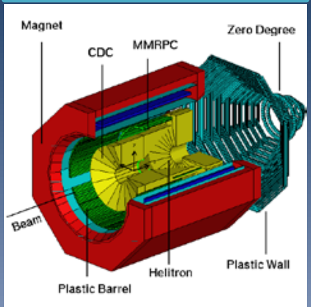

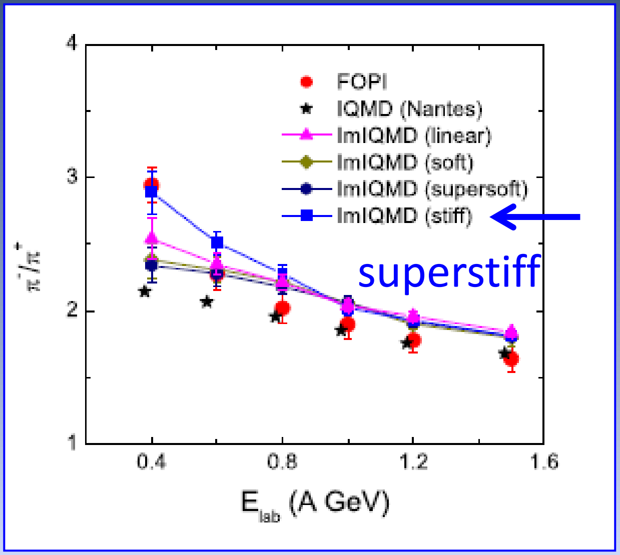

Z. Feng et al. PLB 683 140, 2010

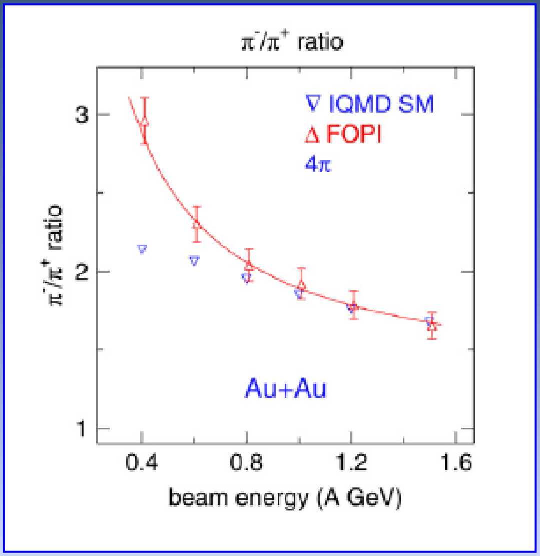

W. Reisdorf et al. NPA 781 459, 2007

Δ resonance:

$Y(\pi-)/Y(\pi+) \approx (N/Z)^2_{dense}$

Statistic model:

$\mu(\pi^+)-\mu(\pi^-)=2\ (\mu_p-\mu_n)$

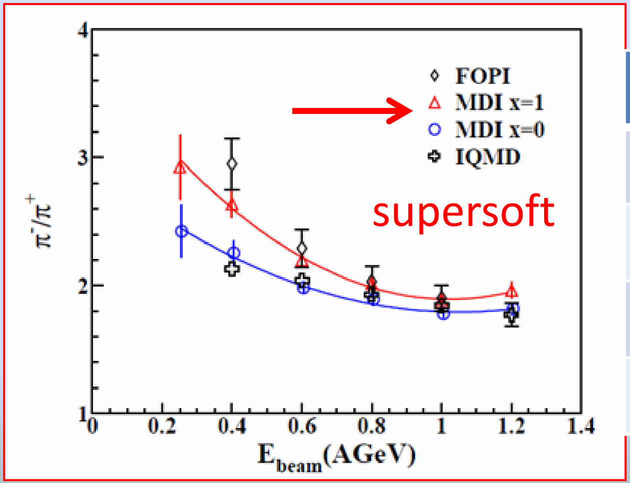

Z. Xiao et al. PRL 102 062509, 2009

Z. Xiao, B-An Li et al.	IBUU4	supersoft
Z. Feng et al.	IMQMD	superstiff
G. Ferini et al.	RMF	stiff (linear)
W. Reisdorf	IQMD	soft (or no influence)
W.J. Xie et al.	ImIBL	supersoft

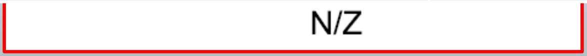

W. Xie et al. PLB 718 1510, 2013

Using Pion and Kaon probes

G. Ferini et al., PRL97, 202301

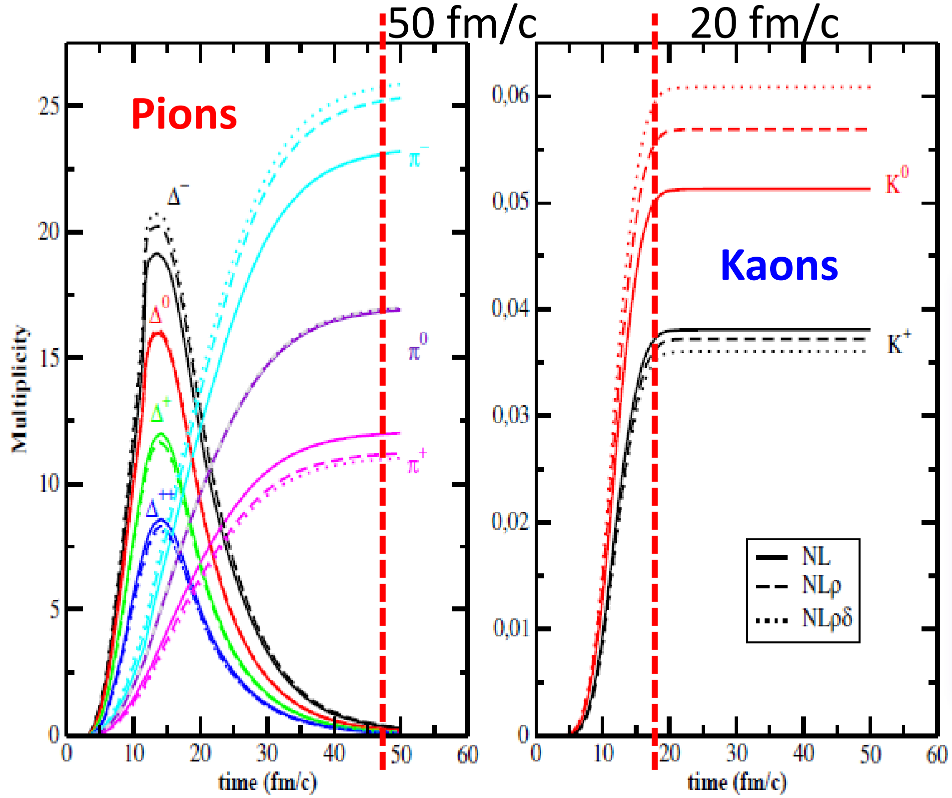

Figure 5.1: Time evolution of $\Delta^{\pm,0,++}$ resonances and pions $\pi^{\pm,0}$ (left) and kaons (right) for a central (b = 0 fm impact parameter) Au+Au collision at 1 AGeV incident energy. Transport calculations using the NL, $NL\rho$ and $NL\rho\delta$ models for the iso-vector part of the nuclear EoS are shown.

Pions and Kaons: different freeze-out times

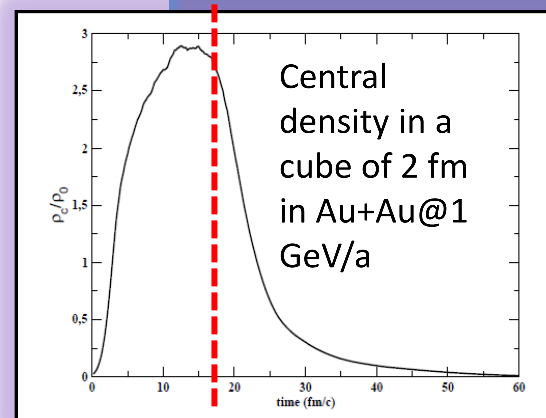

Experiment:

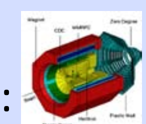

X. Lopez et al., PRC **75**, 011901 (2007).

New observables proposed : using η mesons or high energy photons (G.C. Yong and Bao-An Li Phys. Lett B 723, 388 (2013).

Neutron and proton elliptic flow: the AsyEos experiment at GSI

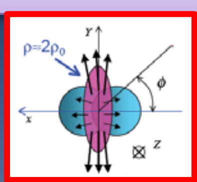

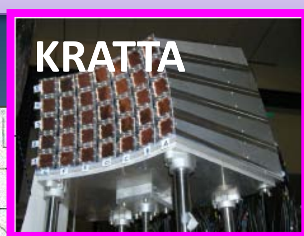

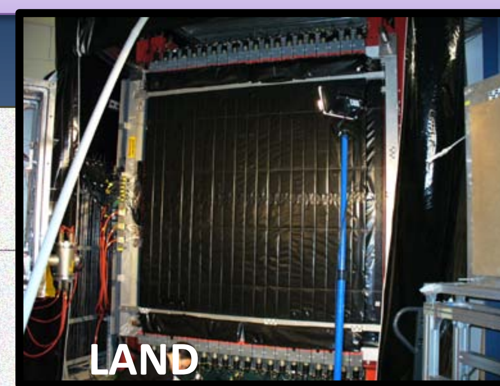

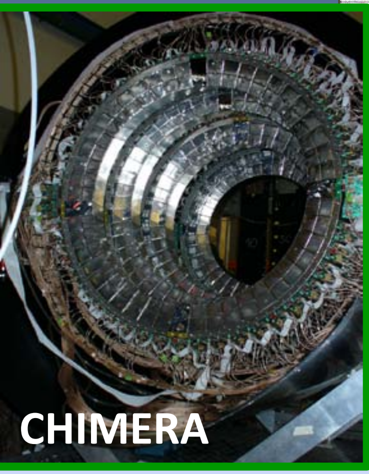

See next talk: P. Russotto

Present: **the Asy-Eos experiment**

Future: **Fair beams (^{132}Sn, ^{106}Sn) R3B/NeuLand, ...**

New projects at Riken with the SAMURAI TPC

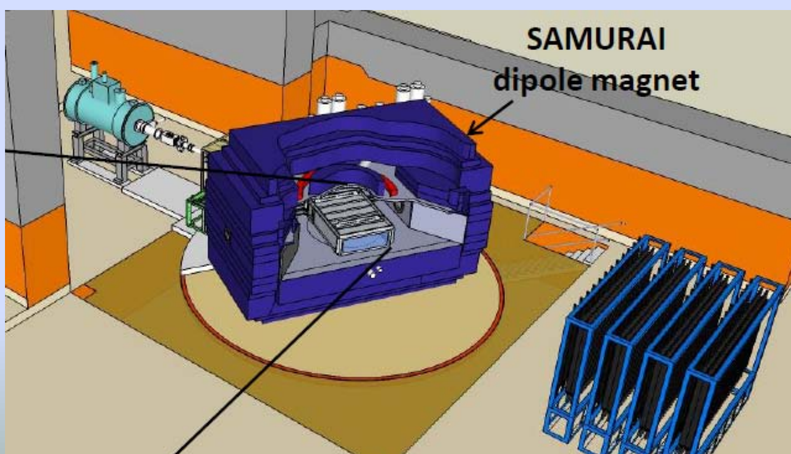

Measure differential flow and ratios for π^+/π^- p/n t/^{3}He at energies around or below 300 A.MeV with RIB beams like ^{132}Sn, ^{108}Sn, ^{52}Ca, ^{36}Ca

WHAT NEXT ?

A relative consistence analysis have been obtained from HIC but with yet large uncertainties.

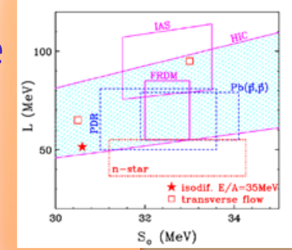

Use of new RIB facilities (exotic neutron rich, proton rich beams: isospin effects are enhanced by increasing the system asymmetry. Comparison with stable beam needed.

Measure different observables in the same experiment: Results have to be consistent for different observables. Different models should describe data in a consisten way.

Models: Look for discrepancies among different modes (the difference between the prediction between two models with the same Iso-parametrization can be larger than the difference between the results obtained by the same model with two different iso-parametrizations. It is important to compare multiple theoretical calculations to the same observable to validate the constraint.

Other signals: use of femtoscopy for a precise space-time sources characterization.

Neutron signals (np correlations, n/p double ratios….). New detectors.

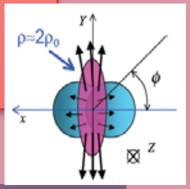

Esperiment to measure the symmetry energy at supra saturation density are now fundamental. FOPI systematics and the ASYEOS@GSI experiment results are a good starting point for the future . Future efforts at RIKEN, FRIB (MSU), FAIR (GSI) with new devices (NEWLAND, SAMURAI TPC, R3B) and new RIB facilities.

FINE

Particle-particle correlations and symmetry energy: a difficult task

IBUU simulations
$^{52}Ca + ^{48}Ca$ E/A=80 MeV, Central collisions
L.W. Chen, V. Greco , C. Ko, B-An Li, PRC68, 014605(2003)

$$1+R(q)=k\cdot\frac{\sum Y_{coinc}(\vec{p}_1,\vec{p}_2)}{\sum Y_{evt.mixing}(\vec{p}_1,\vec{p}_2)}$$

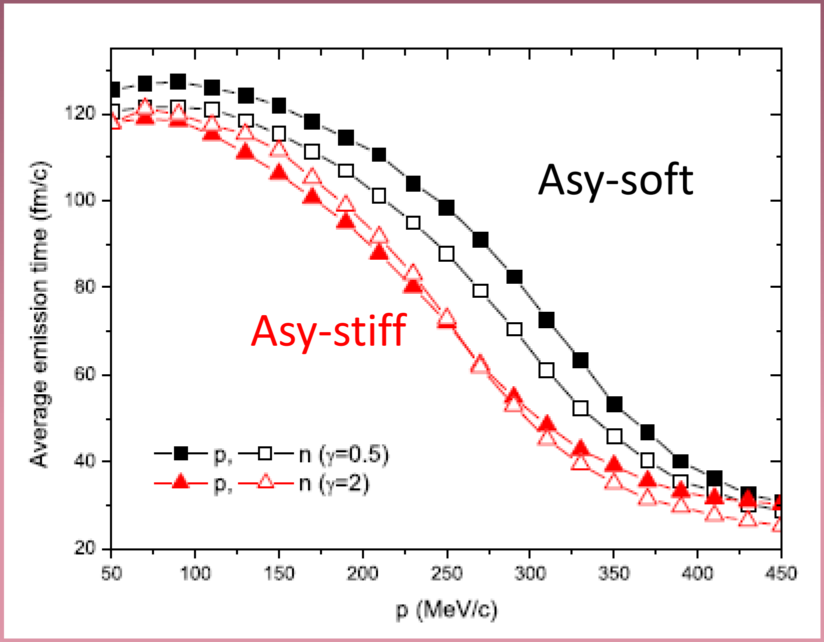

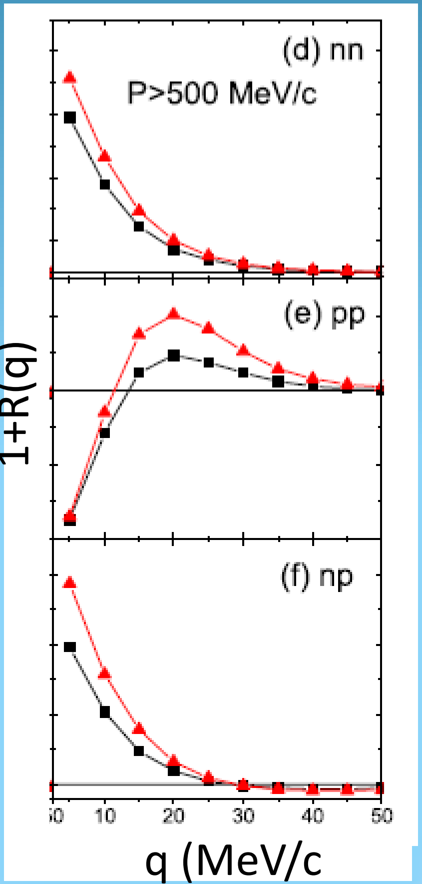

Shorter neutron and proton average emission times and more similar n and p emission times with Esym - stiff

Particle-particle correlations and symmetry energy: a difficult task

IBUU simulations
$^{52}Ca + ^{48}Ca$ E/A=80 MeV, Central collisions
L.W. Chen, V. Greco , C. Ko, B-An Li, PRC68, 014605(2003)

$$1 + R(q) = k \cdot \frac{\Sigma Y_{coinc}(\vec{p}_1, \vec{p}_2)}{\Sigma Y_{evt.mixing}(\vec{p}_1, \vec{p}_2)}$$

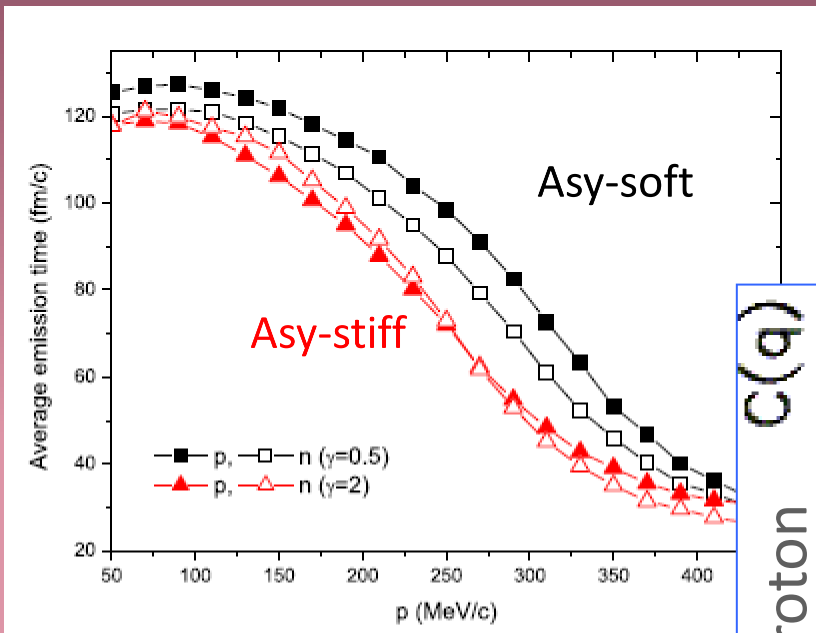

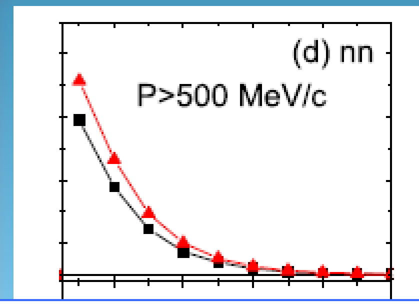

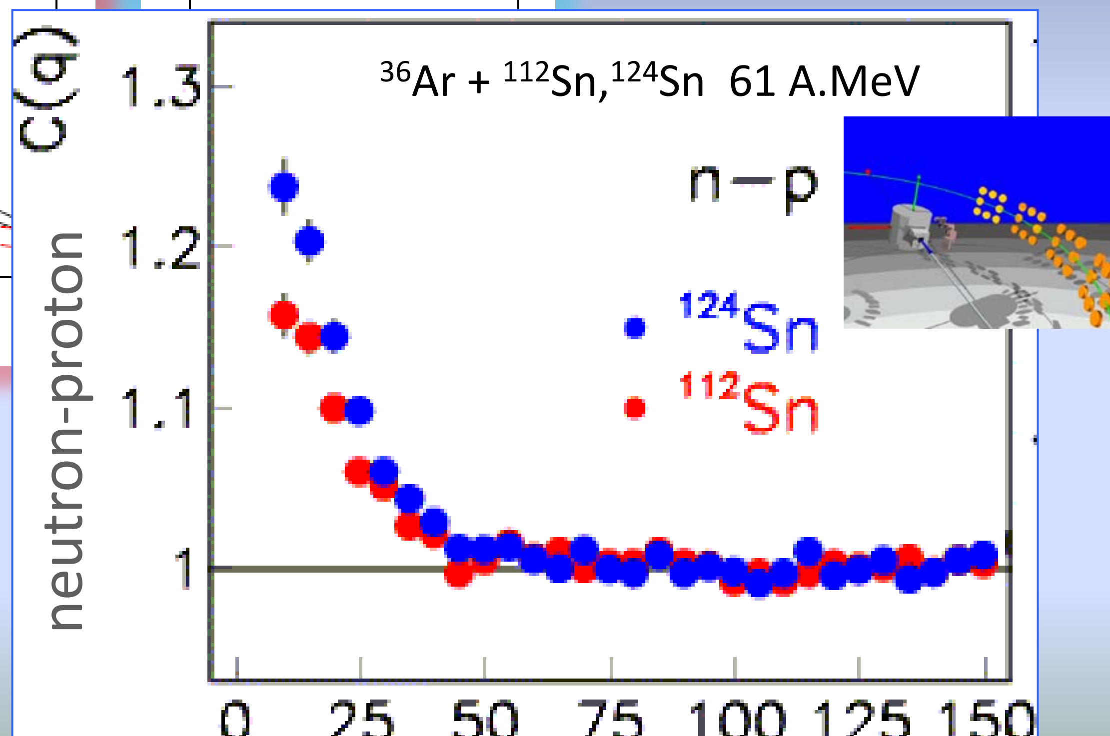

Shorter neutron and proton average emission times and more similar n and p emission times with Esym - stiff

R. Ghetti et al., PRC 69 031605 (2004) CHIC collaboration

Particle-particle correlations and symmetry energy: a difficult task

IBUU simulations
$^{52}Ca + ^{48}Ca$ E/A=80 MeV, Central collisions
L.W. Chen, V. Greco , C. Ko, B-An Li, PRC68, 014605(2003)

$$1+R(q)=k\cdot\frac{\sum Y_{coinc}(\vec{p}_1,\vec{p}_2)}{\sum Y_{evt.mixing}(\vec{p}_1,\vec{p}_2)}$$

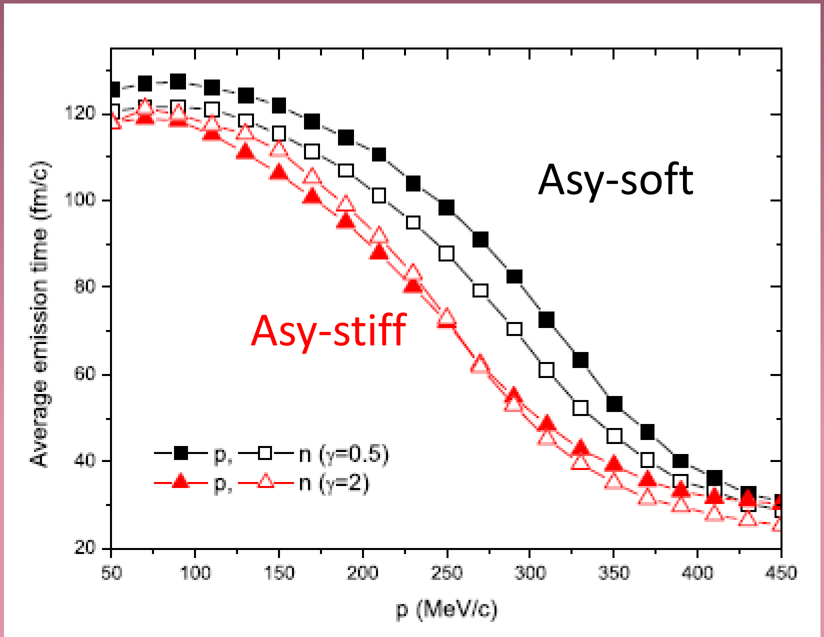

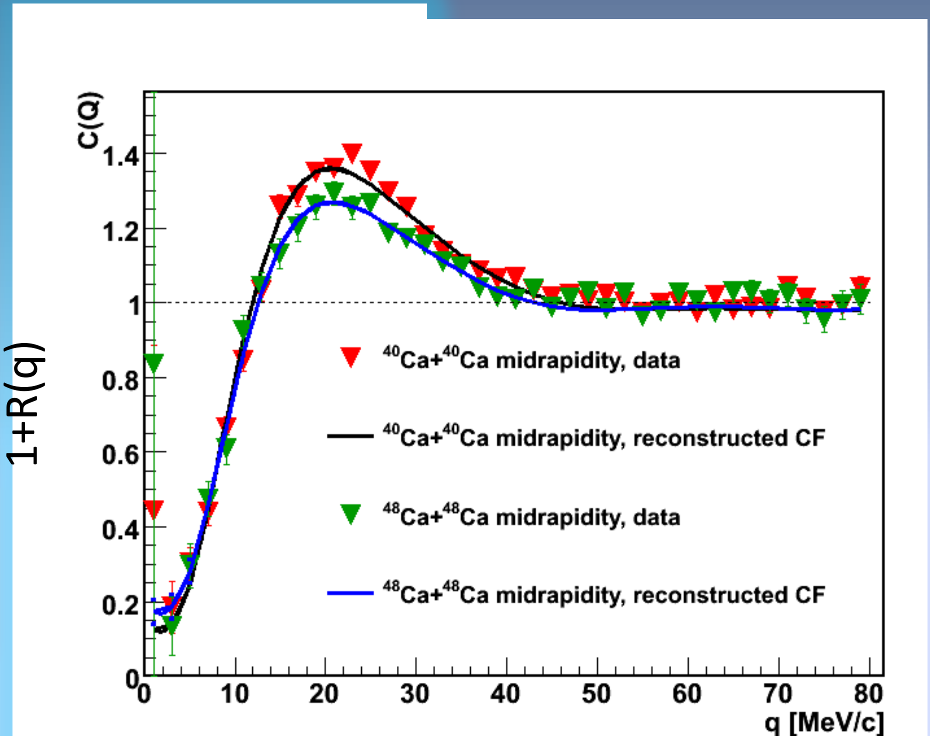

Shorter neutron and proton average emission times and more similar n and p emission times with Esym - stiff

See Henzl et al., PRC85 014606 (2012)
Larger source size for more n-rich systems: Asy-EOS, size effect… ?

A new setup: the 4π CHIMERA + a module of FARCOS prototype

FARCOS: Femtoscope Array for COrrelations and Spectroscopy (INFN, Ganil, Huelva . . .)

- **Based on (62x64x64 mm^3) clusters**
- **1 square (0.3x62x62 mm^3) DSSSD 32+32 strips**
- **1 square (1.5x62x62 mm^3) DSSSD 32+32 strips**
- **4 60x32x32 mm^3 CsI(Tl) crystals**

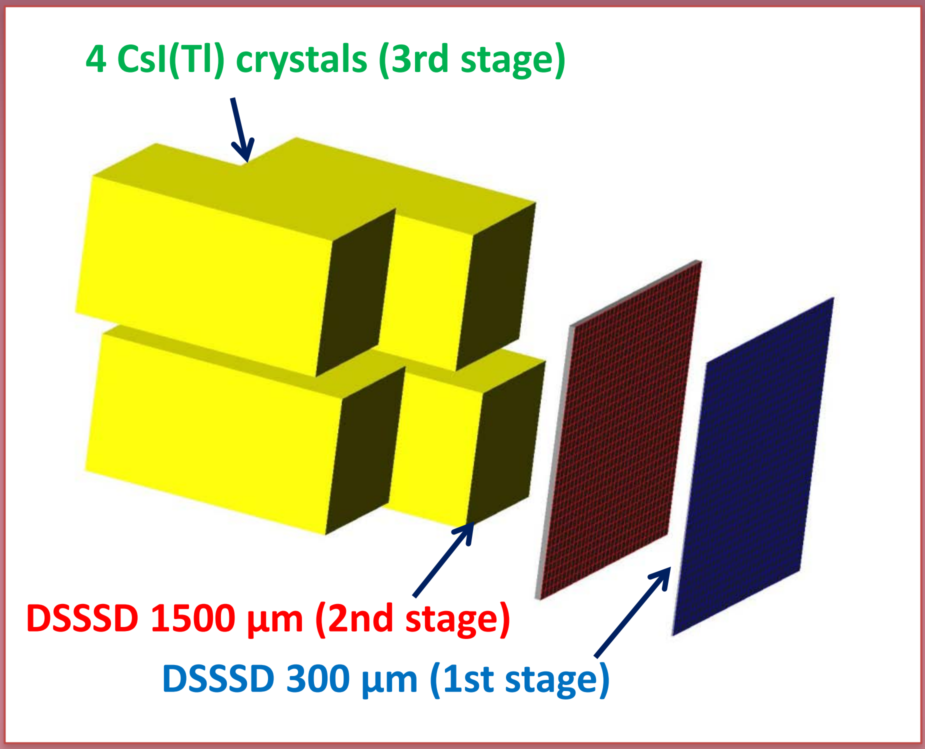

132 channels by each cluster

See T. Minniti talk (Wednesday)

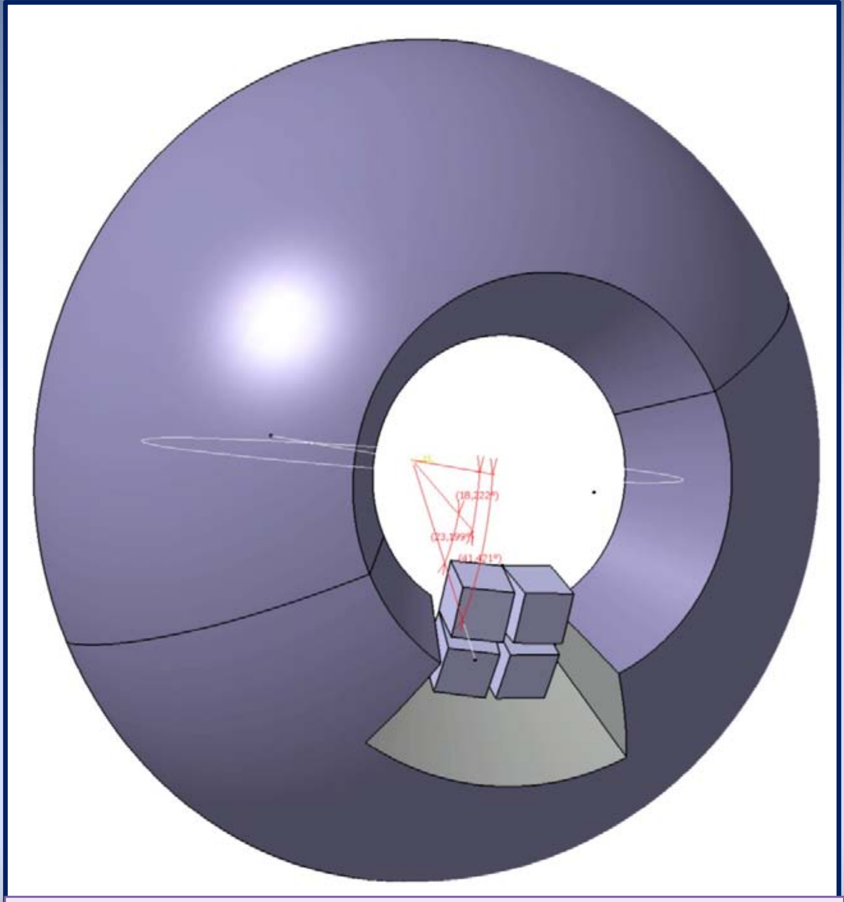

4 telescopes 25 cm from the target
$\theta_{lab} \sim$ 16-44 deg, $\Delta\phi \sim$ 45 deg

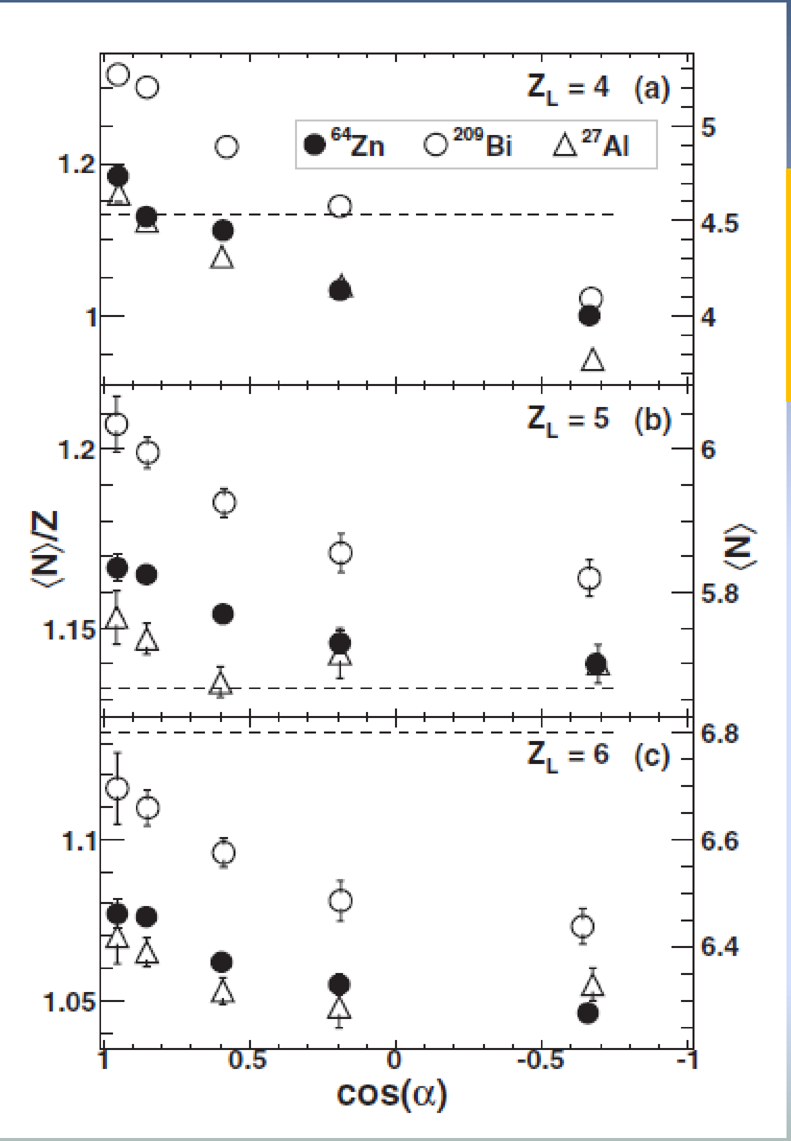

^{64}Zn 45 A.MeV.

Brown et al., PRC87 (2013)